MINISTRY OF EDUCATION AND SCIENCE OF UKRAINE

SUMY NATIONAL AGRARIAN UNIVERSITY

Quilified scientific work (Manuscript)

Chen Rui

UDC: 635.625; 631.527.1; 631.524.86; 577.21

PHD THESIS

SCREENING OF RESISTANT PUMPKIN ROOTSTOCKS AND TRANSCRIPTOMIC ANALYSIS OF RESISTANT/SUSCEPTIBLE PARENTS IN RESPONSE TO *FUSARIUM* WILT AND ROOT-KNOT NEMATODE

Specialty: 201 – Agronomy

Field of study: 20 – Agricultural sciences and food

Submitted for a scientific degree of a Doctor of philosophy

The dissertation contains the results of own research. The use of ideas, results, and texts of other authors have references to the relevant source

_____/CHEN RUI/

Scientific supervisor (consultant)

Volodymyr Dubovyk, Doctor of Agricultural Sciences, Associate Professor

Sumy – 2026

Chen Rui

数字签名者：陈瑞
DN: cn=陈瑞, o=Suny National Agrarian University, ou=Suny National Agrarian University, email=cr15225999975@163.com, c=CN
日期：2026.06.26 18:05:28 +08'00'

АНОТАЦІЯ

ЧЕН ЖУЙ. Стійкість підщеп гарбуза та транскриптомний аналіз реакції батьківських генотипів на фузаріоз та галові нематоди. – Кваліфікаційна наукова праця на правах рукопису.

Дисертація на здобуття наукового ступеня доктора філософії за спеціальністю 201 «Агрономія». – Сумський національний аграрний університет, Міністерство освіти і науки України, Суми, 2026.

Історія досліджень. Гарбуз (*Cucurbita moschata* (Duchesne ex Lam.) Duchesne ex Poir.) є основною підщепою, що використовується у щепленні баштанних культур. Він характеризується добре розвиненою кореневою системою, високою сумісністю та стійкістю до ґрунтових захворювань. Зі стрімким розвитком галузі вирощування баштанних овочів, їх спеціалізоване та інтенсивне вирощування в різних регіонах спричинило серйозні проблеми, пов’язані з неможливістю безперервного вирощування. Фузаріоз та коренева нематода є надзвичайно руйнівними ґрунтовими патогенами баштанних культур, які можуть виживати в ґрунті протягом декількох років і їх важко знищити. Наразі не існує повного вирішення цієї проблеми. Селекція стійких генетичних ресурсів та підщеп є найбільш економічним, ефективним та екологічним заходом боротьби з фузаріозом та *Meloidogyne incognita* у баштанних культурах. Виходячи з цього, виявлення генів стійкості та аналіз механізмів стійкості до патогенів за допомогою транскриптоміки та біоінформатики мають велике значення для прискорення селекції на стійкість до хвороб.

Наукова інноваційність результатів дослідження. Шляхом комбінування різних гібридних комбінацій гарбуза та батьківських сортів, відібраних під час інкубації з фузаріозним в'яненням та *Meloidogyne incognita*, у цьому дослідженні було виявлено гібридні комбінації гарбуза та батьківські сорти, стійкі як до фузаріозного в'янення, так і до *Meloidogyne incognita*, а саме матеріали з подвійною стійкістю. На цій основі було додатково з'ясовано механізм стійкості та механізм регуляції стійких матеріалів до фузаріозного в'янення та *Meloidogyne incognita*.

Практичне значення результатів дослідження. Рекомендується проводити скринінг резистентних ресурсів шляхом окремого зараження фузаріозним в'яненням та *Meloidogyne incognita*, що є специфічним та цілеспрямованим підходом, який забезпечує точність оцінки кожного окремого ресурсу. Необхідно проводити комплексний скринінг у поєднанні з показниками росту та фізіологічними показниками, показниками резистентності, активністю антиоксидантних ферментів та іншими показниками. Результати показують, що окремий показник не може точно відобразити рівень резистентності різних гібридних комбінацій гарбуза та батьківських форм.

Метою даного дослідження було вивчення стійкості різних гібридних комбінацій гарбуза та їх батьківських форм до фузаріозного в'янення та кореневих галових нематод в умовах зараження патогенами, а також попереднє з'ясування молекулярних основ стійкості гарбуза до фузаріозного в'янення та кореневих галових нематод за допомогою високопродуктивного секвенування

транскриптома для аналізу генів з диференційованою експресією. Для досягнення зазначених цілей було поставлено такі завдання: визначити стійкість різних гібридних комбінацій та батьківських форм гарбуза до фузаріозного в'янення в умовах зараження збудником фузаріозу; визначити стійкість різних гібридних комбінацій та батьківських форм гарбуза до кореневих нематод за умов зараження кореневими нематодами; проаналізувати гени, що диференційно експресуються між стійкими та сприйнятливими батьківськими формами гарбуза за умов зараження фузаріозним в'янення та кореневими нематодами, а також зрозуміти механізм стійкості та механізм регуляції стійких форм до фузаріозного в'янення та *Meloidogyne incognita*.

До змісту дослідження увійшла оцінка стійкості 24 гібридних комбінацій гарбуза та 12 батьківських сортів гарбуза до фузаріозного в'янення та кореневих галових нематод, а також аналіз транскриптома та генів з диференційованою експресією, що визначають реакції на стрес, у стійкого батьківського сорту «Хетоу А2» та сприйнятливого батьківського сорту «Лінчуань С1». Об'єктом дослідження був гарбуз (*Cucurbita moschata*). Зміст дослідження включав біологічні стреси (інфікування фузаріозним патогеном, інфікування кореневою галовою нематодою), штучні умови, а також економічну та енергоефективність вирощування гарбуза в сонячних теплицях в Інституті науки і технологій Хенань, місто Сіньсян, провінція Хенань, Китай.

У цьому дослідженні механізми адаптації матеріалів гарбуза до біологічних стресів (інфікування збудником фузаріозу та інфікування кореневими нематодами) вивчалися шляхом вимірювання показників росту та

фізіологічних параметрів, активності антиоксидантних ферментів, вмісту малонового діальдегіду (МДА), розчинних цукрів та розчинних білків у листі, стеблах і коренях саджанців 24 гібридних комбінацій гарбуза та 12 батьківських сортів гарбуза. Матеріал гарбуза штучно інокулювали збудником фузаріозу на стадії саджанців методом занурення коренів, використовуючи суспензію спор у концентрації 1×10^7 спор/мл; суспензію ювенільних особин 2-го віку у концентрації 100 нематод/мл збирали та інокулювали методом проколювання кореневої зони. Сканування коренів проводили в лотках для коренів за допомогою сканера коренів (EPSON Perfection 4990 PHOTO, Seiko Epson (China) Co., Ltd.). Після обробки відскановані зображення коренів аналізували за допомогою професійного програмного забезпечення для аналізу коренів (WinRHIZO Pro 2007, 13 березня 2007 р.) для отримання таких параметрів, як загальна довжина коренів, загальна проекційна площа, площа поверхні коренів, середній діаметр коренів, загальний об’єм коренів та кількість кінчиків коренів. Результати показали, що досліджуваний збудник фузаріозу був високопатогенним, а симптоми були найбільш вираженими через 20 днів після інокуляції. За показниками росту, такими як висота рослини, діаметр стебла та вміст хлорофілу, гібридні комбінації, зокрема 360-3×487, та батьківські сорти, зокрема Renhe-1, 112-2, Xingtai-23, виявилися менш вразливими до ураження патогенами та продемонстрували високу стійкість до фузаріозного в’янення. Гібридна комбінація Yanbian-4×041-1 та батьківські сорти Fangshan, 112-2 продемонстрували високу стійкість до кореневих нематод, а діаметр їх стебел залишався відносно стабільним за обох стресів.

Стійкість до хвороб оцінювали на основі індексу захворюваності. Було відібрано гібридні комбінації з помірною стійкістю до фузаріозного в’янення, зокрема Yanbian-3×360-3, Yanbian-2×041-1 та 360-3×487, а також батьківські сорти з помірною стійкістю, такі як Renhe-1 та Hetou a2. Серед них гібридна комбінація 360-3×487 продемонструвала надзвичайно низький індекс захворюваності стебел та видатну здатність коренів до самозахисту. У поєднанні з кластерним аналізом та значенням функції приналежності Yanbian-3×360-3, Yanbian-2×041-1 та 360-3×487 були визначені як матеріали, стійкі до кореневих нематод, тоді як 112-2 та Lingchuan C1 були визначені як чутливі матеріали. Ці два результати оцінки були в основному узгодженими. Дослідження фізіологічних механізмів показали, що антиоксидантні реакції гарбуза на фузаріозне в’янення та кореневу галову нематоду були специфічними для стресу. CAT відігравав домінуючу роль під час стресу, спричиненого фузаріозним в’яненням, тоді як SOD та CAT спільно брали участь у захисті від кореневої галової нематоди. Вміст MDA можна використовувати як важливий показник для оцінки стресостійкості гарбуза. Аналіз морфології коренів показав, що коренева нематода значно стимулювала проліферацію дрібних коренів та кореневих волосків, підвищуючи стійкість за рахунок поліпшення поглинання та фізичного бар'єру. Натомість збудник фузаріозу в основному уражав судинні пучки, що призводило до зниження функції коренів та слабкого розвитку дрібних коренів і кореневих волосків.

Використовуючи резистентний батьківський сорт гарбуза Hetou a2 та сприйнятливий батьківський сорт Lingchuan C1 як вихідний матеріал, за

допомогою технології RNA-seq було проведено обробку з інфікуванням фузаріозом (48 год, 96 год) та кореневими галовими нематодами (24 год, 48 год). За допомогою секвенування транскриптома та біоінформаційного аналізу було досліджено гени з диференційованою експресією та основні метаболічні шляхи між резистентними та сприйнятливими батьківськими лініями, а також проаналізовано ранні молекулярні механізми реакції гарбуза на два патогена, що передаються через ґрунт. Результати показали, що загалом було отримано 254,55 Гб високоякісних очищених даних та зібрано 33 673 унігени, серед яких 28 977 були функціонально анотовані. Якість даних та цілісність анотацій були надійними, що заклало міцну основу для подальшого аналізу. Аналіз диференціальної експресії показав, що резистентні матеріали значно підвищували експресію великої кількості генів, пов’язаних із захистом, на ранній стадії стресу, тоді як сприйнятливі матеріали демонстрували значне зниження експресії генів на пізній стадії стресу, що вказує на те, що відмінності в резистентності були тісно пов’язані зі швидкістю, інтенсивністю та стабільністю реакцій на стрес. Аналіз збагачення за методами GO та KEGG показав, що гени з диференційованою експресією були значно збагачені в основних захисних шляхах, таких як взаємодія рослина-патоген, сигнальний шлях MAPK, передача сигналів рослинних гормонів та біосинтез фенілпропаноїдів, які були висококонсервативними за обох видів біологічного стресу. Аналіз експресії шляху взаємодії рослина-патоген та ключових генів показав, що резистентні матеріали швидко активували загальну експресію цього шляху. Серед них RBOH демонстрував особливо високу експресію у

стійкості до патогенів за обох стресів, виступаючи ключовим геном для широкого спектру стійкості до патогенів. PR1 та FLS2 виявляли специфічні для стресу партерні реакції. За допомогою WGCNA було ідентифіковано загалом 33 модулі коекспресії генів, серед яких ME17 та ME9 позитивно та негативно регулювали стійкість до широкого спектру захворювань відповідно, а ME20 та ME5 брали участь у специфічних реакціях на стрес, спричинений фузаріозним в'яненням та кореневими нематодами відповідно. Було проведено додатковий скринінг 30 основних генів-хабів, і було підтверджено, що транскрипційні фактори, такі як DOF та ERF, утворюють багаторівневу регуляторну мережу стійкості до хвороб, націлюючись на промоторні ділянки генів-хабів та регулюючи їх. Серед них основна регуляторна вісь CmoDof-PMEI, ідентифікована в цьому дослідженні, продемонструвала високу надійність завдяки порівнянню функцій гомологічних генів та перевірці літературних даних і була ключовою регуляторною одиницею ефективної системи захисту у сорту Rifu. Підсумовуючи, це дослідження дозволило виявити молекулярний механізм широкого спектра стійкості гарбуза до хвороб, що базується на швидкій ранній активації імунних шляхів, специфічній високій експресії ключових генів та синергетичній регуляції численних модулів, що забезпечує важливі генетичні ресурси та теоретичну основу для молекулярної селекції на стійкість до патогенів у баштанних культурах.

Ключові слова: фузаріоз; стрес; забруднення кадмієм, розвиток рослин, сорт, урожайність, шкідники, транскриптомний аналіз, експресія генів, ДНК, ґрунтова інфекція, інокуляція, білок, ареал, хвороба

ABSTRACT

Chen Rui. **Screening of Resistant Pumpkin Rootstocks and Transcriptomic Analysis of Resistant/Susceptible Parents in Response to Fusarium Wilt and Root-Knot Nematode.** – Manuscript.

Dissertation for a Doctor of Philosophy degree (PhD): Specialty 201 – Agronomy. – Sumy National Agrarian University, Ministry of Education and Science of Ukraine – Sumy, 2026.

Research Background. Pumpkin (*Cucurbita moschata* (Duchesne ex Lam.) Duchesne ex Poir.) is the main rootstock used in grafted cultivation of cucurbit crops. It has the characteristics of well-developed root system, good compatibility, and resistance to soil-borne diseases. With the rapid development of the cucurbit vegetable industry, specialized and intensive cultivation in various regions has caused serious problems of continuous cropping obstacles. Fusarium wilt and root-knot nematode are extremely destructive soil-borne diseases of cucurbits, which can survive in soil for several years and are difficult to eliminate. At present, there is no complete solution. Breeding resistant germplasm resources and rootstocks is the most economical, effective and environmentally friendly measure to control fusarium wilt and *Meloidogyne incognita* in cucurbits. On this basis, mining resistance genes and analyzing disease resistance mechanisms via transcriptome and bioinformatics are of great significance for accelerating disease-resistant breeding.

Scientific Innovation of Research Results. By combining different pumpkin hybrid combinations and pumpkin parents screened under inoculation with fusarium wilt and *Meloidogyne incognita*, this study identified pumpkin hybrid combinations

and parents with resistance to both fusarium wilt and *Meloidogyne incognita*, namely dual-resistant materials. On this basis, the resistance mechanism and regulatory mechanism of resistant materials to fusarium wilt and *Meloidogyne incognita* were further revealed.

Practical Significance of Research Results. It is recommended to screen resistant resources under separate inoculation of fusarium wilt and *Meloidogyne incognita*, which is specific and targeted, ensuring the accuracy of evaluation for single resource. It is necessary to conduct comprehensive screening combined with growth and physiological indexes, resistance indexes, antioxidant enzyme activities and other indicators. The results show that a single index cannot accurately reflect the resistance level of different pumpkin hybrid combinations and parents.

This study aimed to investigate the resistance of different pumpkin hybrid combinations and parents to fusarium wilt and root-knot nematode under pathogen and nematode infection, and to preliminarily clarify the molecular basis of resistance to fusarium wilt and root-knot nematode in pumpkin using high-throughput transcriptome sequencing to analyze differentially expressed genes. To achieve the above objectives, the following tasks were set: to determine the resistance of different pumpkin hybrid combinations and parents to fusarium wilt under fusarium pathogen infection; to determine the resistance of different pumpkin hybrid combinations and parents to root-knot nematode under root-knot nematode infection; to analyze differentially expressed genes between resistant and susceptible pumpkin parents under fusarium pathogen and root-knot nematode infection, and to

understand the resistance mechanism and regulatory mechanism of resistant materials to fusarium wilt and *Meloidogyne incognita*.

The research contents included the resistance of 24 pumpkin hybrid combinations and 12 pumpkin parents to fusarium wilt and root-knot nematode, as well as transcriptome and differentially expressed gene analysis of resistance responses in the resistant parent Hetou a2 and susceptible parent Lingchuan C1. The research object was pumpkin (*Cucurbita moschata*). The research contents included biological stresses (fusarium pathogen infection, root-knot nematode infection), artificial conditions, and the economic and energy efficiency of pumpkin cultivation in solar greenhouses at Henan Institute of Science and Technology, Xinxiang City, Henan Province, China.

In this study, the adaptation mechanisms of pumpkin materials to biological stresses (fusarium pathogen infection and root-knot nematode infection) were investigated by measuring growth and physiological parameters, antioxidant enzyme activities, malondialdehyde (MDA) content, soluble sugar and soluble protein contents in leaves, stems and roots of seedlings of 24 pumpkin hybrid combinations and 12 pumpkin parents. Pumpkin materials were artificially inoculated with fusarium pathogen at the seedling stage by root-dipping method using a spore suspension of 1×10^7 spores/mL; a 2nd-stage juvenile suspension of 100 nematodes/mL was collected and inoculated by the root-zone punching method. Root scanning was performed in root trays using a root scanner (EPSON Perfection 4990 PHOTO, Seiko Epson (China) Co., Ltd.). After processing, the scanned root images were analyzed with professional root analysis software (WinRHIZO Pro

2007, March 13, 2007) to obtain parameters such as total root length, total projected area, root surface area, average root diameter, total root volume and number of root tips. The results showed that the tested fusarium pathogen was highly pathogenic, and the symptoms were most significant 20 days after inoculation. Based on growth indexes including plant height, stem diameter and chlorophyll content, hybrid combinations such as 360-3×487 and parents such as Renhe-1, 112-2, Xingtai-23 were less affected by pathogen infection, showing strong resistance to fusarium wilt. Hybrid combination Yanbian-4×041-1 and parents Fangshan, 112-2 exhibited high resistance to root-knot nematode, and their stem diameters were relatively stable under both stresses.

Disease resistance was evaluated based on disease index. Moderately fusarium wilt-resistant hybrid combinations including Yanbian-3×360-3, Yanbian-2×041-1 and 360-3×487, and moderately resistant parents such as Renhe-1 and Hetou a2 were screened. Among them, hybrid combination 360-3×487 showed an extremely low stem disease index and outstanding root defense ability. Combined with cluster analysis and membership function value, Yanbian-3×360-3, Yanbian-2×041-1 and 360-3×487 were identified as root-knot nematode-resistant materials, while 112-2 and Lingchuan C1 were identified as susceptible materials. The two evaluation results were basically consistent. Physiological mechanism studies showed that the antioxidant responses of pumpkin to fusarium wilt and root-knot nematode were stress-specific. CAT played a dominant role under fusarium wilt stress, while SOD and CAT were jointly involved in defense against root-knot nematode. MDA content could be used as an important indicator for stress resistance

evaluation in pumpkin. Root morphology analysis showed that root-knot nematode significantly induced the proliferation of fine roots and root hairs, enhancing resistance by improving absorption and physical barrier. In contrast, fusarium pathogen mainly infected vascular bundles, leading to declined root function and weak development of fine roots and root hairs.

Using the resistant pumpkin parent Hetou a2 and susceptible parent Lingchuan C1 as materials, RNA-seq technology was used to perform treatments of fusarium infection (48 h, 96 h) and root-knot nematode infection (24 h, 48 h). Through transcriptome sequencing and bioinformatics analysis, differentially expressed genes and core metabolic pathways between resistant and susceptible parents were explored, and the early molecular mechanisms of pumpkin in response to two soil-borne diseases were analyzed. The results showed that a total of 254.55 Gb high-quality clean data were obtained, and 33,673 Unigenes were assembled, among which 28,977 were functionally annotated. The data quality and annotation integrity were reliable, laying a solid foundation for subsequent analysis. Differential expression analysis showed that resistant materials significantly up-regulated a large number of defense-related genes at the early stage of stress, while susceptible materials showed extensive down-regulation of genes at the late stage of stress, indicating that resistance differences were closely related to the speed, intensity and stability of stress responses. GO and KEGG enrichment analysis showed that differentially expressed genes were significantly enriched in core defense pathways such as plant-pathogen interaction, MAPK signaling pathway, plant hormone signal transduction, and phenylpropanoid biosynthesis, which were highly conserved under

both biological stresses. Expression analysis of the plant-pathogen interaction pathway and key genes showed that resistant materials rapidly activated the overall expression of the pathway. Among them, *RBOH* showed specifically high expression in disease resistance under both stresses, serving as a key gene for broad-spectrum disease resistance. *PR1* and *FLS2* exhibited stress-specific response patterns. A total of 33 gene co-expression modules were identified by WGCNA, among which ME17 and ME9 positively and negatively regulated broad-spectrum disease resistance, respectively, and ME20 and ME5 participated in specific stress responses to fusarium wilt and root-knot nematode, respectively. Thirty core hub genes were further screened, and transcription factors such as DOF and ERF were confirmed to form a multi-level disease resistance regulatory network by targeting and regulating the promoter regions of hub genes. Among them, the *CmoDof*-PMEI core regulatory axis identified in this study showed high reliability through homologous gene function comparison and literature verification, and was a key regulatory unit of the efficient defense system in the Rifu cultivar. In summary, this study revealed the molecular mechanism of broad-spectrum disease resistance in pumpkin through rapid early activation of immune pathways, specific high expression of key genes, and synergistic regulation of multiple modules, providing important gene resources and theoretical basis for molecular breeding of disease resistance in cucurbit crops.

Keywords: Fusarium wilt, stress, cadmium pollution, plant development, variety, yield, pests, transcriptome analysis, gene expression, DNA, soil infection, inoculation, protein, range, diseases

LIST OF THE APPLICANT'S PUBLICATIONS

Articles in scientific professional publications of Ukraine category «B»:

1. Chen, R. 2024. IDENTIFICATION OF RESISTANCE TO MELON FUSARIUM WILT IN SEVEN HYBRID COMBINATIONS OF PUMPKINS. Bulletin of Sumy National Agrarian University. The series: Agronomy and Biology. 55, 1 (Jun. 2024), 11-17.

DOI:https://doi.org/10.32782/agrobio.2024.1.2.

2. Chen, R. and Dubovyk, V. 2025. GERMINATION OF PUMPKIN SEEDS UNDER CD STRESS. *Bulletin of Sumy National Agrarian University. The series: Agronomy and Biology*. 58, 4 (Mar. 2025), 3-8.

DOI: https://doi.org/10.32782/agrobio.2024.4.1.

Scopus and WoS publication:

3. **Chen, R.,** V. Dubovyk, B. Chen and J. Liu. 2025. Comparison of the effects of seven hybrid combinations of pumpkin root stocks on the growth and antioxidant enzyme activity of grafted cucumber. Pak. J. Bot., 57(3).

DOI: http://dx.doi.org/10.30848/PJB2025-3(37).

Conferences

4. Chen Rui, Dubovyk V. THE INFLUENCE OF PUMPKIN ROOT STOCK IN PRODUCTION, X International Scientific and Practical Conference "Modern

problems of science, education and society" Kyiv, Ukraine 4-6 December 2023. – Pp. 49–52.

5. Chen Rui, Dubovyk V. THE EFFECT OF PUMPKIN ROOT STOCK GRAFTING ON THE GROWTH AND QUALITY OF MELONS, XI International Scientific and Practical Conference "Modern problems of science, education and society" Kyiv, Ukraine 8-10 January 2024. – Pp. 40–42.

CONTENT

LIST OF SYMBOLS AND ABBREVIATIONS

SOD – superoxide dismutase

POD – peroxidase

CAT – catalase

MDA – malondialdehyde

SS – soluble sugar

SP – soluble protein

INTRODUCTION

Reasons for Choosing This Research Topic. Pumpkin (*Cucurbita moschata* (Duchesne ex Lam.) Duchesne ex Poir.) is the main rootstock in grafted cultivation of cucurbit crops. It is characterized by a well-developed root system, good compatibility, and resistance to soil-borne diseases. With the rapid development of the cucurbit vegetable industry, specialized and intensive cultivation in various regions has led to serious problems of continuous cropping obstacles in cucurbit vegetables. Fusarium wilt and root-knot nematode are extremely destructive soil-borne diseases of cucurbits. They can survive in the soil for several years and are difficult to eliminate, and there is currently no complete solution. Breeding resistant germplasm resources and rootstocks is the most economical, effective and environmentally friendly measure to control fusarium wilt and *Meloidogyne incognita* in cucurbits. On this basis, isolating and identifying resistance genes to fusarium wilt and root-knot nematode in cucurbit germplasm, then introducing them into cultivated cucurbit varieties via transgenic technology to directionally breed new varieties with stably inherited resistance traits, is of great significance for solving the damage caused by fusarium wilt and root-knot nematode in cucurbits.

Connection of the Study with Scientific Programs, Plans and Topics. The study was carried out in accordance with the thematic plan of Henan Institute of Science and Technology and national scientific research projects, and was supported by the Special Project for Post Experts of the Bulk Vegetable Industry Technology System of Henan Province (HARS-22-07-G6), the National Natural Science

Foundation of China (No. U2004161), and the Major Science and Technology Special Project of Henan Province in 2024 (241100110200).

This study aimed to investigate the resistance of different pumpkin hybrid combinations and pumpkin parents to fusarium wilt and root-knot nematode under infection of fusarium wilt pathogen and root-knot nematode, and to preliminarily clarify the molecular basis of resistance to fusarium wilt and root-knot nematode in pumpkin by analyzing differentially expressed genes using high-throughput transcriptome sequencing.

To achieve the above objectives, the following tasks were set in the study:

To determine the resistance of different pumpkin hybrid combinations and pumpkin parents to fusarium wilt and root-knot nematode under fusarium wilt pathogen infection.

To determine the resistance of different pumpkin hybrid combinations and pumpkin parents to fusarium wilt and root-knot nematode under root-knot nematode infection.

To analyze differentially expressed genes between resistant and susceptible pumpkin parents under infection of fusarium wilt pathogen and root-knot nematode, and to understand the resistance mechanism and resistance regulation mechanism of resistant materials to fusarium wilt and *Meloidogyne incognita*.

The research contents included the resistance of 24 pumpkin hybrid combinations and 12 pumpkin parents to fusarium wilt and root-knot nematode, as well as transcriptome and differentially expressed gene analysis of resistance responses in the screened resistant pumpkin parent Hetou a2 and susceptible parent

Lingchuan C1.

The research object was pumpkin (*Cucurbita moschata*). The research contents included biological stresses (fusarium wilt pathogen infection, root-knot nematode infection), artificial conditions, and the economic and energy efficiency of pumpkin cultivation in solar greenhouses at Henan Institute of Science and Technology in Xinxiang City, Henan Province, China.

Research Methods. The study adopted general scientific methods (hypothesis, analysis, synthesis, extrapolation and generalization) as well as special research methods. Visual methods were used to observe disease symptoms of plants under infection of fusarium wilt pathogen and root-knot nematode; measurement and weighing methods were used to determine morphological parameters and performance of plants; chemical methods were used for enzyme analysis and determination of soluble sugar and soluble protein contents; mathematical and statistical methods were used for analysis of variance to evaluate the reliability of the obtained results; calculation and comparative analysis were used to evaluate the resistance of different pumpkin hybrid combinations and pumpkin parents to fusarium wilt and root-knot nematode. High-throughput transcriptome sequencing was used to analyze differentially expressed genes to understand the resistance mechanism and resistance regulation mechanism of resistant materials to fusarium wilt and *Meloidogyne incognita*.

Scientific Innovation of the Results Obtained. By combining different pumpkin hybrid combinations and pumpkin parents screened under infection of fusarium wilt and *Meloidogyne incognita*, this study obtained pumpkin hybrid

combinations and parents with resistance to both fusarium wilt and *Meloidogyne incognita*, namely dual-resistant materials. On this basis, the resistance mechanism and resistance regulation mechanism of resistant materials to fusarium wilt and *Meloidogyne incognita* were further revealed.

The research results have important practical significance. It is recommended to screen resistant resources under separate inoculation of fusarium wilt and *Meloidogyne incognita*, which is specific and targeted, ensuring the accuracy of evaluation for a single resource. It is necessary to conduct comprehensive screening combined with growth and physiological indexes, resistance indexes, antioxidant enzyme activities and other indicators. The results show that a single index cannot accurately reflect the resistance level of different pumpkin hybrid combinations and pumpkin parents.

Contribution of the PhD Candidate. The contribution includes: searching, analyzing and systematically organizing scientific research achievements of scientists at home and abroad. The main contents of the experimental part of the study include: implementation of experimental research; generalized summary of results; mathematical and statistical processing of data; formation of conclusions; and proposal of production recommendations. The scientific argumentation of this dissertation was developed by the author under the guidance of the supervisor.

Recognition of Dissertation Achievements. The main research results of the doctoral dissertation have been recognized at several international scientific-practical conferences: X International Scientific and Practical Conference “Modern problems of science, education and society”(Kyiv, Ukraine,2023); XI International

Scientific and Practical Conference “Modern problems of science, education and society”(Kyiv, Ukraine,2024).

Publications. The main contents of this dissertation have been published in 5 scientific works, including 2 articles in professional Ukrainian journals; 1 article indexed in the international scientometric citation databases Scopus and Web of Science; 2 articles in international scientific-practical conferences.

Structure and Scope of the Dissertation. The dissertation includes an introduction, 4 chapters, conclusions, practical recommendations and a list of references, as well as appendices. The main text of the dissertation is 194 pages long, containing 9 tables, 33 figures and 11 appendices. The reference list includes 215 publications.

SECTION 1

LITERATURE REVIEW

1.1. Research Progress on Pumpkin Rootstocks

With the rapid development of the cucurbit vegetable industry, specialized and intensive cultivation in various regions has caused serious continuous cropping obstacles in cucurbit vegetables. The incidence rate increases year by year with continuous cropping, resulting in severe production losses [1-3]. Pumpkin is widely used as a rootstock for cucurbit grafting [4-11]. Grafting is an effective strategy to improve the resistance of cucurbits and solanaceous vegetables to soil-borne diseases and pests [12-15]. Previous studies have shown that grafting can alleviate the stress of continuous cropping obstacles on grafted watermelon seedlings [16, 17], reduce damage caused by adverse stress to watermelon plants [18, 19], enhance plant vigor and yield of small-fruited watermelon, reduce the application of chemical fertilizers and pesticides [20], and improve nitrogen use efficiency in watermelon [21].

It has been reported that after grafting and root replacement of vegetables, grafted plants develop vigorous root systems with enhanced absorption capacity, and exhibit different physiological and ecological responses compared with own-root seedlings [22, 23]. Grafting can significantly enhance cold resistance and promote root nutrient absorption, growth and development [24]. Therefore, the use of disease-resistant pumpkin as rootstocks can reduce the occurrence of soil-borne diseases in

cucurbits, especially fusarium wilt and root-knot nematode [25]. Grafting and root replacement cultivation can effectively control fusarium wilt of cucurbits and increase yield, which has been widely applied in disease-resistant cultivation of watermelon and cucumber [26-28].

The use of interspecific hybrids of disease-resistant pumpkin as rootstocks [29, 30] can significantly enhance the vigor and stress resistance of watermelon, effectively prevent soil-borne diseases, reduce the adverse effects of protected continuous cropping obstacles, and ultimately achieve the goals of disease resistance, high quality and high yield, compared with intervarietal hybrids [31, 32]. Huo Yumeng et al. [33] constructed a cloning vector of a specific expression promoter induced by root-knot nematode, but there is still no simple and feasible method to control root-knot nematode. Breeding root-knot nematode-resistant varieties is also an important approach. Screening rootstocks resistant to root-knot nematode [34] can save a great deal of labor and material resources, reduce vegetable product pollution caused by chemical control, and thus has broad prospects [35-38].

Research on cucurbit grafting technology began in Japan as early as the 1920s. After the 1980s, vegetable grafting also received extensive attention in China, America, Europe and other regions, and has been applied in the production of most cucurbit and solanaceous vegetables [39-44]. According to statistics, 95% of greenhouse watermelons, 92% of open-field watermelons, and 95% of greenhouse cucumbers in Japan are produced using grafting technology [45-47]; more than 90% of watermelons and over 80% of melons in South Korea are cultivated by grafting [48], which can not only increase yield but also improve quality [49-63]. With the

popularization of vegetable grafting [64-67], the demand for rootstocks has increased rapidly. Rootstock breeding has attracted the attention of world-famous seed companies, including Monsanto, Syngenta, Rijk Zwaan, and Nunhems, indicating that commercial rootstock breeding has been widely valued [68].

1.2. Research Progress on *Fusarium* Wilt of Cucurbits

Fusarium wilt of cucurbits, also known as wilt disease or vine blight, is one of the most important diseases of cucurbits. The damage caused by fusarium wilt [69-83] has become a critical problem urgently to be solved in cucurbit production. Cucumber and watermelon are the most severely affected, followed by wax gourd and melon. Symptoms appear successively after flowering and fruiting: leaves turn yellow gradually from bottom to top, wilt as if lacking water, and recover at night; after a period, the whole plant turns yellow and wilts, and the vascular bundle of the root discolors until the plant dies.

Fusarium wilt of cucurbits is a fungal soil-borne disease caused by *Fusarium oxysporum* Schl. of the genus *Fusarium* (Tuberculariaceae, Moniliales, Imperfectifungi). The pathogen infects crops from the roots and damages the host by blocking vessels and secreting toxic substances [84-94]. It generally reduces cucurbit yield by 20%–30%, and can reach 50%–60% or even total crop failure under severe conditions [95, 96]. It was first reported in Minnesota, USA [97]. The pathogen overwinters as mycelium, sclerotia and chlamydospores in soil, diseased residues, uncomposted fertilizer, and also on seeds [98-105]. Fusarium wilt pathogen

can survive in soil for several years, and new populations can emerge through continuous variation, making it difficult to prevent and eliminate [106-117]. According to surveys, the incidence rate of fusarium wilt in common disease fields ranges from 12.30% to 56.75%, while in severely infested fields it exceeds 85% or even leads to total death, causing huge economic losses to cucurbit production [118-124].

In terms of resistance and control, resistance to fusarium wilt in cucurbits is mainly inherited as a quantitative trait, regulated by both major QTLs and minor polygenes. At present, several fusarium wilt resistance-related genes have been isolated and cloned from cucurbit crops, and phenylpropanoid metabolism, pathogenesis-related (PR) proteins, and hormone signaling (SA, JA/ET) have been identified as core defense pathways. Grafting, crop rotation, chemical pesticides and biological control are the main control measures in production, among which pumpkin rootstock grafting is the most stable and efficient green control strategy [125-128].

1.3. Research Progress on Root-Knot Nematode of Cucurbits

Root-knot nematodes (*Meloidogyne* spp.) are a group of plant-parasitic nematodes with numerous species, wide host ranges and severe damage [129-131]. They mainly damage plant roots, forming bead-like root knots, destroying the differentiation and physiological activities of root tissues, and affecting the growth and development of aboveground parts [132-138]. According to statistics, there are

more than 90 species, which can infect more than 3,000 plant species [139], causing annual economic losses of billions of dollars worldwide [140].

Root-knot nematodes mainly infect Cucurbitaceae, Solanaceae, Brassicaceae and other plants [132], and are particularly severe on vegetables such as tomato and cucumber [141, 142]. They are mainly transmitted via soil, diseased residues, irrigation water and agricultural machinery [143]. At present, nearly 100 species of root-knot nematodes have been reported worldwide [144, 145]. The common species in agricultural production include *Meloidogyne incognita*, *M. arenaria*, *M. hapla* and *M. javanica* [146, 147], among which *M. incognita* is dominant [148]. Crop losses caused by these four species account for more than 90% of the total losses caused by root-knot nematodes [149, 150].

At present, root-knot nematode-resistant varieties of tomato and pepper have been bred and applied in production [151-154]. Many nematode resistance genes have also been mapped in potato [155, 156]. Louws F J et al. reported that grafting cultivated watermelon onto wild watermelon accessions conferred resistance or moderate resistance to *M. incognita*, while four gourd rootstocks and one pumpkin hybrid (*C. moschata* × *C. maxima*) were highly susceptible, with only partially tolerant materials obtained [157-159]. Studies by Bin Liu et al. showed that African wild cucurbits are highly resistant to *M. incognita* and fusarium wilt [160]. Overall, root-knot nematode-resistant germplasm in cucurbits is still scarce, and further exploration of new resistance resources and broad-spectrum resistance genes is needed to meet production needs.

1.4. Overview of Transcriptomics in Plant Response to Biotic Stress

Transcriptomics (RNA-seq) enables global analysis of gene expression dynamics under stress and systematic identification of key genes, regulatory pathways and transcription factor networks, and has become a core technical tool in the study of plant biotic stress response mechanisms [161]. Under biotic stresses including fungi, nematodes and bacteria, transcriptomics can efficiently screen differentially expressed genes (DEGs) and reveal the response patterns of conserved pathways such as pattern recognition receptors (PRRs), MAPK cascades, hormone signaling (SA/JA/ET), secondary metabolism (phenylpropanoids, terpenoids), and ROS metabolism. Meanwhile, combined with transcription factors (WRKY, NAC, MYB, etc.) and co-expression network analysis, the regulatory hierarchy of stress response can be constructed and core hub genes rapidly identified.

In stress resistance research of cucurbits and pumpkin, transcriptomics has been widely used in studies of fusarium wilt [162, 163], root-knot nematode [164-167], and grafting rootstock-scion interaction [168], successfully identifying numerous candidate genes for disease and stress resistance, and clarifying the key roles of multiple metabolic and signaling pathways. The recently developed spatiotemporal transcriptomics, single-cell transcriptomics and multi-omics integration have further enabled precise analysis at the cellular and dynamic temporal levels, promoting mechanistic research from the tissue level to the cellular and molecular levels.

Conclusions to section 1

Resistant rootstocks are ideal materials for controlling soil-borne diseases and improving stress resistance in cucurbits, and have important value in both production and basic research. Fusarium wilt and root-knot nematode of cucurbits are both highly destructive soil-borne diseases; single infection alone can cause significant yield loss, while combined infection aggravates damage, forms complex interactions, and greatly increases the difficulty of control.

At present, considerable progress has been made in physiological and biochemical characteristics, resistance genetics and molecular mechanisms under single stress. Transcriptomics provides a powerful tool for mining stress resistance genes and analyzing regulatory pathways. However, most existing studies focus on single disease, and systematic understanding is still lacking regarding the immune crosstalk, signal crosstalk, defense trade-offs and molecular networks of cucurbits under combined fusarium wilt and root-knot nematode stress. Meanwhile, the screening of pumpkin rootstock resources adapted to combined resistance, as well as the cloning and mechanistic analysis of key genes, are obviously insufficient, which can hardly meet the needs of precise breeding and green control.

Therefore, conducting transcriptomic analysis of pumpkin in response to combined fusarium wilt and root-knot nematode stress, systematically mining core resistance genes and regulatory pathways, and clarifying the molecular mechanism of combined stress response, have important theoretical significance and application value for breeding multi-resistant rootstocks, overcoming continuous cropping obstacles, and ensuring high-quality and high-yield cucurbit production.

References to section 1

1. Zhao, S.M., Xiao, Z.L., Shen, Y.G. Grafting cultivation experiment of thin-skin melon in greenhouse[J]. China Cucurbits and Vegetables, 2010, 23(4): 27–30. DOI:10.3969/j.issn.1673-2871.2010.04.009.

2. Liu, G., Yang, X.P., Xu, J.H., et al. Research progress on grafting cultivation techniques of watermelon and melon[J]. China Cucurbits and Vegetables, 2009, 22(1): 4. DOI:10.3969/j.issn.1673-2871.2009.01.010.

3. Fan, H.J., Zhou, B.L., Lin, G.R. Grafting cultivation techniques of eggplant[J]. Journal of Henan Agricultural Sciences, 2001(4): 2. DOI:CNKI:SUN:HNNY.0.2001-04-023.

4. Li, H., Wang, Z.W., Sun, X.W. Research progress on pumpkin rootstocks[C]//Member Congress and Academic Symposium of Pumpkin Branch, Chinese Society for Horticultural Science. 2013.

5. Wei, M., Ma, H. Application of grafting rootstocks for cucurbit vegetables[J]. Northern Horticulture, 1999. DOI:CNKI:SUN:BFYY.0.1999-02-048.

6. Zhou, J.G., Li, X.Z. Utilization of pumpkin in cucurbit grafting cultivation and research progress on salt tolerance of cucurbit rootstocks[C]//The 5th Academic Symposium of Pumpkin Branch, Chinese Society for Horticultural Science. 2007.

7. Gao, X.Y., Wang, Y.Y. Benefits of cucurbit grafting[J]. Life World, 1981(3): 1–2, 2.

8. Liu, D.H., Xiao, W., Luo, Z.Y., et al. Discussion on grafting cultivation

techniques of cucurbits[J]. Southwest Horticulture, 2005, 33(1): 3. DOI:CNKI:SUN:XNYY.0.2005-01-005.

9. Li, H.Z., Gong, G.Y., Zhang, F., et al. Breeding of Jingxin Rootstock 4, a special rootstock for watermelon[C]//Conference on Research and Application of Grafting Seedling for Cucurbit Crops, 2009.

10. Wei, M., Ma, H. Application of grafting rootstocks for cucurbit vegetables[J]. Northern Horticulture, 1999(2): 55–56.

11. Wang, P.C., Liu, K., Zhang, Q.A., et al. Research and application of cucurbit rootstock breeding and high-efficiency seedling raising techniques[J]. China Science and Technology Achievements, 2017(24): 2. DOI:10.3772/j.issn.1009-5659.2017.24.030.

12. Shi, X.J., Zheng, G.F., Guo, S.Y., et al. Grafting cultivation techniques of seedless watermelon[J]. Journal of Henan Agricultural Sciences, 1998(11): 2. DOI:CNKI:SUN:HNNY.0.1998-11-017.

13. Dong, Y.M., Jiao, Z.G., Wang, C.Q., et al. Grafting cultivation techniques of winter-spring muskmelon[J]. Shandong Agricultural Sciences, 2007(2): 120–121.

14. Zhou, J.Y., Liu, F.R., Wang, H.W. Eggplant grafting cultivation techniques and yield-increasing effects[C]//Liaoning Agricultural Science Symposium, 2004. DOI:ConferenceArticle/5aa519edc095d72220d52c18.

15. Qian, W., Xu, Z.H. Grafting cultivation techniques of vegetables[J]. Agriculture and Forestry Science Experiment, 1994(9): 12–14.

16. Hassell, R.L., Memmott, F., Liere, D.G. Grafting methods for watermelon production[J]. HortScience, 2008, 43(6): 1677–1679.

17. Chen, K., Sun, J.Q., Liu, R.J., et al. Effects of arbuscular mycorrhizal fungi on growth and root defensive enzyme activities of grafted watermelon seedlings[J]. Chinese Journal of Applied Ecology, 2013, 24(1): 135–141.

18. Lee, J.M., Kubota, C., Tsao, S.J., et al. Current status of vegetable grafting: Diffusion, grafting techniques, automation[J]. Scientia Horticulturae, 2010, 127(2): 93–105.

19. Mohamed, F.H., Abd El-Hamed, K.E., Elwan, M.W.M., et al. Evaluation of different grafting methods and rootstocks in watermelon grown in Egypt[J]. Scientia Horticulturae, 2014, 168: 145–150.

20. Ying, Q.S., Wang, Y.E., Wang, Y.H., et al. Technology for preventing premature senescence of long-season grafted watermelon in protected cultivation in Zhejiang[J]. Yangtze Vegetables, 2014(1): 45–46.

21. Nawaz, M.A., Han, X., Chen, C., et al. Nitrogen Use Efficiency of Watermelon Grafted onto 10 Wild Watermelon Rootstocks under Low Nitrogen Conditions[J]. Agronomy, 2018, 8(11).

22. Zhou, B.L., Lin, G.R., Li, N.Y. Grafting Cultivation of Vegetables. Beijing: China Agriculture Press, 1997: 1–9, 19.

23. Arai, K. Physiological and ecological responses in roots of grafted plants[J]. Abstract Autumn Meet. J. Jpn. Soc. Hort. Sci., 1980: 67–73.

24. Li, J., Xu, B., Li, H., et al. Research and application overview of vegetable grafting[J]. Yunnan Agriculture, 2013(5): 37–38. DOI:10.3969/j.issn.1005-1627.2013.05.024.

25. Zhang, H.H. Morphological character analysis and disease resistance

evaluation of pumpkin germplasm for rootstocks[D]. Guangxi: Guangxi University, 2015. DOI:10.7666/d.Y2888458.

26. Lei, M. Effects of grafting on resistance to fusarium wilt of watermelon[J]. Journal of Anhui Agricultural Sciences, 2001, 29(5): 655–656. DOI:10.3969/j.issn.0517-6611.2001.05.047.

27. Jiang, Y.T., Zhang, M.F., Sun, L.X. Progress and prospect of cucurbit grafting cultivation in China[J]. Yangtze Vegetables, 1998(6): 1–4, 39.

28. Li, G.Q. Studies on breeding of cucumber rootstocks and grafting cultivation techniques[J]. Journal of Anhui Agricultural Sciences, 2008, 36(14): 2. DOI:10.3969/j.issn.0517-6611.2008.14.065.

29. Zhang, H.H. Morphological character analysis and disease resistance evaluation of pumpkin germplasm for rootstocks[D]. Guangxi: Guangxi University, 2015. DOI:10.7666/d.Y2888458.

30. Wang, J.W., Dai, X.Z., Yu, F.S. High-yield and high-quality cultivation techniques for hybrid seed production of pumpkin for rootstocks[J]. Jilin Vegetables, 2008(3): 2. DOI:10.3969/j.issn.1672-0180.2008.03.002.

31. Jin, G.Y., Wei, W.X., Chen, J.Y., et al. Preliminary study on interspecific sexual hybridization of Cucurbita[J]. Fujian Journal of Agricultural Sciences, 1999(S1): 97–101.

32. Lin, D.P. Genetic genes and interspecific hybridization of Cucurbita plants[J]. China Watermelon and Muskmelon, 2000(3): 41–44. DOI:10.3969/j.issn.1673-2871.2000.03.016.

33. Huo, Y.M., Wang, W., Xu, Y.F., et al. Cloning and sequence analysis of

root-knot nematode-inducible promoter RKNIP[J]. Shandong Agricultural Sciences, 2009(4): 5–8, 15.

34. Gu, X.F., Zhang, S.P., Zhang, S.Y., et al. Screening of cucumber rootstocks resistant to *Meloidogyne incognita*[J]. China Vegetables, 2006(2): 5. DOI:10.3969/j.issn.1000-6346.2006.02.002.

35. Dong, D.F., Cao, Z.P., Wang, X.H., et al. Effects of root-knot nematode-resistant rootstocks on growth and yield of tomato[J]. Acta Horticulturae Sinica, 2007, 34(5): 4. DOI:10.3321/j.issn:0513-353x.2007.05.041.

36. Chen, Z.D., Wang, P.S., Zhou, Y., et al. Effects of different rootstocks grafting on tomato yield, quality and control effect of *Meloidogyne incognita*[J]. China Vegetables, 2012(20): 83–87.

37. Jia, S.S. Identification of resistance of tomato rootstocks to *Meloidogyne incognita* and studies on resistance mechanism[D]. Shandong Agricultural University, 2012. DOI:10.7666/d.y2117201.

38. Jin, G.L., Wang, F., Huo, Y.M., et al. Screening of cucurbit rootstocks resistant to root-knot nematode[J]. Shandong Agricultural Sciences, 2010(5): 89–91.

39. Wang, B.J., Wu, Z.H. Research progress on vegetable grafting seedling techniques[J]. Hans Journal of Agricultural Sciences, 2018, 8(1): 6. DOI:10.12677/HJAS.2018.81009.

40. Zheng, Q., Song, W.H. Research progress of vegetable grafting techniques at home and abroad (I)[J]. Yangtze Vegetables, 2000. DOI:CNKI:SUN:CJSC.0.2000-08-000.

41. Zheng, Q., Song, W.H. Research progress of vegetable grafting

techniques at home and abroad (II)[J]. Yangtze Vegetables, 2000. DOI:CNKI:SUN:CJSC.0.2000-09-000.

42. Li, M.X., Fan, J. Research status and development trend of vegetable grafting techniques[J]. 2023.

43. Xing, G.M., Kang, X.P., Ji, Q.Y., et al. Research progress on grafting cultivation of solanaceous vegetables[J]. Journal of Shenyang Agricultural University, 2000(1): 144–146. DOI:10.3969/j.issn.1000-1700.2000.01.041.

44. Liu, G., Yang, X.P., Xu, J.H., et al. Current status and development trend of cucurbit grafting rootstock breeding[C]//The 7th Yangtze River Delta Horticultural Forum. 2013.

45. Liu, A.H. Grafting techniques for horticultural crops[J]. New Agricultural Technology, 2006(3): 2. DOI:CNKI:SUN:BJNK.0.2006-03-048.

46. Wang, Y.H., Huang, Y.P. Cucurbit grafting seedling techniques[J]. Ningbo Agricultural Science and Technology, 2006(4): 22–24.

47. Li, H.J. Improving vegetable quality and yield by using vegetable grafting techniques[J]. Henan Agriculture, 2008(21).

48. Bie, Z.L. Current status, problems and countermeasures of cucurbit grafting seedling production in China[J]. Yangtze Vegetables, 2009(4): 1–5. DOI:10.3865/j.issn.1001-3547(x).2009.02.001.

49. Huang, J. Analysis of key links in grafting cultivation management of melons and vegetables and their effects on yield and quality[J]. Farmers' Guide to Wealth, 2025(29).

50. Lu, Y.H. Effects of different pumpkin rootstocks on growth, fruit quality

and disease resistance of grafted cucumber[D]. Shandong Agricultural University, 2024.

51. Wang, H.Y., Wang, Y., Wang, J., et al. Effects of grafting on disease resistance, stress resistance and fruit quality of calabash[J]. Journal of Nuclear Agricultural Sciences, 2025, 39(1): 191–200. DOI:10.11869/j.issn.1000-8551.2025.01.0191.

52. Zhu, Y.Q., Ding, J.T., Zhang, P., et al. Effects of different grafting combinations on growth and quality of mini cucumber[J]. Journal of Zhejiang Agricultural Sciences, 2024, 65(5): 1025–1030.

53. Han, X.Y., Huang, Q.W., Xiao, R.S., et al. Effects of different rootstocks grafting on pepper quality and yield[J]. Yangtze Vegetables, 2014(10): 2. DOI:10.3865/j.issn.1001-3547.2014.10.011.

54. Tao, M.Q., Zhou, G., Yao, C.Y., et al. Effects of rootstock types on growth, quality and yield of grafted cucumber[J]. Yangtze Vegetables, 2018(2): 6. DOI:CNKI:SUN:CJSC.0.2018-02-021.

55. Su, S.W., Chen, X.Z., Zhou, Y.H., et al. Effects of different pumpkin rootstock varieties on growth and yield of grafted cucumber[J]. Vegetables, 2018(2): 4. DOI:CNKI:SUN:SCZZ.0.2018-02-004.

56. Wang, M.Z., Wang, K.L. Effects of different rootstock varieties with double-cut root grafting on growth of watermelon seedlings[J]. Vegetables, 2015(8): 2. DOI:CNKI:SUN:SCZZ.0.2015-08-007.

57. Chen, Y.G., Lv, W.J., et al. Effects of different rootstocks on quality and yield of grafted cucumber[J]. Journal of Anhui Agricultural Sciences, 2017, 45(4):

4. DOI:10.13989/j.cnki.0517-6611.2017.04.010.

58. Zhang, Y.X., Pang, Q.Y., Ren, M., et al. Effects of different rootstocks grafting on fruit yield and quality of line pepper[J]. Acta Agriculturae Boreali-Occidentalis Sinica, 2018, 27(11): 8. DOI:10.7606/j.issn.1004-1389.2018.11.010.

59. Lin, Y.S., Chen, Y. Effects of different loofah rootstocks grafting on yield, quality and disease resistance of bitter melon[J]. China Vegetables, 2024(7).

60. Li, D., Fan, S.J., He, X.Y., et al. Effects of different rootstocks grafting on tomato resistance and fruit quality[J]. Yangtze Vegetables, 2024(10): 52–55. DOI:10.3865/j.issn.1001-3547.2024.10.015.

61. Li, L.Z., Gu, B.Q., Gao, T.Y. Effects of different rootstocks grafting on growth, quality and comprehensive field disease resistance of tomato[J]. Vegetables, 2021(10): 5.

62. Zhu, N., Yu, J.S., Qi, C.H., et al. Effects of different rootstock types on peel of grafted cucumber fruit[J]. Vegetables, 2018(11): 5. DOI:CNKI:SUN:SCZZ.0.2018-11-003.

63. Chu, Z.S., Chen, H.L., Wu, Z., Liu, M.C. Effects of double rootstocks grafting on growth, yield and quality of greenhouse cucumber[J]. China Vegetables, 2010(8): 14–20.

64. Zhang, J.W., Nie, C.H., Zhang, S.H. Ten advantages of vegetable grafting[J]. Rural Science and Technology Development, 2000. DOI:CNKI:SUN:NCKF.0.2000-04-017.

65. Qin, D., Li, G., Lu, F., et al. Screening and application of thin-skin melon grafting rootstocks[J]. Yangtze Vegetables, 2017(2): 4. DOI:10.3865/j.issn.1001-

3547.2017.02.022.

66. Wang, Y.K., Li, Y., Hu, X.H., et al. Effects of different rootstocks grafting on tomato quality and economic benefit[J]. Yangtze Vegetables, 2007(10): 2. DOI:10.3865/j.issn.1001-3547.2007.10.027.

67. Zhou, C.Y. Comparative study on new protected vegetable varieties and grafting rootstocks[D]. Shandong Agricultural University, 2006. DOI:10.7666/d.y903706.

68. Bie, Z.L. New international trends of vegetable grafting and discussion on several issues of vegetable grafting development in China: Enlightenment from "2011 International Conference on Vegetable Grafting"[J]. China Vegetables, 2012(6): 1–4.

69. Zang, J.C., Luo, W.D., Meng, Z.P., et al. Occurrence, damage and integrated control of watermelon fusarium wilt[J]. Plant Protection, 2001, 27(5): 43–44. DOI:10.3969/j.issn.0529-1542.2001.05.022.

70. Jin, Y.X., Xie, G.L., Sun, X.L., et al. Relationship between garlic rotation and fusarium wilt of cucurbits[J]. Journal of Shanghai Jiaotong University (Agricultural Science Edition), 2003, 21(1): 4. DOI:10.3969/j.issn.1671-9964.2003.01.003.

71. She, X.M., He, Z.F., Luo, F.F., et al. Fusarium wilt of cucurbits and its integrated control techniques[J]. Guangdong Agricultural Sciences, 2011, 38(2): 4. DOI:10.3969/j.issn.1004-874X.2011.02.034.

72. Shen, W.Y. Biological characteristics of four special forms of fusarium wilt pathogen of cucurbits and studies on biological control of fusarium wilt of

cucurbits[D]. Sichuan Agricultural University, 2012.

73. Shi, F.H., Dai, M.F. Causes and prevention of fusarium wilt in grafted seedless watermelon[J]. Modern Agricultural Science and Technology, 2004(10): 11.

74. Li, X.P. Preliminary study on control techniques of watermelon fusarium wilt[J]. Green World, 2010.

75. Han, J.X., Hong, R.X., Zhou, L., et al. Research progress on fusarium wilt of watermelon, cucumber, melon and other cucurbits[J]. China Cucurbits and Vegetables, 2009, 22(2): 4. DOI:10.3969/j.issn.1673-2871.2009.02.012.

76. Li, M.Y., Li, X.H., Huang, J.B., et al. Fusarium wilt of cucurbits and its control[J]. China Vegetables, 2008(9): 4. DOI:CNKI:SUN:ZGSC.0.2008-09-026.

77. Yang, Z.J. Control of fusarium wilt of cucurbits[J]. China Cucurbits and Vegetables, 2003(6): 40. DOI:10.3969/j.issn.1673-2871.2003.06.021.

78. Wu, X.L. Occurrence and control of fusarium wilt of cucurbits[J]. Northern Horticulture, 2003. DOI:CNKI:SUN:BFYY.0.2003-05-035.

79. Tian, C.Q. Characteristics and control measures of fusarium wilt of cucurbits[J]. Sichuan Agricultural Science and Technology, 2002(9): 1. DOI:10.3969/j.issn.1004-1028.2002.09.037.

80. Hu, L.H. Control of fusarium wilt of cucurbits[J]. Rural Practical Science and Technology Information, 2002(8): 1. DOI:CNKI:SUN:NCXX.0.2002-08-046.

81. Sun, Y., Sun, S.M. Integrated control of fusarium wilt of cucurbits[J]. Hebei Agriculture, 2015(5): 1. DOI:CNKI:SUN:HBLI.0.2015-05-012.

82. Jin, Y.L., Guo, L.M. Research progress on fusarium wilt of cucurbits[J]. Vegetables, 2023(1): 26–29.

83. Du, X.L., Tan, H.M. Occurrence and control of root-knot nematode disease of cucurbits[C]//Chinese Society for Horticultural Science. 2009.

84. Qiao, Y.C., Lin, J.Y., Xie, W.P., et al. Research progress on fusarium wilt of cucurbits[J]. Subtropical Plant Science, 2013, 42(3): 272–278.

85. Oumouloud, A., Otmani, M.E., Rouhou, H.C., et al. Breeding melon for resistance to Fusarium wilt: recent developments[J]. Euphytica, 2013, 192: 155–169.

86. Wang, Q., Lin, L. Research progress on fusarium wilt of cucurbits[J]. China Cucurbits and Vegetables, 2016, 29(3): 6. DOI:10.3969/j.issn.1673-2871.2016.03.001.

87. Wang, J.T. Control of fusarium wilt of cucurbits[J]. Yunnan Agriculture, 1994(6): 26–27. DOI:CNKI:SUN:YNNY.0.1994-06-035.

88. Xiao, R.F., Liu, B., Chen, L., et al. Isolation, identification and distribution of fusarium wilt pathogen of cucurbits in plants[C]//Academic Annual Conference of Chinese Society of Plant Protection, 2009.

89. Zhang, S. Physiological differentiation of three fusarium wilt pathogens (*Fusarium oxysporum* Schl.) of cucurbits and differential expression of pathogenic gene *FochsV*[D]. Shenyang Agricultural University, 2013.

90. Shen, W.Y. Biological characteristics of four special forms of fusarium wilt pathogen of cucurbits and studies on biological control of fusarium wilt of cucurbits[D]. Sichuan Agricultural University, 2012.

91. Yao, H. Screening and characteristic analysis of high-efficiency antagonistic actinomycetes against melon fusarium wilt[D]. Jilin Agricultural University, 2014.

92. Qiao, S.W. Isolation, identification and related characteristics of an antagonistic bacterium against cucumber fusarium wilt[D]. Nanjing Agricultural University, 2010. DOI:10.7666/d.Y1763041.

93. Dai, H.X. Fusarium wilt of cucurbits and its control techniques[J]. Shanghai Vegetables, 1997(4): 1. DOI:CNKI:SUN:SHSC.0.1997-04-028.

94. Man, H. Beware of fusarium wilt of cucurbits[J]. Hebei Agriculture, 2012(5): 2. DOI:CNKI:SUN:HBLI.0.2012-05-022.

95. Lv, G.Y., Guo, S.G., Zhang, H.Y., et al. Expressed sequence tag analysis of incompatible interaction between watermelon and fusarium wilt pathogen[J]. Scientia Agricultura Sinica, 2010, 43(9): 1883–1894.

96. Lv, G.Y., Zhang, H.Y., Guo, S.G., et al. Research progress on interaction mechanism between host plants and fusarium wilt pathogen[J]. China Vegetables, 2010(4): 1–7.

97. Ficcadenti, N., Sestili, S., Annibali, S., Campanelli, G., Belisario, A., Maccaroni, M., Corazza, L. Resistance to *Fusarium oxysporum* f. sp. *melonis* race 1,2 in muskmelon lines Nad-1 and Nad-2[J]. Plant Disease, 2002, 86(8): 897–900.

98. Han, J.X., Hong, R.X., Zhou, L., et al. Research progress on fusarium wilt of watermelon, cucumber, melon and other cucurbits[J]. China Cucurbits and Vegetables, 2009, 22(2): 32–35. DOI:10.3969/j.issn.1673-2871.2009.02.012.

99. Lin, L.L. Studies on cucumber fusarium wilt[J]. Agricultural Disaster Research, 2011(2): 7. DOI:CNKI:SUN:NZYJ.0.2011-02-010.

100. Zhou, X.L., Yang, X.J., Ding, G.J., et al. Chemical control experiment of melon fusarium wilt[J]. Shanghai Vegetables, 2007(6): 105–107.

DOI:10.3969/j.issn.1002-1469.2007.06.074.

101. Li, J. Screening of attenuated strains of cucumber fusarium wilt pathogen after treatment with celery root rot extract and mechanism of attenuation[D]. Inner Mongolia Agricultural University, 2014.

102. Sun, B.T. Diagnosis and control of three soil-borne diseases of bitter melon[J]. Farmers' Technology, 2007(5): 1. DOI:CNKI:SUN:NJKK.0.2007-05-018.

103. Zhang, S.P. Integrated control techniques of fusarium wilt in cucumber seed production fields[J]. Yangtze Vegetables, 2001(3): 29. DOI:10.3865/j.issn.1001-3547.2001.03.018.

104. Ding, L.T., Li, D.C., Xu, H.Y. Efficacy test of several formula fungicides on watermelon fusarium wilt[J]. Modern Horticulture, 2008(3): 2. DOI:CNKI:SUN:JXYA.0.2008-03-029.

105. Yi, J. Efficacy test of fungicides against melon fusarium wilt[J]. Contemporary Vegetables, 2006(6): 2. DOI:CNKI:SUN:NCFZ.0.2006-06-043.

106. Yang, K.K., Liu, X.H., Chen, C., et al. Research progress on cucumber fusarium wilt[J]. Hunan Agricultural Sciences, 2019(6): 121–124. DOI:10.16498/j.cnki.hnnykx.2019.006.032.

107. Wang, H.L. Monitoring the effect of cucumber root exudates on biomass of fusarium wilt pathogen in soil by real-time fluorescence quantitative PCR[J]. Journal of Shanghai Jiaotong University (Agricultural Science Edition), 2010(1): 5. DOI:10.3969/j.issn.1671-9964.2010.01.008.

108. Li, S.G. Biocontrol effects of two Trichoderma strains on cucumber fusarium wilt pathogen and their impacts on rhizosphere soil microorganisms[D].

Chinese Academy of Agricultural Sciences, 2010.

109. Zhang, L.J., Li, S.D., Miao, Z.Q. Changes in pathogenicity and population genetic structure of cabbage fusarium wilt pathogen in soil under continuous cropping[J]. Acta Phytopathologica Sinica, 2013, 43(1): 58–68. DOI:10.3969/j.issn.0412-0914.2013.01.008.

110. Zou, J., Li, H.P. Analysis of survival status of banana fusarium wilt pathogen in soil[C]//Academic Annual Conference of Chinese Society for Plant Pathology, 2016.

111. Zhang, L.J. Pathogenic variation and population genetic structure differentiation of cabbage fusarium wilt pathogen in continuous cropping soil[D]. Chinese Academy of Agricultural Sciences, 2012.

112. Lan, J.L., Su, M.X., Ge, C.B., et al. Correlation between distribution of *Fusarium oxysporum* and disease process of watermelon fusarium wilt[J]. Chinese Agricultural Science Bulletin, 2007, 23(12): 4. DOI:10.3969/j.issn.1000-6850.2007.12.066.

113. Huang, F.L. Identification of antagonistic bacteria against cucumber fusarium wilt and their effects on soil microecology[D]. Zhejiang A&F University, 2013.

114. Li, D., Qin, W.Y., Liu, Z.P., et al. Allelopathic effects of watermelon root exudates on watermelon fusarium wilt pathogen and its biocontrol bacteria[C]//Academic Annual Conference of Chinese Society for Plant Pathology, 2017.

115. Zhang, W., Liu, B.Y., Gai, Z.S., et al. Biological characteristics of

cucumber fusarium wilt pathogen[J]. Shandong Agricultural Sciences, 2011(10): 70–73.

116. Huang, X.Q. Changes in pathogenicity of cucumber fusarium wilt pathogen in continuous cropping soil and transcriptome analysis of strong and weak pathogenic strains[D]. Chinese Academy of Agricultural Sciences, 2018. DOI:CNKI:CDMD:1.1018.151855.

117. Liu, X., Li, Z.W., Liu, L. Analysis of occurrence regularity and control measures of melon fusarium wilt[J]. Vegetables, 2010(12): 2. DOI:10.3969/j.issn.1001-8336.2010.12.015.

118. Ju, X.X., Huang, R.K., Huang, X.J., et al. Research progress on genetic breeding for resistance to fusarium wilt of cucurbits[J]. Chinese Journal of Tropical Agriculture, 2022, 42(4): 33–38. DOI:10.12008/j.issn.1009-2196.2022.04.006.

119. Ling, N., Wang, Q.J., Yang, X.M., et al. Control of watermelon fusarium wilt in continuous cropping by rhizosphere application of microbial organic fertilizer[J]. Plant Nutrition and Fertilizer Science, 2009, 15(5): 1136–1141. DOI:10.3321/j.issn:1008-505X.2009.05.022.

120. Ma, G.B., Lin, D.P., Wang, Y.J., et al. Preliminary study on mechanism of fusaric acid from watermelon fusarium wilt pathogen on watermelon seedlings[J]. Acta Phytopathologica Sinica, 2000. DOI:CNKI:SUN:ZWBL.0.2000-04-017.

121. Hao, X.J., Liu, B., Xie, G.L. Research progress on biological control of plant fusarium wilt[J]. Chinese Agricultural Science Bulletin, 2005, 21(7): 5. DOI:10.3969/j.issn.1000-6850.2005.07.095.

122. Xu, W.H., Zhou, Y., Wu, F.Z. Research progress on watermelon fusarium

wilt[J]. China Vegetables, 2013. DOI:CNKI:SUN:ZGSC.0.2013-08-004.

123. Jin, Y.X., Xie, G.L. Research progress on control of fusarium wilt of cucurbits[J]. Plant Protection, 2002, 28(6): 3. DOI:10.3969/j.issn.0529-1542.2002.06.014.

124. Zhang, Z.Z., Lv, L.X., Huang, B.Q., et al. Research progress on control techniques of watermelon fusarium wilt[J]. China Vegetables, 2005(7): 3. DOI:10.3969/j.issn.1000-6346.2005.07.017.

125. Liu, S.T., Liu, X.J., Liu, J.X., Guo, Y., Gao, Y., Zhao, W., Gao, M.L., Yuan, C.Z. Research progress on breeding for resistance to fusarium wilt in cucurbit crops[J]. 2025.

126. Chu, X.P. Screening of tomato fusarium wilt-resistant rootstocks and mechanism of disease resistance by grafting[D]. Hebei Agricultural University, 2020.

127. Chen, Z.D. Identification, genetic diversity of bitter melon fusarium wilt pathogen and differential proteins in host-pathogen interaction[D]. Guangxi University, 2014. DOI:10.7666/d.Y2888245.

128. Wang, G.C., Ye, Q.M. Role of *Fusarium* in biological control[C]//Proceedings of the 3rd National Symposium on Mycology and Lichenology. Beijing: Mycological Society of China, Botanical Society of China, 1990: 204.

129. Zhao, H., Peng, D.L., Zhu, J.L. Research status of root-knot nematodes[J]. Plant Protection, 2003, 29(6): 6–9. DOI:10.3969/j.issn.0529-1542.2003.06.002.

130. Sun, Y.D., Wang, X.J. Occurrence characteristics and integrated control

techniques of root-knot nematode disease in vegetable fields[J]. China Vegetables, 1996. DOI:CNKI:SUN:ZGSC.0.1996-06-012.

131. Wang, L.F., Yang, B.J., Li, C.D. Research progress on biological control of root-knot nematodes[J]. Journal of Nanjing Forestry University (Natural Sciences Edition), 2002, 26(1): 5. DOI:10.3969/j.issn.1000-2006.2002.01.016.

132. Liu, W.Z. Plant Pathogenic Nematology. Beijing: China Agriculture Press, 2000.

133. Zhu, M.L., Li, T.F., Zhang, K.Q., et al. Overview and progress of biocontrol resources for root-knot nematodes[J]. Microbiology China, 2004, 31(1): 100–104. DOI:10.3969/j.issn.0253-2654.2004.01.023.

134. Cao, A.C., Guo, M.X. Control techniques of root-knot nematodes in soil[J]. China Vegetables, 2002(6): 60–61. DOI:10.3969/j.issn.1000-6346.2002.06.034.

135. Lei, J.C., Huang, H.Q. Research progress on biological control of *Meloidogyne incognita*[J]. Chinese Journal of Biological Control, 2007(S1): 6. DOI:CNKI:SUN:ZSWF.0.2007-S1-016.

136. Lu, X.J., Liao, X.L., Cheng, F.X., et al. Research progress on biological control of root-knot nematodes[J]. Chinese Journal of Agricultural Science and Technology, 2010(4): 5. DOI:10.3969/j.issn.1008-0864.2010.04.09.

137. Zhang, B., Wang, H.L., Mu, L.Y. Occurrence and control of vegetable root-knot nematodes[J]. Agrochemicals, 2002, 43(9): 11. DOI:10.3969/j.issn.1006-0413.2002.09.002.

138. Kong, X.Y., Chen, M.C. Research progress on control of root-knot

nematode disease[J]. Chinese Journal of Tropical Agriculture, 2006, 26(2): 6. DOI:10.3969/j.issn.1009-2196.2006.02.021.

139. Zhang, S.S. Diagnosis and Management of Plant Nematode Diseases. Fuzhou: Fujian Science and Technology Press, 1999.

140. Jin, N., Liu, Q., Jian, H. New advances in biological control of plant parasitic nematodes[J]. Chinese Journal of Biological Control, 2015, 31(5): 789–800. DOI:10.16409/j.cnki.2095-039x.2015.05.019.

141. Wu, C.Q., Yang, Z.M., Wu, C.J., et al. Research progress on damage and control mechanism of root-knot nematodes in protected vegetables[J]. Northern Horticulture, 2018(11): 164–172.

142. Li, R., Li, H.X., Xie, B.Y., et al. Mechanism of *Trichoderma longibrachiatum* strain TL16 against *Meloidogyne incognita*[J]. Journal of Plant Protection, 2020, 47(2): 384–393. DOI:10.13802/j.cnki.zwbhxb.2020.2019109.

143. Dang, J.H. Identification and control of root-knot nematodes in protected tomato and fig in Kunyu City[MS Thesis]. Alar: Tarim University, 2021.

144. Chen, Z.J., Zhang, S.L., Zhang, F. Basis and Technology for Control of Root-Knot Nematodes in Protected Vegetables. Beijing: Science Press, 2013.

145. Wang, L.F., Yang, B.J., Li, C.D. Investigation of root-knot nematodes in East China[J]. Forest Research, 2001, 14(5): 484–489. DOI:10.3321/j.issn:1001-1498.2001.05.004.

146. Walters, S.A., Wehner, T.C., Barker, K.R. Root-knot nematode resistance in cucumber and horned cucumber[J]. HortScience, 1993, 28(2): 151–154.

147. Peng, D.L. Integrated management of vegetable diseases and pests (10):

Occurrence and control of vegetable nematode diseases[J]. China Vegetables, 1998(4): 57–58.

148. Moens, M., Perry, R.N., Starr, J.L. *Meloidogyne* species: a diverse group of novel and important plant parasites[M]//Perry, R.N., Moens, M., Starr, J.L. Root-Knot Nematodes. Wallingford: CABI Publishing, 2009: 1–117.

149. Jin, N. Production technology of *Streptomyces roseogriseus* HDZ-9-47 and its effect on soil biological community[PhD Thesis]. Beijing: China Agricultural University, 2016.

150. Zhao, H.H. Species identification of root-knot nematodes in parts of China and intraspecific morphological variation of the four most common species[J]. Acta Phytopathologica Sinica, 2000, 30(3): 288. DOI:10.1038/sj.cr.7290036.

151. Zhang, Y., Zheng, J.Q., Shi, Y.C., Chen, L.W., Wang, Z.J., Shen, G.Y., Cui, X.Y., Shi, G.R., He, Q., Jian, H., Xiao, C.T. Screening of tomato varieties resistant to root-knot nematode[J]. China Vegetables, 2006(10): 23–24.

152. Liu, D.W., Sun, M.M., Liu, X.J., Wu, H.Y. Evaluation of resistance of different pepper varieties to *Meloidogyne incognita*[J]. China Vegetables, 2015(10): 42–44.

153. Peng, D.L., Tang, W.H. Research progress on *Mi* gene for resistance to root-knot nematode in tomato[J]. Journal of Shenyang Agricultural University, 2001, 32(3): 220–223.

154. Niu, J.H., Guo, Y.D., Jian, H. Research progress on genomics of plant root-knot nematodes[C]//Proceedings of the 2009 Academic Annual Conference of the Chinese Society for Plant Pathology, 2009.

DOI:ConferenceArticle/5aa03126c095d72220697112.

155. Van Der Vossen, E.A.G., Rouppe Van Der Voort, J.N.A.M., Kanyuka, K., Bendahmane, A., Sandbrink, H., Baulcombe, D.C., Bakker, J., Stiekema, W.J., Klein-Lankhorst, R.M. Homologues of a single resistance-gene cluster in potato confer resistance to distinct pathogens: a virus and a nematode[J]. The Plant Journal, 2000, 23: 567–576.

156. Bakker, E., Butterbach, P., Rouppe van der Voort, J., van der Vossen, E., van Vliet, J., Bakker, J., Goverse, A. Genetic and physical mapping of homologues of the virus resistance gene *Rx1* and the cyst nematode resistance gene *Gpa2* in potato[J]. Theoretical and Applied Genetics, 2003, 107(8): 1524–1531.

157. Louws, F.J., Rivard, C.L., Kubota, C. Grafting fruiting vegetables to manage soilborne pathogens, foliar pathogens, arthropods and weeds[J]. Scientia Horticulturae, 2010, 127(2): 127–146.

158. Jin, G.L., Wang, F., Huo, Y.M., et al. Screening of cucurbit rootstocks resistant to root-knot nematode[J]. Shandong Agricultural Sciences, 2010(5): 89–91. DOI:10.3969/j.issn.1001-4942.2010.05.028.

159. Izuogu, N.B., Oyedunmade, E.E.A., Babatola, J.O. Screenhouse assessment of reaction of fluted pumpkin, *Telfairia occidentalis* Hook f. to root-knot nematode *Meloidogyne incognita*[J]. Journal of Agricultural Science, 2010, 2(3): 169.

160. Liu, B., Ren, J.J., Zhang, Y., An, J.B., Chen, M.Y., Chen, H.M., Xu, C., Ren, H.Z. A new grafted rootstock against root-knot nematode for cucumber, melon, and watermelon[J]. Agronomy for Sustainable Development, 2015: 251–259.

161. Liu, H.L., Zheng, L.M., Liu, Q.Q., et al. Transcriptome research of non-model organisms[J]. Hereditas, 2013, 35(8): 955–970.

162. Sun, H.B., Lv, G.Y., Xu, Y., et al. Transcriptomic analysis of incompatible interaction between watermelon and fusarium wilt pathogen[J]. China Cucurbits and Vegetables, 2019, 32(8): 1. DOI:CNKI:SUN:ZGXG.0.2019-08-058.

163. Kou, Q.H., Liang, Z.H., Wang, Z.W., Xiao, G.H., Liu, J.X. Research progress on physiological race identification and disease-resistant breeding of watermelon fusarium wilt pathogen[J]. China Vegetables, 2012(14): 9–17.

164. Mao, Z.C., Xie, B.Y., Yang, Z.W., et al. Molecular interaction between root-knot nematodes and plants[J]. Acta Horticulturae Sinica, 2006, 33(4): 7. DOI:10.3321/j.issn:0513-353X.2006.04.052.

165. Li, K. Screening of watermelon and melon rootstock resources resistant to *Meloidogyne incognita* and transcriptomic analysis of their resistance response[D]. Chinese Academy of Agricultural Sciences, 2016.

166. Zhu, C.X., Liao, W.M., Liu, J.P., et al. Genome-wide identification of *MATE* gene family in cucumber and their expression analysis in response to root-knot nematode and powdery mildew infection[J]. Acta Agriculturae Universitatis Jiangxiensis, 2022, 44(2): 1–12. DOI:10.13836/j.jjau.2022034.

167. Wang, X., Cheng, C.Y., Zhang, K.J., et al. Transcriptomic study on resistance to *Meloidogyne incognita* in cucumber[C]//Manual of the 8th Cucumber Academic Symposium and New Variety Exhibition of Chinese Society for Horticultural Science, 2018.

168. Li, H.Y. Transcriptomic study on two types of black-seed pumpkin in

response to fusarium wilt pathogen infection[D]. Yunnan Agricultural University, 2022.

SECTION 2

OBJECTIVES AND CONTENTS

2.1. Research Objectives

Pumpkin (Cucurbita moschata (Duchesne ex Lam.) Duchesne ex Poir.) is one of the most widely used grafting rootstocks for cucurbit crops and has been extensively applied in protected cultivation[1].

Fusarium wilt and root-knot nematode (RKN) are extremely destructive soil-borne diseases of cucurbits. They can survive in soil for several years and have become major constraints limiting the development of the protected vegetable industry. Due to the difficulties in eradication, no fully effective control method is currently available. Breeding resistant germplasm and rootstocks is the most economical, effective, and environmentally friendly strategy for managing cucurbit fusarium wilt and Meloidogyne incognita.

Isolating and identifying resistance genes to fusarium wilt and RKN in cucurbit germplasm, then introducing them into cultivated cucurbit varieties via transgenic technology to directionally breed new cultivars with stably inherited resistance, can greatly shorten the breeding cycle, representing a novel approach in crop breeding in recent years[2].

With the deepening understanding of plant resistance mechanisms to fusarium wilt and RKN, as well as the clarification of molecular mechanisms underlying pathogen-host interactions, progress has been made in screening resistant germplasm and applying resistant rootstocks in grafting[3-5]. However, the number of resistant germplasm resources identified so far remains limited, and they are far

from being applied in production to reduce losses caused by fusarium wilt and RKN.

Benefiting from the rapid development of bioinformatics, transcriptome sequencing combined with bioinformatic analysis can reveal the resistance and regulatory mechanisms of resistant materials to cucurbit fusarium wilt and M. incognita, laying a foundation for further dissecting resistance mechanisms and mining resistance genes[6].

2.2. Research Contents

In this study, 24 pumpkin hybrid combinations and 12 parental lines were used as materials to evaluate their resistance to cucurbit fusarium wilt and root-knot nematode. Highly resistant pumpkin hybrid combinations were screened as potential rootstocks, providing a reference for grafted cultivation in production.

Transcriptome sequencing and differentially expressed gene (DEG) analysis were performed on the resistant parent Hetou a2 and susceptible parent Lingchuan C1 using the Illumina NovaSeq6000 high-throughput sequencing platform. Several DEGs closely related to resistance to fusarium wilt and RKN were identified, preliminarily revealing the molecular mechanism of pumpkin resistance to these two diseases, and providing a basis for subsequent functional verification.

Conclusions to section 2

Pumpkin is an important grafting rootstock for cucurbits. Fusarium wilt and root-knot nematode are soil-borne diseases that severely restrict protected cucurbit production. Breeding disease-resistant rootstocks is an economical and efficient control strategy.

At present, disease-resistant germplasm resources are scarce and the resistance mechanisms remain unclear. Mining resistance genes and dissecting disease resistance mechanisms via transcriptomics and bioinformatics are of great significance for accelerating resistance breeding.

In this study, 24 pumpkin hybrid combinations and 12 parental lines were used to screen elite rootstocks with comprehensive resistance to cucurbit fusarium wilt and root-knot nematode. The resistant parent Hetou a2 and susceptible parent Lingchuan C1 were selected for high-throughput transcriptome sequencing to analyze differentially expressed genes, which preliminarily clarified the molecular basis of pumpkin resistance to fusarium wilt and root-knot nematode. The results provide a theoretical foundation for further mining and functional verification of disease resistance genes.

References to section 2

1. Wang, M.M. Functional and mechanistic analysis of cold resistance genes CmRCC1 and CmHVA22 in pumpkin rootstocks[D]. Huazhong Agricultural University, 2021.

2. Ding, Y.M. Response mechanism of Cucurbita ficifolia to fusarium wilt infection and screening of NBS-type resistance genes[D]. Southwest University, 2026.

3. Wang, F.T., Zhao, F.S., Qiao, K.B., et al. Research progress on molecular mechanisms of rootstock-scion interaction in vegetable grafting[J]. Biotechnology Bulletin, 2024, 40(10). DOI:10.13560/j.cnki.biotech.bull.1985.2024-0284.

4. Zhao, R.Z. Transcriptomic analysis of resistance response to Meloidogyne incognita and control by red light induction in watermelon[D]. Chinese Academy of Agricultural Sciences, 2026. DOI:CNKI:CDMD:2.1018.160788.

5. Bao, W.X. Comprehensive evaluation of melon rootstock germplasm for resistance to fusarium wilt and Meloidogyne incognita[D]. Guangxi University, 2026. DOI:10.7666/d.Y3276382.

6. Li, K. Screening of watermelon and melon rootstock resources resistant to Meloidogyne incognita and transcriptomic analysis of their resistance response[D]. Chinese Academy of Agricultural Sciences, 2016.

SECTION 3

SCREENING OF PUMPKIN ROOTSTOCKS AND RESISTANT/SUSCEPTIBLE PARENTS FOR RESISTANCE TO *FUSARIUM* WILT AND ROOT-KNOT NEMATODE

With the rapid development of the cucurbit vegetable industry, specialized and intensive cultivation in various regions has caused serious problems of continuous cropping obstacles. In particular, the incidence of soil-borne diseases of cucurbits has increased year by year, resulting in severe production losses.

Cucurbit fusarium wilt, also known as blight disease, occurs from the seedling stage to the adult plant stage. After infection by fusarium wilt fungi, the most intuitive phenotypic change is plant morphological alteration. At the seedling stage, infected plants show wilting of the apex, wilting and drooping of cotyledons and true leaves, browning and rot at the base of stems and vines, leading to damping-off of seedlings[1]. The pathogen can survive in soil for several years and overwinter on seeds, making it extremely difficult to eradicate.

Root-knot nematodes (Meloidogyne spp.) are plant-parasitic nematodes with a wide host range and high damage, and have become one of the major constraints limiting the development of the protected vegetable industry, causing billions of dollars in economic losses worldwide annually. At present, there is no complete solution to fusarium wilt and root-knot nematode. In production, screening rootstocks resistant to fusarium wilt and root-knot nematode to reduce the damage caused by these pathogens can not only save a lot of labor and material resources,

but also reduce vegetable product pollution caused by chemical control.

In this experiment, 24 pumpkin hybrid combinations and 12 pumpkin parents were used as materials to evaluate their resistance to fusarium wilt and root-knot nematode. Highly resistant pumpkin hybrid rootstocks and parents were screened, providing a reference for the selection of resistant varieties to cucurbit fusarium wilt and root-knot nematode in practical production.

3.1. Materials and Methods

3.1.1 Materials

A total of 24 pumpkin hybrid combinations (rootstocks) and 12 pumpkin parents were provided by the Pumpkin Research Group, College of Horticulture and Landscape Architecture, Henan Institute of Science and Technology. 24 pumpkin hybrid combinations (rootstocks): Hetou a2 × 041-1, Yanbian-3 × Lingchuan C1, Yanbian-3 × 360-3, Hetou a2 × 360-3, Yanbian-4 × Lingchuan C1, Yanbian-2 × 041-1, 360-3 × 041-1, Renhe-1 × 041-1, 041-1 × Xingtai, Yanbian-4 × 041-1, Xingtai × Lingchuan C1, Xingtai × Yanbian-4, 041-1 × Hetou a2, Xingtai × 487, Xingtai × 041-1, Hetou a2 × Lingchuan C1, Lingchuan C1 × 360-3, Lingchuan C1 × Xingtai, Hetou a2 × 112-2, Zhangzhou × 041, Renhe-1 × 360-3, Yanbian-4 × 360-3, 360-3 × 487, Renhe-1 × Lingchuan C1. 12 pumpkin parents: 041-1, 112-2, 360-3, 487, Renhe-1, Hetou a2, Yanbian-3, Xingtai-23, Lingchuan C1, Fangshan, Wan 95-24, Daziwang-24. Fungus: Fusarium oxysporum f. sp. cucumerinum; Nematode: Meloidogyne incognita. Both were provided by the Institute of Vegetables and

Flowers, Chinese Academy of Agricultural Sciences.

The experiment was conducted in the solar greenhouse (east campus) and the Physiology and Biochemistry Laboratory of the College of Horticulture and Landscape Architecture, Henan Institute of Science and Technology, from August 2023 to December 2024.

3.1.2 Methods

3.1.2.1 Seedling Preparation

Uniform and plump seeds were selected and disinfected in hot water at 55 °C for 10 min with constant stirring. After the water temperature cooled to room temperature, the seeds were soaked for 8 h.

The soaked seeds were spread evenly on wet towels, wrapped, and placed in a 28 °C incubator for germination. After approximately 24 h, when the radicles reached 2–3 mm in length, the seeds were sown in plug trays filled with mixed substrate previously sterilized with carbendazim.

Seedlings were grown in a greenhouse at about 28 °C and used for inoculation when two cotyledons were fully expanded and the first true leaf emerged.

3.1.2.2 Preparation of Fusarium Wilt Inoculum

The pathogen strain was retrieved from the stock culture, inoculated onto potato dextrose agar (PDA) slants, and activated at 28 °C. After mycelial growth, a small agar block was transferred to a PDA plate and cultured at 28 °C for 8–10 days.

The spores were washed off with sterile water, and the suspension was filtered through three layers of sterile gauze to remove mycelia. Spore concentration was determined using a hemocytometer under a microscope with three replicates.

The spore density was calculated as: average spores per grid × 4×10^6 per mL. The spore suspension was adjusted to 1×10^7 spores/mL with sterile distilled water for inoculation.

Fusarium Wilt Inoculation Method. Seedling root-dipping method was used for artificial inoculation. Roots of pumpkin seedlings were rinsed with water, slightly wounded at the root tips, and dipped in the prepared spore suspension for 30 min. Seedlings were then transplanted into plastic pots filled with nursery substrate. Each material included 3 biological replicates, with 20 plants per replicate (60 plants total). A control group was included with 10 plants per material treated with sterile water only.

During the first week after inoculation, plants were watered 1–2 times daily to maintain soil moisture. The greenhouse temperature was maintained at 23–30 °C and relative humidity at 60%–80%[2].

Measurement of Experimental Indicators.

Growth and Physiological Indicators. At 10, 20, and 30 days after inoculation (DAI), plant height, stem diameter, chlorophyll content, and leaf number were measured in inoculated and control plants. Plant height: distance from soil surface to apical meristem, measured with a ruler. Stem diameter: measured at half the distance between the stem base and cotyledons using a vernier caliper. Chlorophyll content: SPAD value of the second true leaf from the base, measured with a portable chlorophyll meter (SPAD-502). Each treatment was performed in triplicate, with three plants per replicate, and the relative growth of pumpkin materials was calculated (1).

$$Relative\ growth\ rate = (value\ of\ inoculated\ plants / value\ of\ control\ plants) \times 100\% \quad (1)$$

(2) Antioxidant Enzyme Activities and MDA Content. At 30 DAI, the second true leaf from the base was sampled to measure the activities of superoxide dismutase (SOD), peroxidase (POD), catalase (CAT), and malondialdehyde (MDA) content. Three replicates were used per material, with three plants per replicate. Activities of SOD, POD, CAT and MDA content were determined according to Li et al.[3].

Fresh leaf samples (0.5 g) were ground in an ice bath with 1 mL pre-cooled phosphate buffer, then buffer was added to a final volume of 5 mL. The homogenate was centrifuged at 3000 rpm for 10 min, and the supernatant was used as the crude enzyme extract. SOD activity: NBT method, absorbance at 560 nm. POD activity: guaiacol method, absorbance at 470 nm. CAT activity: potassium permanganate titration method. MDA content: thiobarbituric acid (TBA) method. 0.5 g leaf tissue was homogenized in 5 mL 5% trichloroacetic acid (TCA) and centrifuged at 3000 rpm for 10 min. 2 mL supernatant was mixed with 2 mL 0.67% TBA, heated in a 100 °C water bath for 30 min, cooled, and centrifuged again. Absorbance was measured at 450 nm, 532 nm, and 600 nm.

(3) Root Morphological Indicators. At 30 DAI, three plants per material were randomly selected. Roots were washed gently with tap water and placed in a root scanning tray (EPSON Perfection 4990 PHOTO). Root images were analyzed using WinRHIZO Pro 2007 to determine total root length, total projected area, root surface area, average root diameter, total root volume, and number of root tips.

(4) Soluble Sugar Content. Anthrone-acetic acid reagent was prepared by

dissolving 2 g of anthrone in 100 mL ethyl acetate and stored in the dark. A 0.3 g leaf sample (second true leaf) was extracted twice in 10 mL distilled water in a boiling water bath for 30 min each. The extract was filtered into a 25 mL volumetric flask and diluted to volume. Sucrose standard solutions (0, 20, 40, 60, 80, 100 μg/L) were prepared. 0.5 mL of standard or sample solution was mixed with 1.5 mL distilled water, 0.5 mL anthrone reagent, and 5 mL concentrated sulfuric acid. After mixing, the mixture was incubated in a boiling water bath for 1 min, cooled to room temperature, and absorbance was measured at 630 nm. Soluble sugar content was calculated based on the standard curve.

(5) Soluble Protein Content. Coomassie Brilliant Blue G-250 reagent was prepared and stored in the dark. Standard protein solutions (20, 40, 60, 80, 100 μg/mL) were prepared. A 0.2 g leaf sample was homogenized in 5 mL distilled water and centrifuged at 10000 rpm at 4 °C for 10 min. 1 mL supernatant was mixed with 5 mL Coomassie brilliant blue reagent and incubated for 2 min. Absorbance was measured at 595 nm. Soluble protein content was calculated using the standard curve.

(6) Disease Resistance Indexes. Disease incidence was investigated at 10, 20, and 30 DAI. Leaf symptoms were graded and recorded. At 30 DAI, stems were dissected, and vascular discoloration was scored. Leaf disease grading was performed according to Luo et al.[4] (Table 3.1). Stem-dissection disease grading was performed according to Zhang[2] (Table 3.2). Resistance evaluation was classified according to Luo et al.[4] (Table 3.3). Disease incidence (2) and disease index (3) were calculated according to Guo et al.[5].

$$Disease\ incidence\ (\%) = (number\ of\ diseased\ plants / total\ number\ of\ plants) \times 100\% \quad (2)$$

$$Disease\ index\ (DI)\ = \frac{\sum(disease\ grade \times number\ of\ plants\ in\ that\ grade)}{(highest\ disease\ grade \times total\ number\ of\ plants)} \times\ 100\% \quad (3)$$

Table 3.1 Leaf Grading Standard for Fusarium Wilt

Grade	Symptoms of plant diseases
0	No symptoms;
1	1–2 cotyledons slightly yellowed, normal growth;
2	1–2 cotyledons yellowed or necrotic; true leaves slightly yellowed and wilted;
3	Cotyledons dead; true leaves obviously wilted; growth inhibited and slight dwarfing;
4	Whole plant severely wilted, leaves yellow and dry;
5	Plant dead or lodged.

Table 3.2 Stem-dissection Grading Standard for Fusarium Wilt

Grade	Symptoms of plant diseases
0	Vascular bundle without discoloration;
1	Discolored area ≤ 1/4 of total;
2	Discolored area 1/4–1/2 of total;
3	Discolored area 1/2–2/3 of total;
4	Plant dead.

Table 3.3 Resistance Evaluation Standard for Fusarium Wilt

Resistance	DI range
High Resistant (HR)	0＜DI≤15.0
Resistant (R)	15.0＜DI≤35.0
Moderately Resistant (MR)	35.0＜DI≤55.0
Susceptible (S)	55.0＜DI≤75.0
High Susceptible (HS)	DI＞75.0

3.1.2.3 Hatching of Root-Knot Nematode Second-Stage Juveniles

Egg masses of root-knot nematode were placed on two layers of gauze in a Petri dish containing sterile water, and incubated at 28 °C in a growth chamber for 3–5 d. Sterile water below the sieve was collected every 1 d to obtain second-stage juveniles (J2).

Inoculation Method for Root-Knot Nematode. Root-zone punching was used for inoculation. The collected J2 suspension was inoculated onto the roots of pumpkin seedlings, with 500 J2s per plant. Each material included 3 biological replicates, with 20 plants per replicate (60 plants total). A control group was included with 10 plants per material. Plants were carefully uprooted 60 d after inoculation to investigate root damage[6,7,8,9,10].

Measurement of Experimental Indicators.

(1) Growth indicators. At 35 d after inoculation with root-knot nematode, plant height, stem diameter, chlorophyll content (SPAD-502), and leaf number were measured in inoculated and control plants. Three replicates were used per material, with three plants per replicate. Each treatment was performed in triplicate, with three

plants per replicate, and the relative growth of pumpkin materials was calculated (4).

$$Relative\ growth\ rate = (value\ of\ inoculated\ plants / value\ of\ control\ plants) \times 100\% \quad (4)$$

(2) Physiological indicators. (3) Root morphological indicators. (4) Soluble sugar content. (5) Soluble protein content. All were determined as described in 3.1.2.2.

(6) Disease resistance indicators. Root gall grading was performed according to Zhang[11] (Table 3.4), Gall index (GI) (5), egg granule index (EI) (6), reproduction frequency (RF) (7), and disease index (DI) (8) were calculated using the integrated method of Boiteox & Charchar[12] and Liu[13], using the following formulas:

$$Root\ nodule\ index(GI) = \frac{number\ of\ root\ nodules\ of\ a\ single\ pumpkin\ rootstock}{fresh\ weight\ of\ roots\ of\ a\ single\ pumpkin\ rootstock} \quad (5)$$

$$Egg\ Index(EI) = \frac{number\ of\ eggs\ in\ the\ root\ system\ of\ a\ single\ pumpkin\ rootstock}{fresh\ weight\ of\ the\ root\ system\ of\ a\ single\ pumpkin\ rootstock} \quad (6)$$

$$Nematode\ reproduction\ coefficient(RF) = \frac{number\ of\ eggs\ in\ the\ root\ system\ of\ a\ single\ pumpkin\ rootstock}{inoculation\ amount\ of\ a\ single\ pumpkin\ rootstock} \quad (7)$$

$$Disease\ index(DI) = \frac{\sum(number\ of\ diseased\ pumpkin\ rootstocks\ at\ all\ levels)\times(the\ disease\ level)}{(investigate\ the\ total\ number\ of\ pumpkin\ rootstock\times highest\ disease\ level)} \times 100\% \quad (8)$$

(7) Subordinate function values after nematode infection. Subordinate function values were calculated according to Song et al.[14]. Subordinate function values for growth indices of pumpkin materials were calculated according to Formula (9), and those for disease resistance indices of pumpkin rootstocks according to Formula (10). A higher subordinate function value indicates stronger resistance to Meloidogyne incognita.

$$X(\mu) = (X - X_{min})/(X_{max} - X_{min}) \quad (9)$$

$$X(\mu) = 1 - (X - X_{min})/(X_{max} - X_{min}) \quad (10)$$

Where:

X = each index of pumpkin materials;

Xmax = maximum value of the index;

Xmin = minimum value of the index.

Table 3.4 Root Gall Grading Standard

Grade	Symptoms of plant diseases
0	No galls in the whole root system;
1	Galls indistinct, accounting for 1%–5% of the total root area;
2	Galls accounting for 6%–25% of the total root area;
3	Galls accounting for 26%–50% of the total root area;
4	Galls accounting for 51%–75% of the total root area;
5	Galls covering more than 75% of the total root area.

3.1.3 Data Processing

Experimental data were analyzed and averaged using Excel 2003. Analysis of variance (ANOVA) and cluster analysis were performed using SPSS 27, and cluster analysis was conducted using the Euclidean distance method.

3.2 Results and Analysis

3.2.1 Effects of Fusarium oxysporum Infection on Growth Indicators of Pumpkin

Relative growth can reflect the resistance level of pumpkin to fusarium wilt. Higher relative growth indicates weaker inhibition by fusarium wilt and stronger resistance, and vice versa.

At the early stage (Figure 3.1-A1), Xingtai×Yanbian-4 was significantly higher than other hybrid combinations in plant height. 360-3×487 was significantly higher

in stem diameter. Lingchuan C1×Xingtai was significantly higher in chlorophyll content. Renhe-1×041-1 was significantly higher in leaf number. At the middle stage (Figure 3.1-A2), 360-3×487 and Zhangzhou×041 were significantly higher in plant height. Xingtai×487 was significantly higher in stem diameter. Lingchuan C1×360-3 was significantly higher in chlorophyll content. Renhe-1×Lingchuan C1 was significantly higher in leaf number. At the late stage(Figure 3.1-A3), Hetou a2×112-2 was significantly higher in plant height. Lingchuan C1×360-3, Hetou a2×Lingchuan C1, and Xingtai×041-1 were significantly higher in stem diameter. Lingchuan C1×360-3 was significantly higher in chlorophyll content. Hetou a2×Lingchuan C1 was significantly higher in leaf number.

At the early stage (Figure 3.1-B1), Xingtai-23 was significantly higher than other parents in plant height. Renhe-1 and 112-2 were significantly higher in stem diameter. Yanbian-3 and 112-2 were significantly higher in chlorophyll content. Renhe-1 was significantly higher in leaf number. At the middle stage (Figure 3.1-B2), Renhe-1 was significantly higher in plant height. 112-2 was significantly higher in stem diameter. Wan 95-24 and Hetou a2 were significantly higher in chlorophyll content. Yanbian-3 was significantly higher in leaf number. At the late stage(Figure 3.1-B3), Xingtai-23 was significantly higher in plant height. Yanbian-3 was significantly higher in stem diameter. Renhe-1 was significantly higher in chlorophyll content. Daziwang-24 and 360-3 were significantly higher in leaf number.

According to the coefficient of variation (Table 3.5), for pumpkin hybrids, the coefficient of variation for leaf number was the largest at 10 d and 20 d (13.23% and

10.93%, respectively). At 30 d, chlorophyll content showed the largest coefficient of variation (12.17%), and leaf number was the second (10.92%). For pumpkin parents, chlorophyll content showed the largest coefficient of variation at all three stages (8.14%, 11.19%, and 9.93%, respectively). The coefficient of variation for stem diameter was the lowest in both hybrids and parents at all stages, indicating that stem diameter was less affected by pathogen infection.

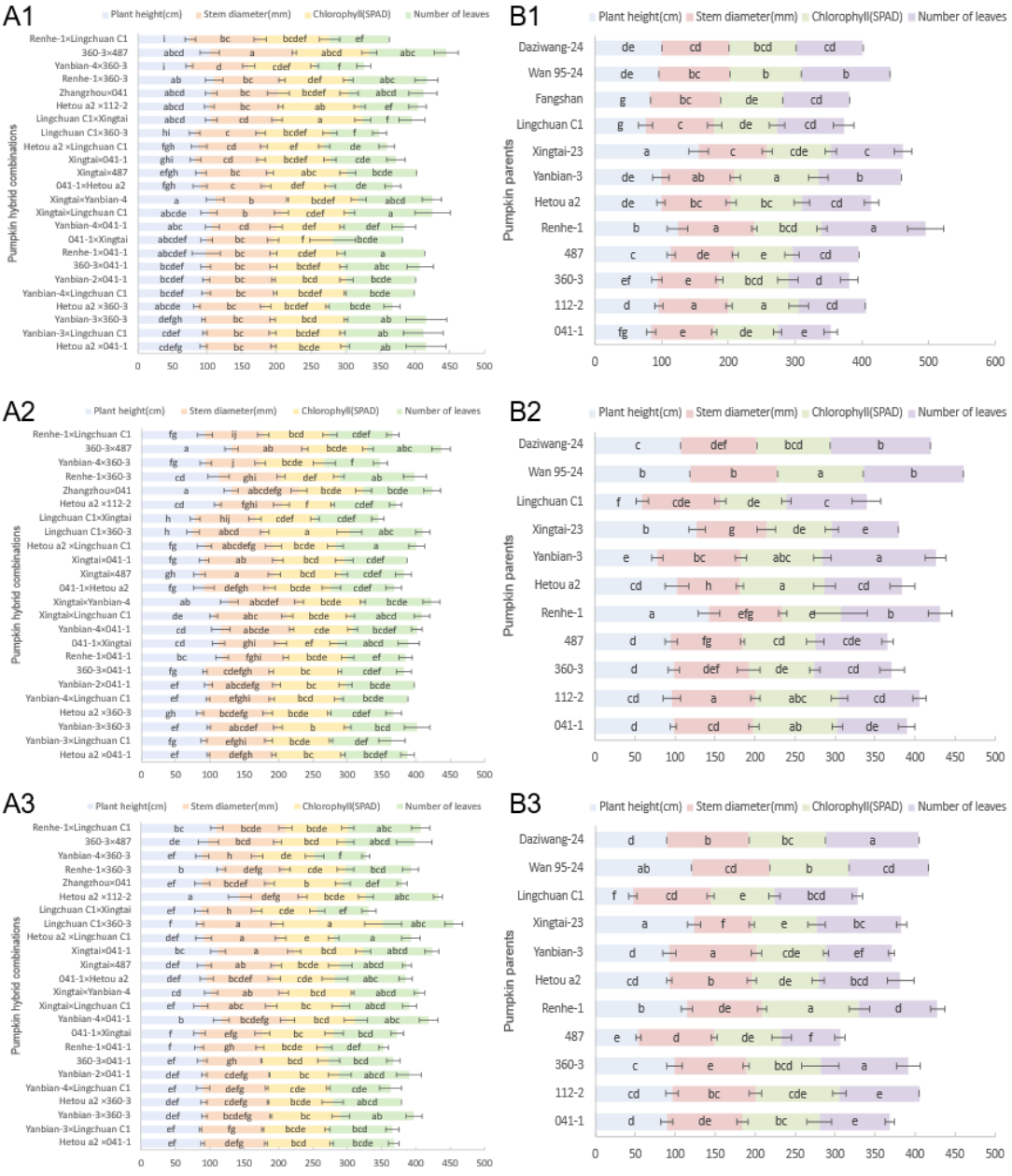

Figure 3.1. Growth and physiological indicators of pumpkin materials at 10,

20, and 30 d after inoculation with Fusarium oxysporum.

(A1, A2, A3) Pumpkin hybrids; (B1, B2, B3) Pumpkin parents.

Table 3.5 Coefficients of variation of relative growth of pumpkin after Fusarium oxysporum infection

Pumpkin Materials	Coefficient of Variation / %			
	Plant Height	Stem Diameter	Chlorophyll	Leaf Number
Hybrids 10 d	8.94	6.32	8.85	13.23
Hybrids 20d	7.67	7.08	8.50	10.93
Hybrids 30d	8.76	6.35	12.17	10.92
Parents 10 d	6.98	4.71	8.14	6.83
Parents 20 d	7.76	6.09	11.19	8.96
Parents 30 d	6.20	4.57	9.93	6.56

3.2.2 Effects of Fusarium oxysporum Infection on Resistance Indicators of Pumpkin

Disease incidence and disease index were calculated after inoculation. 30 days after inoculation, among the 24 pumpkin hybrid combinations (Figure 3.2-A), Yanbian-3×360-3, Yanbian-2×041-1, 041-1×Xingtai, 041-1×Hetou a2, and 360-3×487 were classified as moderately resistant (MR). Their leaf disease indices were 52.67, 54.67, 48.67, 48.67, and 53.33, and stem-dissection disease indices were 37.92, 45.83, 52.92, 47.50, and 5.00, respectively. Yanbian-3×Lingchuan C1, Hetou a2×360-3, Yanbian-4×Lingchuan C1, 360-3×041-1, and Lingchuan C1×360-3 were classified as susceptible (S). Their leaf disease indices were 83.00, 83.33, 80.00, 82.67, and 71.33, and stem-dissection disease indices were 59.58, 74.58, 62.92, 67.92, and 59.17, respectively. Hetou a2×041-1 was classified as highly susceptible (HS), with a leaf disease index of 95.33 and a stem-dissection disease index of 87.92.

30 days after inoculation, among the 12 pumpkin parents (Figure 3.2-B),

Renhe-1 and Hetou a2 were classified as moderately resistant (MR). Their leaf disease indices were 44.67 and 51.33, and stem-dissection disease indices were 48.75 and 33.33, respectively. 112-2, Lingchuan C1, and Daziwang-24 were classified as susceptible (S). Their leaf disease indices were 64.67, 64.67, and 60.00, and stem-dissection disease indices were 72.08, 72.08, and 75.00, respectively. Fangshan was classified as highly susceptible (HS), with a leaf disease index of 100.00 and a stem-dissection disease index of 100.00.

Comprehensive analysis showed that there were significant differences between the disease index, resistance classification, and growth performance of the tested materials, indicating that good plant growth could not directly reflect strong disease resistance.

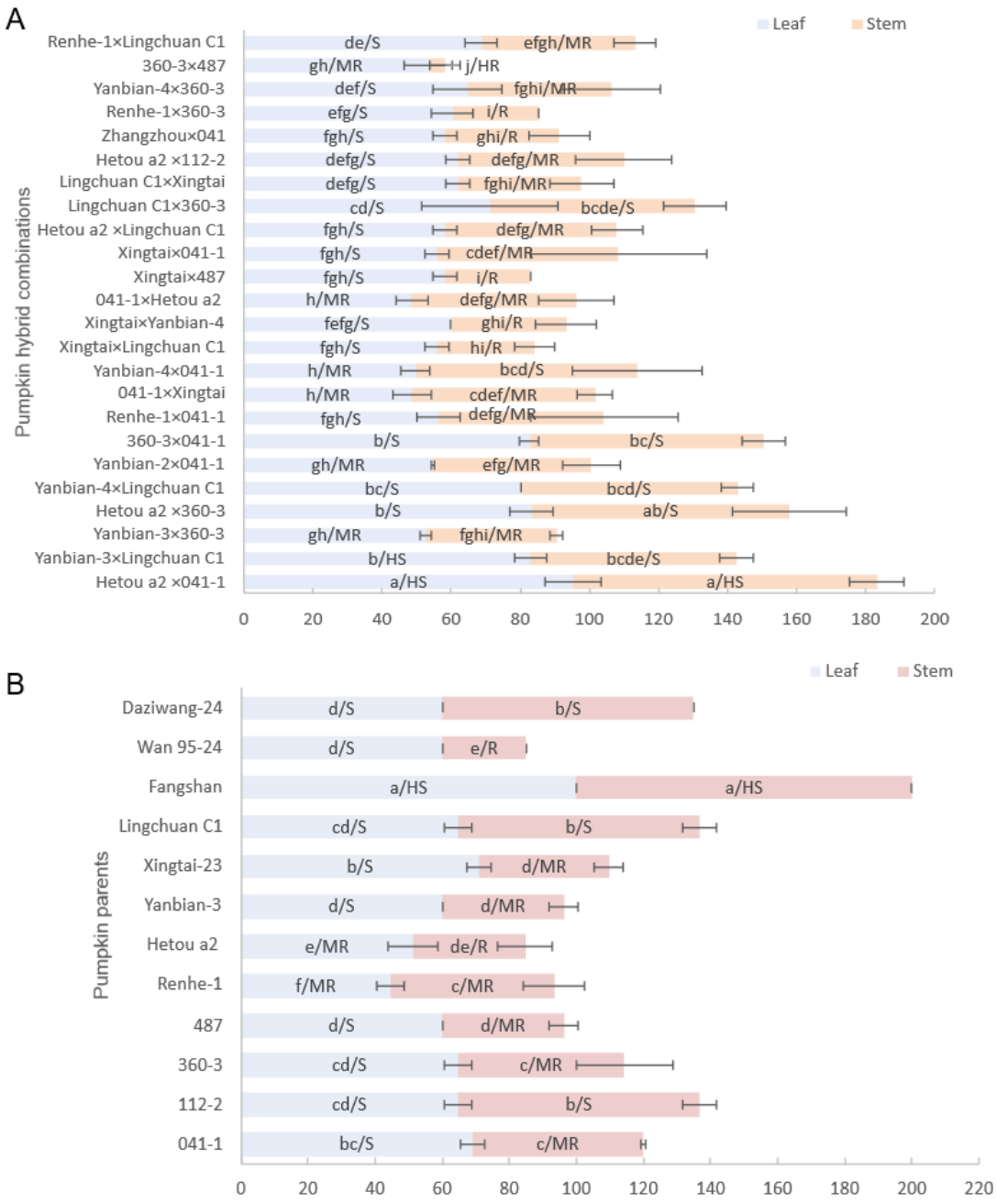

Figure 3.2. Disease index and resistance grades of pumpkin materials at 30 d after inoculation with *Fusarium oxysporum*.

(A) Pumpkin hybrids; (B) Pumpkin parents.

Note: In resistance grades, HR = highly resistant, MR = moderately resistant, S = susceptible, HS = highly susceptible.

3.2.3 Effects of Root-Knot Nematode Infection on Growth Indicators of Pumpkin Rootstock Hybrids

Relative growth reflects the resistance of pumpkin rootstock hybrids to root-knot nematode. Higher relative growth indicates weaker inhibition by nematodes and stronger resistance, and vice versa.

Xingtai×041-1 and Yanbian-4×041-1 were significantly higher than other hybrids in plant height. Yanbian-4×041-1 and Renhe-1×041-1 were significantly higher in stem diameter. No significant difference was observed in chlorophyll content among all hybrids. Xingtai×Lingchuan C1 was significantly higher in leaf number (Figure 3.3-A). Fangshan was significantly higher than other parents in plant height and chlorophyll content. 112-2 was significantly higher in stem diameter and leaf number (Figure 3.3-B).

According to the coefficient of variation (Table 3.6), chlorophyll showed the largest coefficient of variation in both hybrids (10.59%) and parents (19.67%). Stem diameter showed the smallest coefficient of variation (4.83% and 6.91%, respectively). These results indicate that chlorophyll was strongly affected by root-knot nematode infection, while stem diameter was less affected.

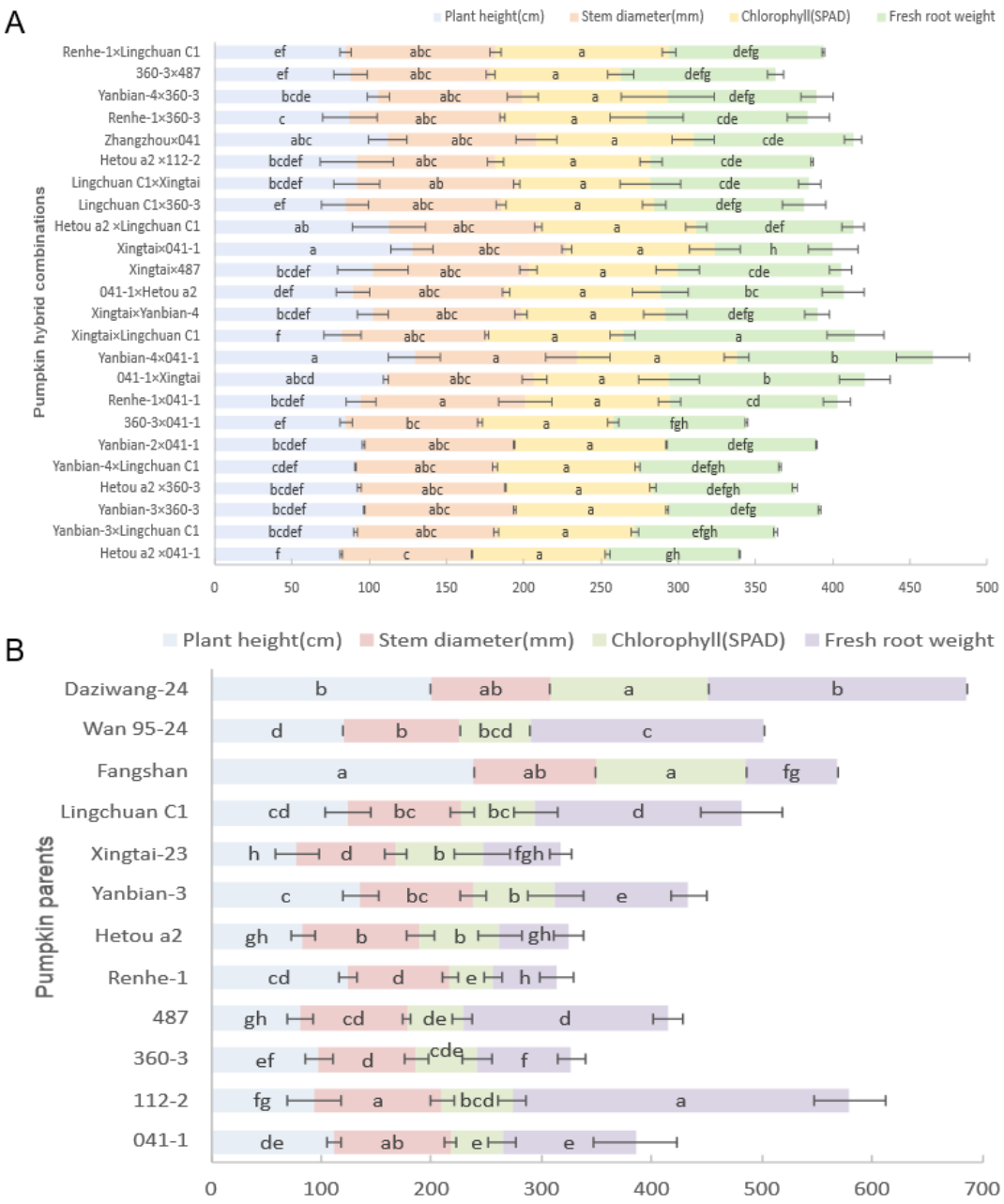

Figure 3.3. Growth and physiological indicators of pumpkin materials inoculated with root-knot nematode.

(A) Pumpkin hybrids; (B) Pumpkin parents.

Table 3.6 Coefficients of variation of relative growth of pumpkin after root-knot nematode infection

Pumpkin Materials	Coefficient of Variation / %			
	Plant Height	Stem Diameter	Chlorophyll	Root Fresh Weight
Hybrids	9.97	4.83	10.59	7.06
Parents	11.06	6.91	19.67	13.11

3.2.4 Effects of Root-Knot Nematode Infection on Resistance Indicators of Pumpkin Rootstock Hybrids

Resistance indicators reflect the resistance level of pumpkin rootstock hybrids to root-knot nematode. Higher values indicate lower resistance, and vice versa.

Yanbian-3×360-3 was significantly lower than other hybrids in all four resistance indicators. No significant differences were observed in egg index and reproduction factor between Yanbian-3×360-3, Hetou a2×112-2, and 360-3×487. No significant difference was observed in disease index between Yanbian-3×360-3 and Yanbian-2×041-1. Zhangzhou×041 was significantly higher than other hybrids in gall index. Hetou a2×041-1 and 360-3×041-1 were significantly higher in reproduction factor. Renhe-1×041-1, Xingtai×Lingchuan C1, and Xingtai×Yanbian-4 were significantly higher in disease index. Xingtai×041-1 was significantly higher in egg index (Figure 3.4-A1, 3.4--A2, 3.4- A3).

360-3 was significantly lower than other parents in all four resistance indicators, with no significant differences from Hetou a2 and Xingtai-23. No significant difference in disease index was observed between 360-3 and Renhe-1. Lingchuan C1 was significantly higher than other parents in disease index. 112-2 was significantly higher than other parents in gall index, egg index, and reproduction factor (Figure 3.4-B1, 3.4-B2, 3.4-B3).

According to the coefficient of variation (Table 3.7), gall index showed the largest coefficient of variation in both hybrids (23.72%) and parents (35.04%). Disease index showed the smallest coefficient of variation (4.29% and 20.16%, respectively). These results indicate that gall index is more effective for evaluating

the resistance of pumpkin rootstocks to root-knot nematode.

A1

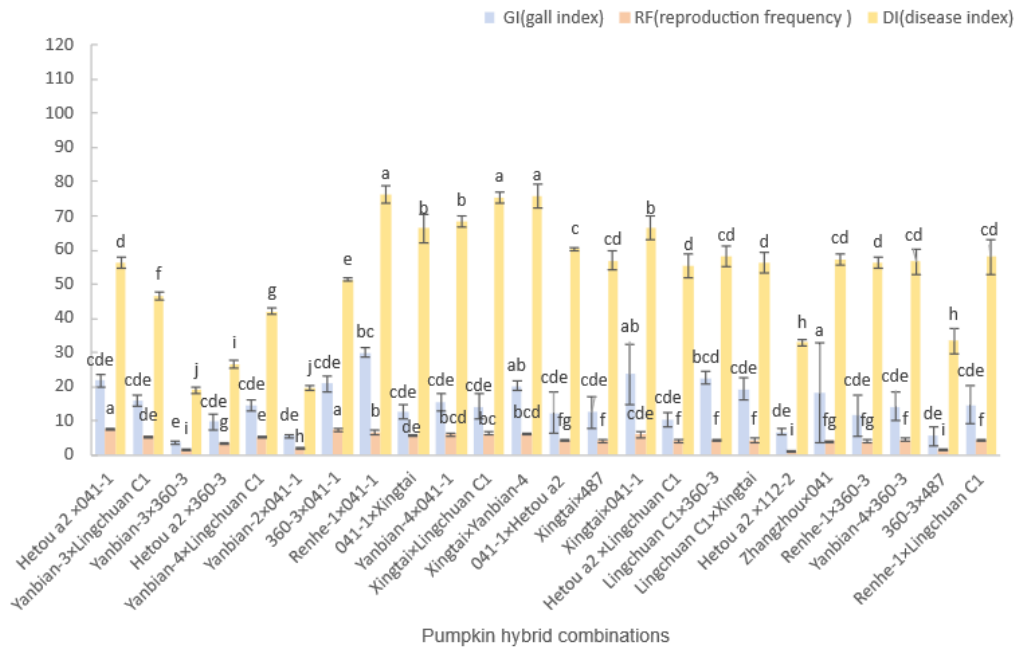

A2

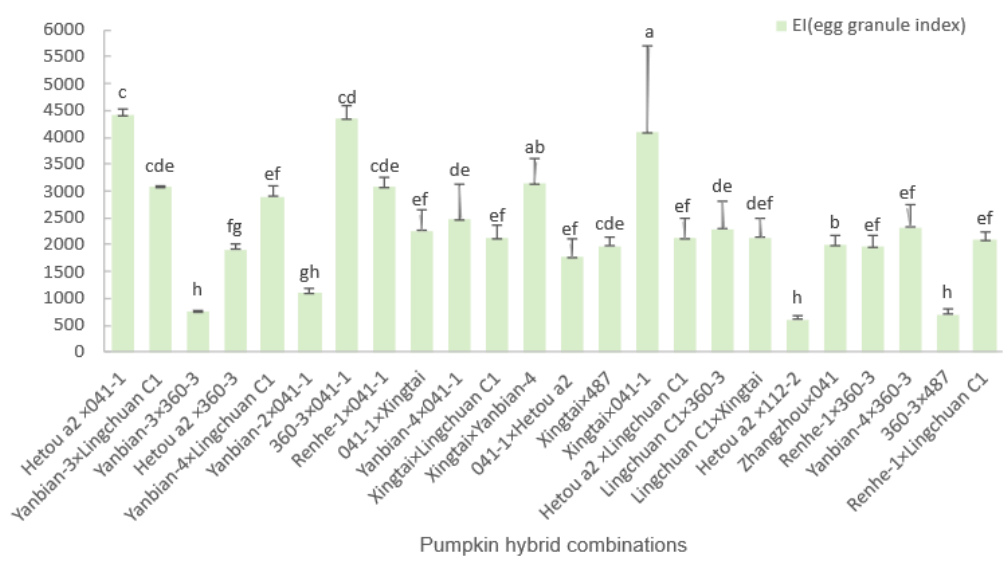

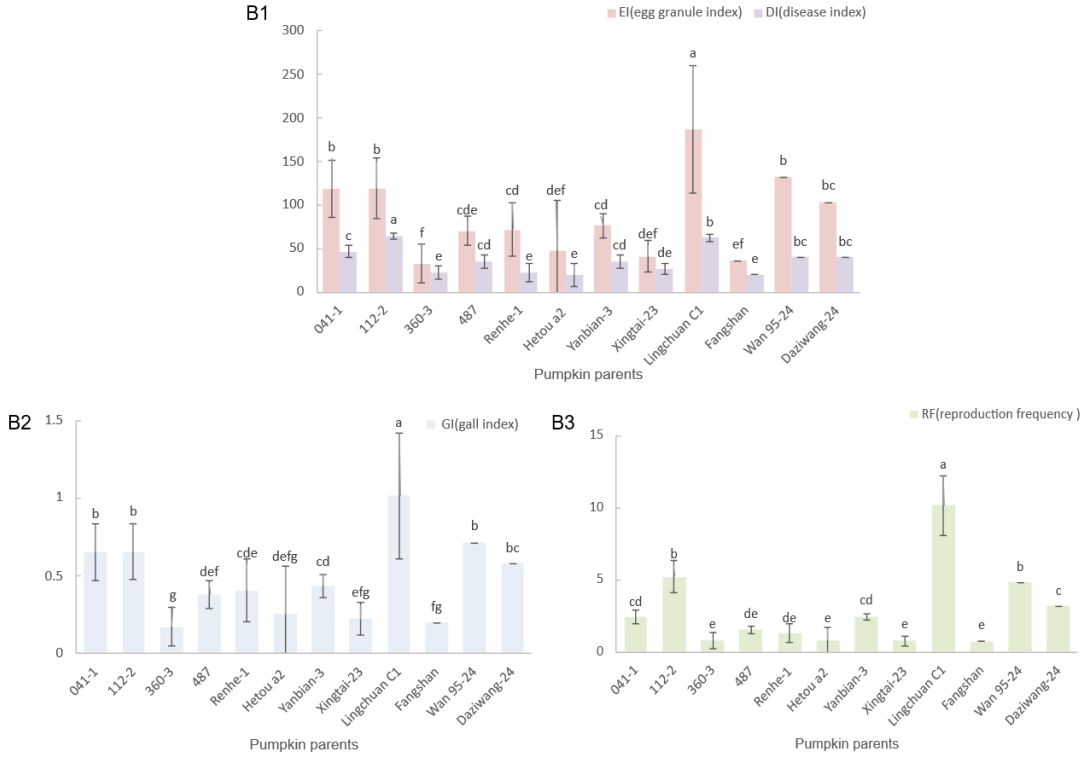

Figure 3.4. Resistance indicators of pumpkin materials inoculated with root-knot nematode.

(A1, A2) Pumpkin hybrids; (B1-B3) Pumpkin parents.

Table 3.7 Coefficients of variation of resistance indicators of pumpkin after root-knot nematode infection

Pumpkin Materials	Coefficient of Variation / %			
	Gall Index	Egg Index	Reproduction Factor	Disease Inde
Hybrids	23.72	12.52	8.11	4.29
Parents	35.04	34.70	30.43	20.16

3.2.5 Subordinate Function Values of Related Indicators of Pumpkin Infected by Root-Knot Nematode

Yanbian-3×360-3 had the largest total subordinate function value (7.10), while Xingtai×Yanbian-4 had the smallest (1.74) (Figure 3.5-A). Fangshan had the largest total subordinate function value (6.04), and Lingchuan C1 had the smallest (2.02) (Figure 3.5-B). These results indicated that the hybrid combination Yanbian-3×360-

3 and the parent line Fangshan exhibited the strongest resistance to root-knot nematode, whereas Xingtai×Yanbian-4 (hybrid) and Lingchuan C1 (parent) showed the weakest resistance.

Based on the total subordinate function values, the resistance order of pumpkin hybrids to root-knot nematode was: Yanbian-3×360-3 > Yanbian-2×041-1 > Hetou a2×360-3 > Hetou a2×112-2 > 360-3×487 > Yanbian-3×Lingchuan C1 > Yanbian-4×Lingchuan C1 > Hetou a2×041-1 > 360-3×041-1 > Hetou a2×Lingchuan C1 > Renhe-1×Lingchuan C1 > Xingtai×487 > Renhe-1×360-3 > Yanbian-4×041-1 > Yanbian-4×360-3 > 041-1×Hetou a2 > Lingchuan C1×360-3 > 041-1×Xingtai > Lingchuan C1×Xingtai > Zhangzhou×041 > Xingtai×Lingchuan C1 > Renhe-1×041-1 > Xingtai×041-1 > Xingtai×Yanbian-4.

The resistance order of pumpkin parents was: Fangshan > 360-3 > Xingtai-23 > Hetou a2 > Daziwang-24 > Yanbian-3 > Renhe-1 > 487 > 041-1 > Wan 95-24 > 112-2 > Lingchuan C1.

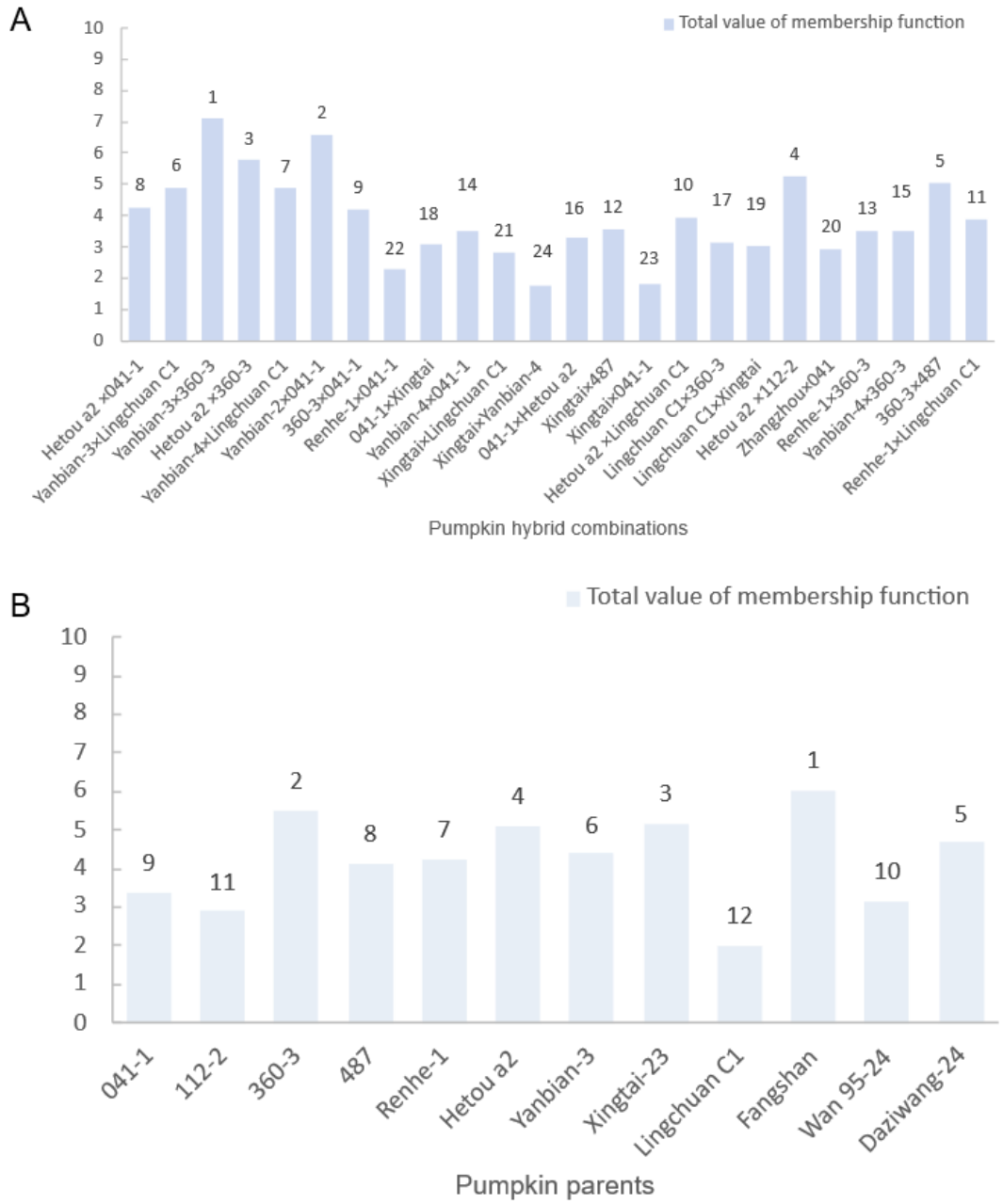

Figure 3.5. Subordinate function values of related indicators of pumpkin materials inoculated with root-knot nematode.

(A) Pumpkin hybrids; (B) Pumpkin parents.

3.2.6 Cluster Analysis of Resistance Indicators of Pumpkin Infected by Root-Knot Nematode

Cluster analysis was performed for pumpkin hybrid combinations based on the four resistance indicators (Figure 3.6-A1). At an Euclidean distance of 25, the

hybrids were divided into two groups: resistant and susceptible. The resistant group included: Hetou a2×360-3, Yanbian-2×041-1, Yanbian-3×360-3, 360-3×487, Hetou a2×112-2. Cluster analysis was performed based on gall index (which had the largest coefficient of variation) (Figure 3.6-A2). At an Euclidean distance of 25, hybrids were divided into resistant and susceptible groups, with Renhe-1×041-1 as the resistant combination. Cluster analysis based on egg index (Figure 3.6-A3) showed that at an Euclidean distance of 25, resistant group was Xingtai×041-1. Cluster analysis based on reproduction factor (Figure 3.6-A4) showed that at an Euclidean distance of 25, resistant hybrids included: Yanbian-2×041-1, Hetou a2×112-2, 360-3×487, Yanbian-3×360-3. Cluster analysis based on disease index (Figure 3.6-A5) showed that at an Euclidean distance of 25, resistant hybrids included: Hetou a2×360-3, 360-3×487, Hetou a2×112-2, Yanbian-2×041-1, Yanbian-3×360-3. These results indicated that the clustering result based on disease index was completely consistent with that based on the four resistance indicators, suggesting that disease index can accurately reflect the nematode resistance of pumpkin hybrids.

Cluster analysis was performed for pumpkin parents based on the four resistance indicators (Figure 3.6-B1). At an Euclidean distance of 25, parents were divided into resistant and susceptible groups. Resistant parents: 360-3, Fangshan, Hetou a2, Xingtai-23, 487, Yanbian-3, Renhe-1, 041-1, Daziwang-24, Wan 95-24, 112-2. Susceptible parent: Lingchuan C1. Cluster analyses based on gall index, egg index, and reproduction factor (Figure 3.6-B2, 3.6-B3, 3.6-B4) showed the same grouping at an Euclidean distance of 25. Cluster analysis based on disease index (Figure 3.6-B5) showed that at an Euclidean distance of 25, resistant parents: 360-3,

Fangshan, Hetou a2, Xingtai-23, 487, Yanbian-3, Renhe-1, 041-1, Daziwang-24, Wan 95-24. Susceptible parents: Lingchuan C1, 112-2. These results indicated that clustering results based on gall index, egg index, and reproduction factor were completely consistent with those based on the four resistance indicators. Although the result of disease index was not fully identical, Lingchuan C1 was always identified as susceptible, demonstrating that all four resistance indicators can reliably evaluate the nematode resistance of pumpkin parents.

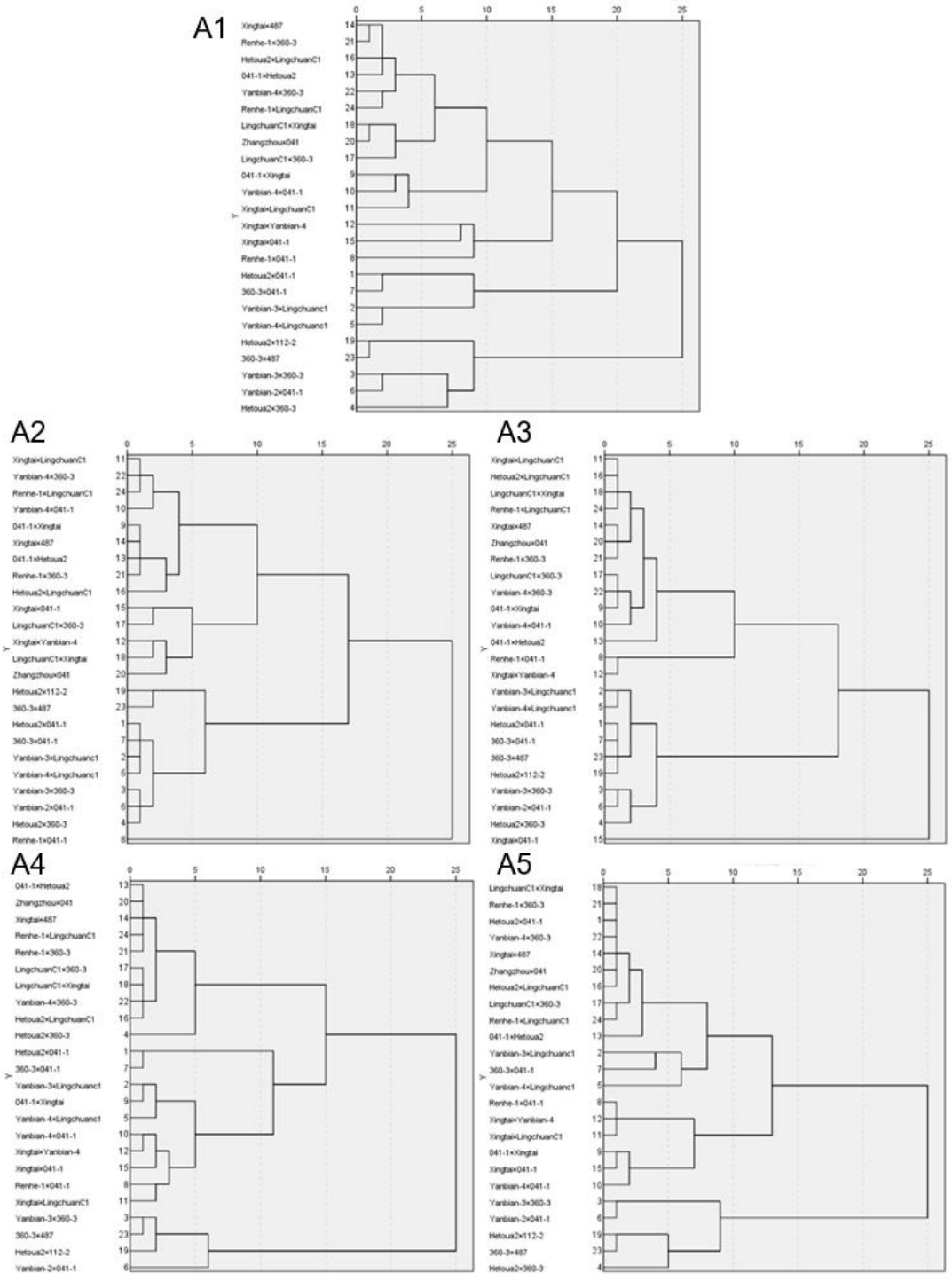
A1
Xingtai×487
Renhe-1×360-3
Hetoua2×LingchuanC1
041-1×Hetoua2
Yanbian-4×360-3
Renhe-1×LingchuanC1
LingchuanC1×Xingtai
Zhangzhou×041
LingchuanC1×360-3
041-1×Xingtai
Yanbian-4×041-1
Xingtai×LingchuanC1
Xingtai×Yanbian-4
Xingtai×041-1
Renhe-1×041-1
Hetoua2×041-1
360-3×041-1
Yanbian-3×Lingchuanc1
Yanbian-4×Lingchuanc1
Hetoua2×112-2
360-3×487
Yanbian-3×360-3
Yanbian-2×041-1
Hetoua2×360-3
A2
A3
A4
A5

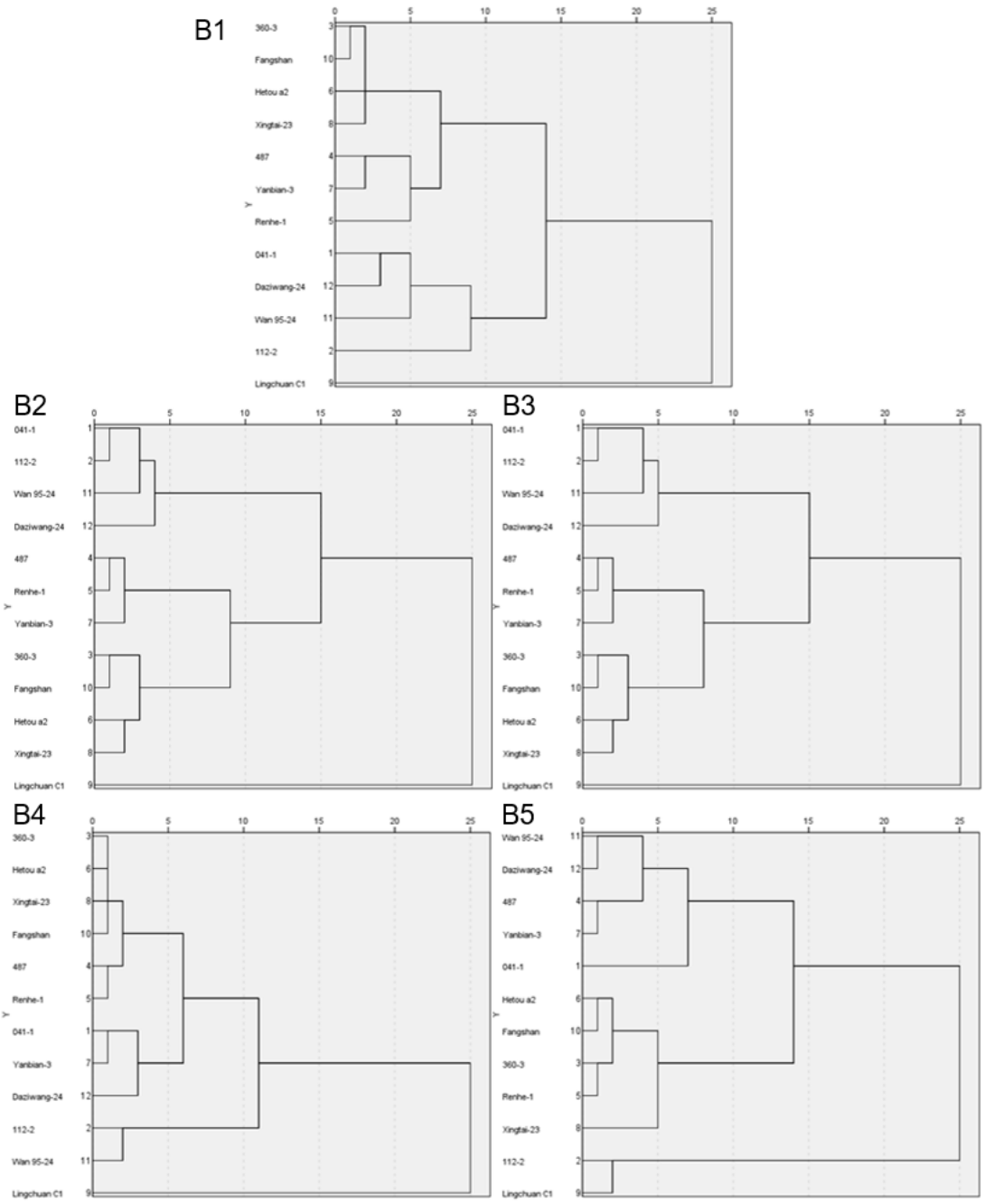

Figure 3.6. Subordinate function values of related indicators of pumpkin materials inoculated with root-knot nematode.

(A1-A5) Pumpkin hybrids; (B1-B5) Pumpkin parents.

3.2.7 Effects of Fusarium oxysporum and Root-Knot Nematode Infection on Antioxidant Enzyme Activities and MDA Content in Pumpkin Parents

Under *Fusarium oxysporum* infection (Figure 3.7-A), significant differences were observed in antioxidant enzyme activities and MDA content among different pumpkin parents. SOD and POD activities showed no significant differences among parents, indicating that they were not the core antioxidant enzymes in response to fusarium wilt stress. In contrast, Fangshan and Wan 95-24 exhibited significantly higher CAT activity than other parents, suggesting that they could alleviate cell damage caused by oxidative stress by efficiently scavenging H_2O_2. MDA content was significantly negatively correlated with antioxidant enzyme activities. Fangshan and Wan 95-24 had significantly lower MDA content, with slighter membrane lipid peroxidation and higher integrity of cell membrane structure. However, 112-2 showed significantly higher MDA content, with serious cell membrane damage and relatively weak disease resistance.

Under root-knot nematode infection (Figure 3.7-B), the response pattern of the antioxidant system was obviously different from that under fusarium wilt stress. 112-2 showed significantly higher SOD and CAT activities than other parents, while POD activity showed no significant difference among parents. Renhe-1 also showed high SOD activity and significantly lower MDA content than other parents, with the least membrane damage, indicating strong antioxidant defense and membrane protection ability.

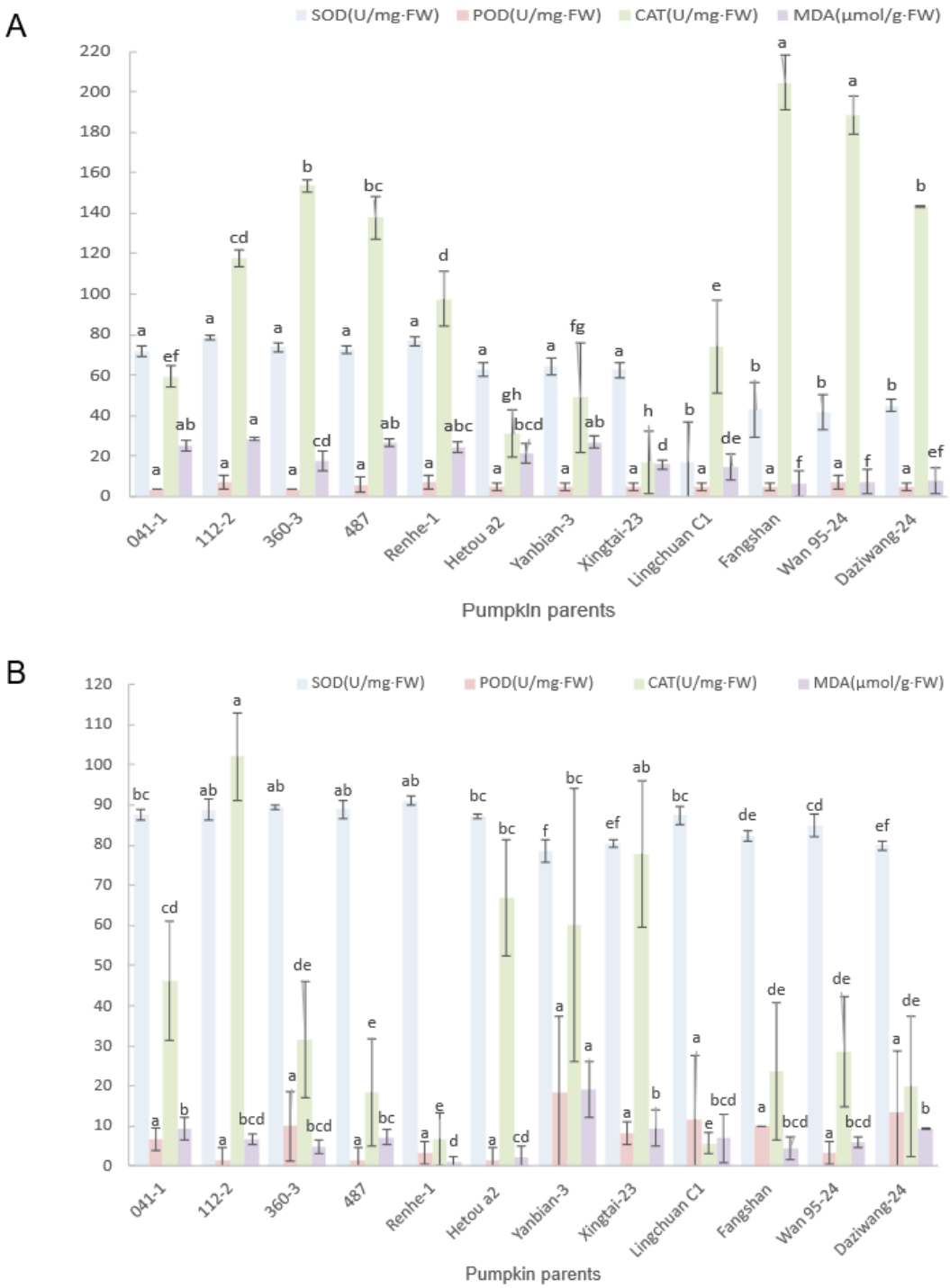

Figure 3.7. Antioxidant enzyme activities and MDA content of different pumpkin parents under biotic stress.

(A) After *Fusarium oxysporum* infection; (B) After root-knot nematode infection.

SOD: Superoxide dismutase activity (U/mg FW);

POD: Peroxidase activity (U/mg FW);

CAT: Catalase activity (U/mg FW);

MDA: Malondialdehyde content (μmol/g FW).

Different lowercase letters above bars indicate significant differences among different pumpkin parents at $P < 0.05$.

3.2.8 Effects of Fusarium oxysporum and Root-Knot Nematode Infection on Soluble Sugar and Soluble Protein Contents in Pumpkin Parents

Under Fusarium oxysporum infection (Figure 3.8-A), soluble sugar content remained at an extremely low level (<0.01%) with no significant differences among parents.Soluble protein content differed significantly, and Wan 95-24 showed significantly higher soluble protein content than other materials, indicating that it may enhance cell structural stability and disease-related enzyme activities by accumulating defense-related proteins, thereby improving resistance to fusarium wilt. Under root-knot nematode infection (Figure 3.8-B), no significant differences were observed in soluble sugar or soluble protein content among parents.

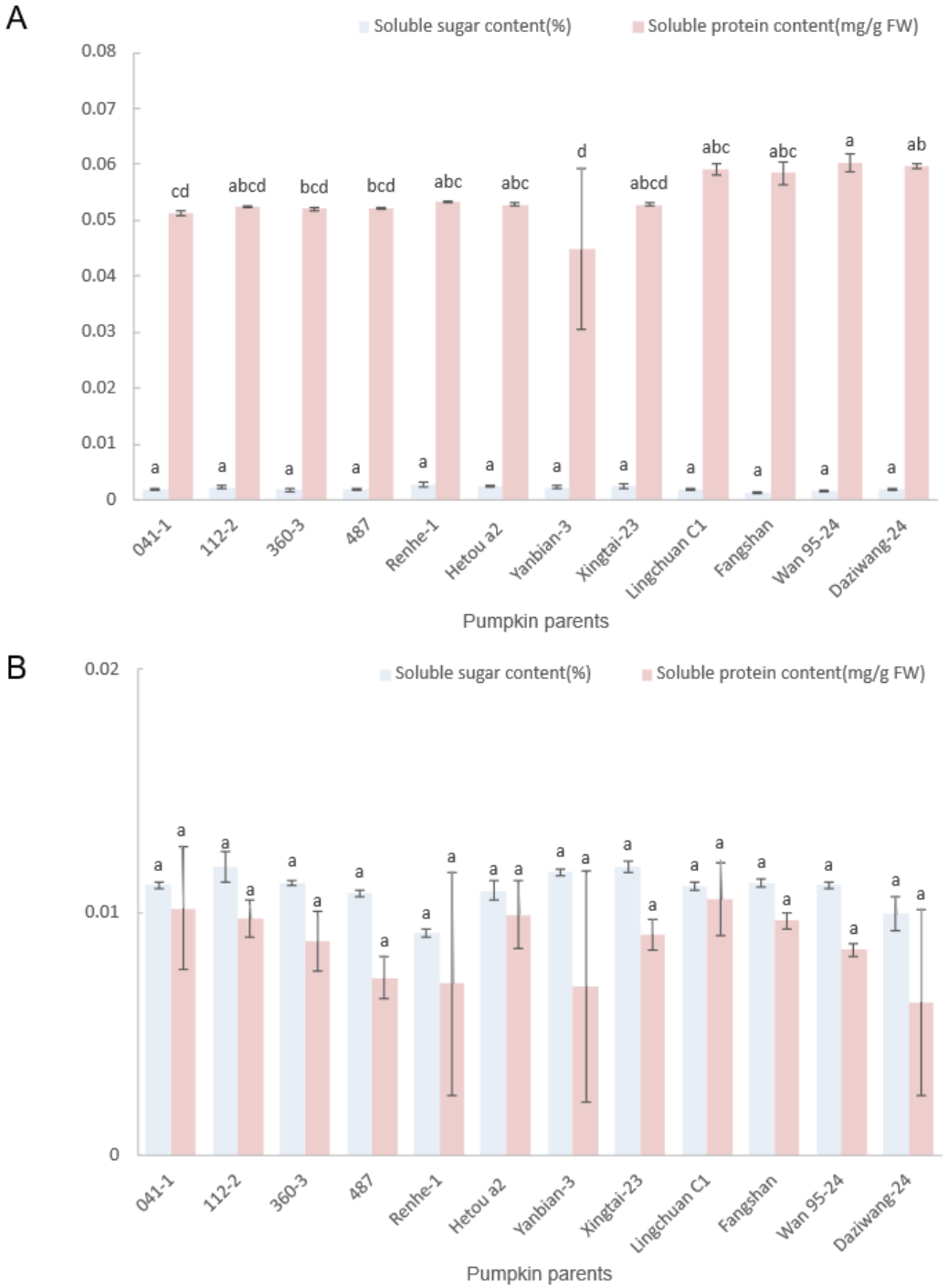

Figure 3.8. Soluble sugar and soluble protein contents of different pumpkin parents under biotic stress.

(A)After Fusarium oxysporum infection; (B) After root-knot nematode infection. Different lowercase letters above bars indicate significant differences at $P < 0.05$.

3.2.9 Root Hair Number and Root Morphological Indicators of Pumpkin Parents after Fusarium oxysporum and Root-Knot Nematode Infection

After scanning with a root system scanner, root images were observed to evaluate root hair number of different pumpkin parents under *Fusarium oxysporum* and root-knot nematode infection. By comparison (Figure 3.9-A, 3.9-B), under root-knot nematode infection, the number of fine roots and root hairs was significantly higher than under *Fusarium oxysporum* infection, indicating that root-knot nematode stress significantly induced the development of fine roots and root hairs in pumpkin.

Under *Fusarium oxysporum* infection (Figure 3.9-A1, 3.9-A2, 3.9-A3), significant differences were observed in root morphological indicators among different pumpkin parents. 360-3 showed significantly higher projected area, root surface area, and root volume than other parents, with no significant differences from Xingtai-23 and Daziwang-24. Meanwhile, 360-3 had significantly longer root length than other parents, with no significant difference in projected area and root surface area from Yanbian-3, and no significant difference in root volume from 041-1. Yanbian-3 had the highest number of root tips, and Lingchuan C1 had the largest average root diameter, both significantly higher than other parents. These results indicated that 360-3, Yanbian-3, and Lingchuan C1 had strong root expansion ability and high biomass accumulation, which could effectively expand the absorption range and strengthen the physical barrier against pathogens, showing strong disease resistance. In contrast, root length, number of root tips, projected area, and root

surface area of Lingchuan C1, as well as average root diameter and root volume of 487, were significantly lower than those of other parents, indicating poor root development and weak disease resistance.

Under root-knot nematode infection (Figure 3.9-B1, 3.9-B2, 3.9-B3), the response pattern of root morphological indicators was obviously different from that under fusarium wilt stress. 041-1 showed significantly higher root length, number of root tips, projected area, root surface area, and root volume than other parents. Yanbian-3 had the largest average root diameter, significantly higher than other parents. These results indicated active development of fine roots and root hairs, which could compensate for root function damage caused by nematodes and maintain water and nutrient balance. However, root length, number of root tips, projected area, and root surface area of Yanbian-3, average root diameter of Fangshan, and root volume of Renhe-1 were significantly lower than those of other parents, indicating serious root atrophy and weak nematode resistance.

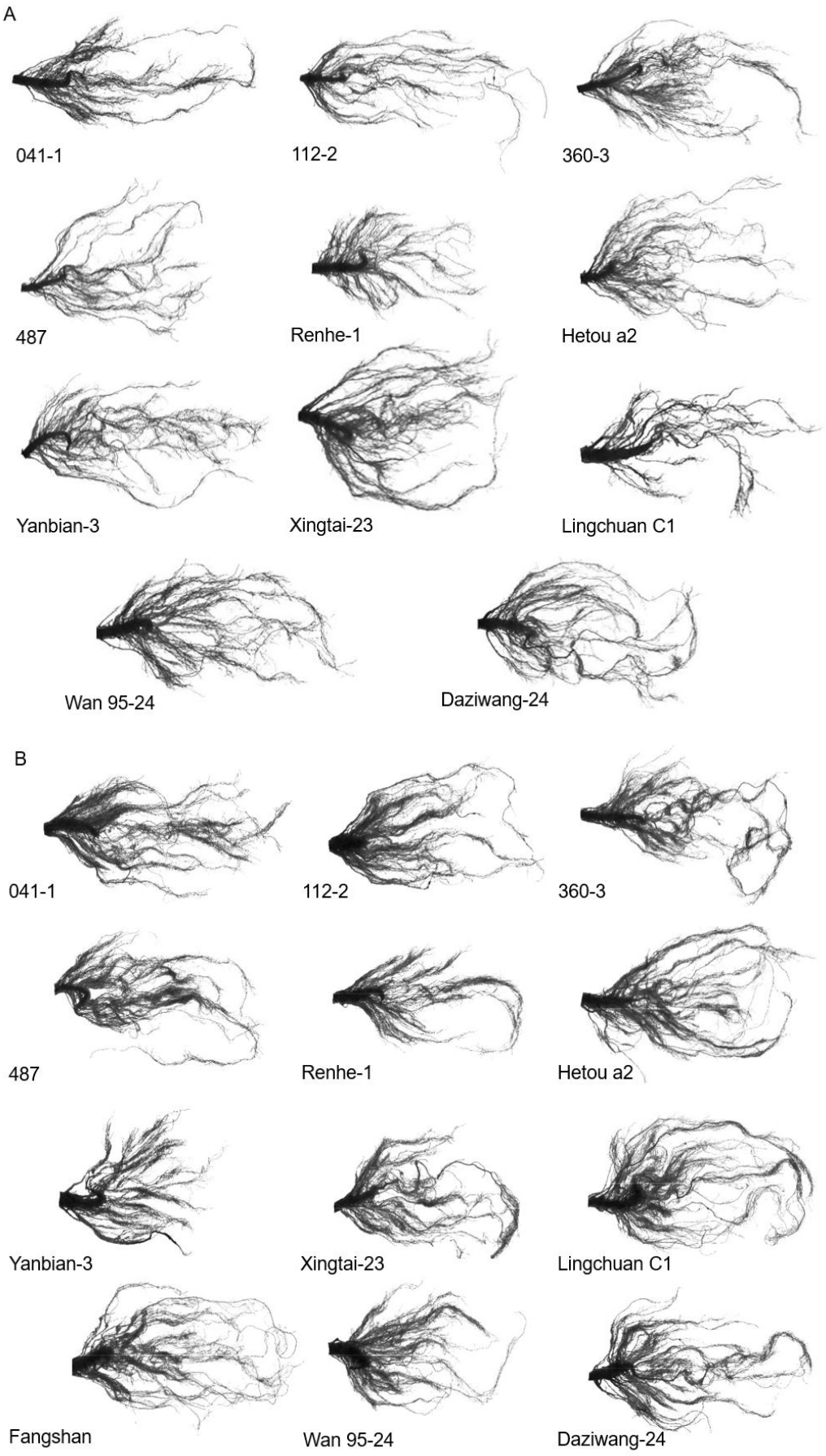
A
041-1
112-2
360-3
487
Renhe-1
Hetou a2
Yanbian-3
Xingtai-23
Lingchuan C1
Wan 95-24
Daziwang-24
B
041-1
112-2
360-3
487
Renhe-1
Hetou a2
Yanbian-3
Xingtai-23
Lingchuan C1
Fangshan
Wan 95-24
Daziwang-24

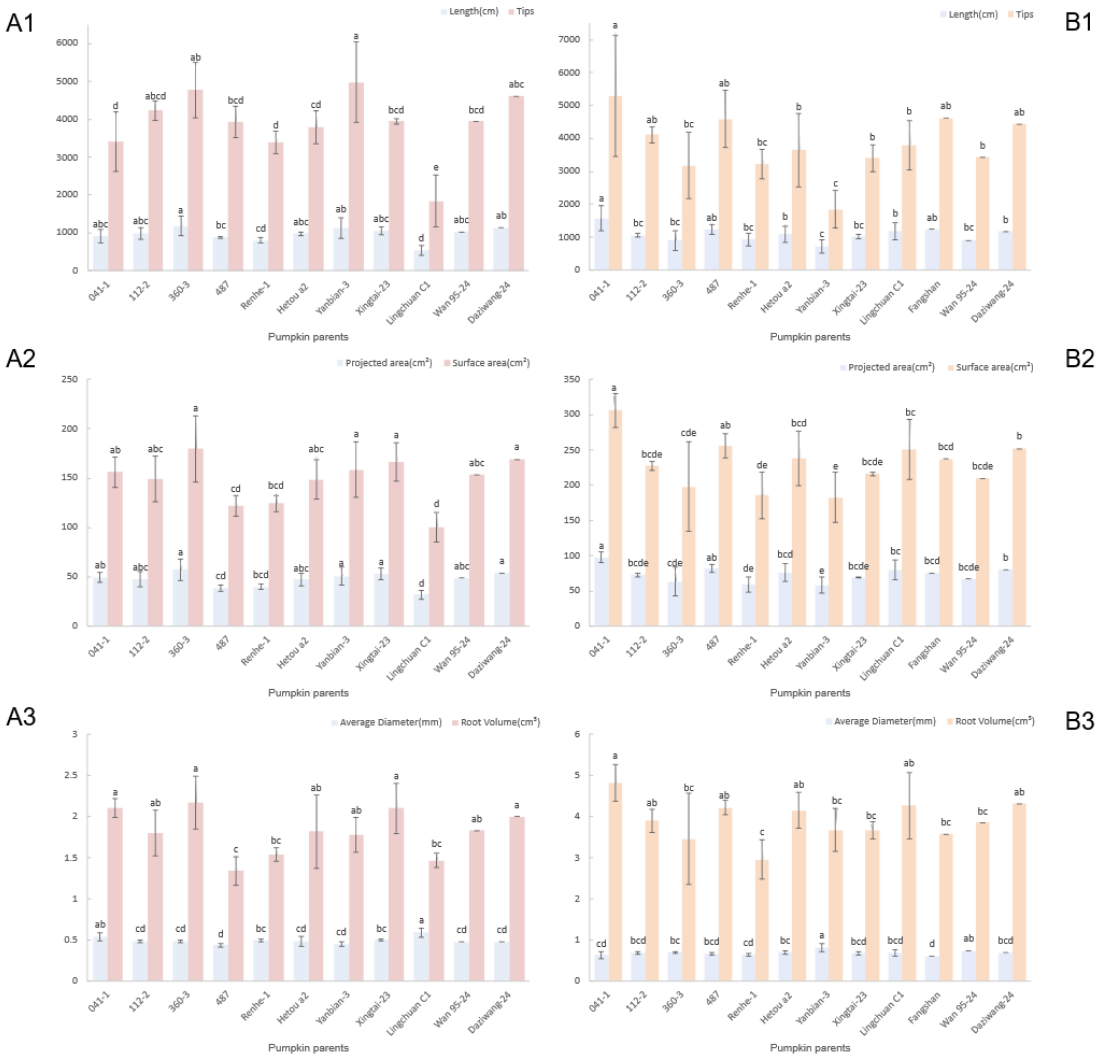

Figure 3.9. Root scanning images and root morphological indicators of different pumpkin parents under biotic stress.

(A, A1–A3) *Fusarium oxysporum* infection;

(B, B1–B3) root-knot nematode infection.

Conclusions to section 3

1. Investigation showed that control plants of all pumpkin hybrids and parents grew normally without disease symptoms. After inoculation with Fusarium oxysporum, plants showed typical symptoms: At the early stage, seedlings were stunted; cotyledons turned yellow, developed necrotic spots, and gradually shrank and dried. At the middle stage, true leaves chlorotic and yellowed; stem base constricted with longitudinal cracks; white or pink mold appeared under humid conditions; brown streaks occurred at nodes. At the late stage, severely infected plants became fully yellow, collapsed, and died. These results confirmed that the Fusarium oxysporum isolate used in this study had strong pathogenicity.

2. Disease tolerance generally refers to the ability of plants to maintain growth under disease stress. Disease incidence and mortality rate reflect tolerance level; high incidence with low mortality usually indicates strong tolerance. Wang et al. (2020) [15] reported that symptoms appeared at 7 d, and developed most rapidly from 9 to 11 d after inoculation. In this study, the most obvious symptoms were observed at 20 d after inoculation, which was consistent with the results of Xu et al. (2021) [16].

3. Analysis of growth and physiological indicators showed that, under Fusarium oxysporum infection: Among hybrids, 360-3×487 performed best in early plant height and late stem diameter; Lingchuan C1×360-3 was superior in middle and late chlorophyll content and late stem diameter; Hetou a2×Lingchuan C1 excelled in late stem diameter and leaf number. Among parents, Xingtai-23 had the

highest early and late plant height; Renhe-1 performed best in early stem diameter, leaf number, middle plant height, and late chlorophyll content; 112-2 was superior in early and middle stem diameter and early chlorophyll; Yanbian-3 excelled in early chlorophyll, middle leaf number, and late stem diameter. These materials showed the highest overall relative growth, were less affected by pathogen infection, and exhibited strong resistance to fusarium wilt.

Under root-knot nematode infection, the hybrid Yanbian-4×041-1 performed best in plant height and stem diameter. Among parents, Fangshan excelled in plant height and chlorophyll content, and 112-2 in stem diameter and leaf number, indicating strong resistance to root-knot nematode. Comparison of coefficients of variation showed that stem diameter was relatively stable and less affected by both stresses in both hybrids and parents.

4. For the classification of fusarium wilt resistance, Luo (2011) [4] used the disease index as the evaluation criterion, and Martyn et al. (1989) [17] based their evaluation on disease incidence. Although the two methods were slightly different, both could effectively evaluate disease resistance. In this study, the resistance grades of all pumpkin materials were evaluated according to the method of Luo (2011) [4], based on the disease index.

The results showed that among the hybrid combinations, Yanbian-3×360-3, Yanbian-2×041-1, 041-1×Xingtai, 041-1×Hetou a2, and 360-3×487 were classified as moderately resistant (MR). Their leaf disease indices were 52.67, 54.67, 48.67, 48.67, and 53.33, and stem-dissection disease indices were 37.92, 45.83, 52.92, 47.50, and 5.00, respectively. Among them, 360-3×487 had a stem-dissection

disease index of only 5.00, indicating that its root system had extremely strong defense ability against fusarium wilt pathogen. Among the pumpkin parents, Renhe-1 and Hetou a2 were classified as moderately resistant (MR), with leaf disease indices of 44.67 and 51.33, and stem-dissection disease indices of 48.75 and 33.33, respectively.

Analysis of resistance indicators to root-knot nematode showed that the hybrid combination Yanbian-3×360-3 and the parents 360-3, Hetou a2, Xingtai-23, and 360-3×487 exhibited the lowest values in all four resistance indicators, and were the least affected by root-knot nematode, with the strongest resistance. Comparison of coefficients of variation showed that the gall index had the largest coefficient of variation in both pumpkin hybrids and parents, indicating that gall index could more accurately reflect the resistance of pumpkin hybrids and parents to root-knot nematode.

In a seed germination experiment conducted under cadmium (Cd) stress, 19 distinct pumpkin hybrid combinations were evaluated. Seven hybrids with strong Cd tolerance were ultimately identified. Among these, the combinations Yanbian-3×360-3 and Yanbian-2×041-1 exhibited superior cadmium tolerance, verifying their resistance not only to fusarium wilt and root-knot nematode but also to cadmium toxicity[18].

5. Cluster analysis groups materials based on genetic distance and trait similarity without artificial thresholds, thus reducing subjective bias. However, it cannot directly quantify resistance level. Subordinate function value can quantitatively reflect resistance but is inconvenient for classification. Therefore, this

study comprehensively evaluated materials using both methods.

Based on four resistance indicators to root-knot nematode, 24 hybrids and 12 parents were divided into resistant and susceptible groups. Combined with subordinate function values: Resistant hybrids had total values higher than 4.88, mainly including Yanbian-3×360-3, Yanbian-2×041-1, Hetou a2×360-3, Hetou a2×112-2, 360-3×487. Susceptible hybrids ranged from 1.74 to 4.88. Resistant parents had values higher than 2.90; susceptible parents (mainly 112-2, Lingchuan C1) lower than 2.90. Overall, the clustering results were consistent with the order of subordinate function values.

6. Antioxidant responses of different pumpkin parents showed obvious stress specificity to fusarium wilt and root-knot nematode. CAT activity played a dominant role under fusarium wilt stress. Fangshan and Wan 95-24 exhibited significantly higher H_2O_2-scavenging capacity and effectively alleviated oxidative damage. Under nematode stress, SOD and CAT jointly participated in defense, and 112-2 showed significantly higher SOD and CAT activities. Notably, 112-2 had significantly higher MDA content under fusarium wilt stress, indicating more severe membrane damage. MDA content can be used as an important physiological index for evaluating stress resistance in pumpkin. Renhe-1 had the lowest MDA content and high SOD activity under nematode stress, showing strong antioxidant and membrane protection ability.

7. Analysis of root hair number and root morphological indicators showed that the number of fine roots and root hairs was significantly higher under nematode infection than under fusarium wilt infection, indicating that root-knot nematode

stress significantly induced the development of fine roots and root hairs. Fine roots and root hairs are the main sites for water and nutrient uptake and important structural barriers against biotic stress. Under nematode stress, pumpkin compensated for root function damage and strengthened physical defense by increasing fine roots and root hairs.

In contrast, fine root and root hair development was weak under fusarium wilt, possibly due to vascular infection and root lignification caused by Fusarium oxysporum. This stress-specific root response pattern reflects the adaptive regulatory mechanism of pumpkin to different biotic stresses and provides important morphological evidence for elucidating molecular mechanisms and breeding broad-spectrum resistant rootstocks.

References to section 3

1. Niu X C. Occurrence and control of watermelon fusarium wilt. Rural Practical Science and Technology Information, 2011, 1: 34-34.

2. Zhang Y, Liu Z X. Screening of watermelon fusarium wilt resistant rootstocks and determination of pathogenicity[J]. Rural Science & Technology, 2018(5): 45-47. DOI:10.3969/j.issn.1002-6193.2018.05.023.

3. Li H S, Sun Q, Zhao S J, et al. Principles and techniques of plant physiological biochemical experiment[J]. Higher Education, Beijing, 2000: 195-197.

4. Luo F, Han X Y, Xu Y, et al. Comparative study on resistance to fusarium wilt and fruit quality of different rootstocks for watermelon[J]. Chinese Journal of Tropical Agriculture, 2011, 31(8): 26-29. DOI:10.3969/j.issn.1009-2196.2011.08.009.

5. Guo T X, Mo J Y. Resistance evaluation of several bitter gourd varieties to fusarium wilt[J]. Guangxi Agricultural Sciences, 2007, 38(4): 408-410. DOI:10.3969/j.issn.2095-1191.2007.04.014.

6. Winstead N N, Sasser J N. Reaction of cucumber varieties to five root knot nematodes (Meloidogyne spp.). Plant Disease Reporter, 1956, 40(4): 272-275.

7. Fassuliotis G, Rau G J. Evaluation of Cucumis spp. for resistance to the cotton root knot nematode, Meloidogyne incognita Acrita. Plant Disease Reporter, 1963, 47(9): 809.

8. Fassuliotis G. Species of Cucumis resistant to the root knot nematode, Meloidogyne incognita Acrita. Plant Disease Reporter, 1967, 51(9): 720-723.

9. Fassuliotis G. Resistance of Cucumis spp. to the root knot nematode,

Meloidogyne incognita Acrita. Journal of Nematology, 1970, 2(2): 174-178.

10. Fassuliotis G. Plant breeding for root knot nematode resistance. In: J. N. Sasser and C. C. Carter (eds). Root knot nematodes: Systematics, biology and control. Academic Press, New York, 1979, 425-453.

11. Zhang M Z. Correlation analysis of resistance to tobacco root-knot nematode[D]. Henan Agricultural University, 2017. DOI:10.27117/d.cnki.ghenu.2017.000045.

12. Boiteox L S, Charchar J M. Genetic resistance to root-knot nematode (Meloidogyne javanica) in eggplant (Solanum melongena)[J]. Plant Breeding, 1996, 115(3): 198-200.

13. Liu W Z. Plant Pathogenic Nematology[M]. Beijing: China Agriculture Press, 2000.

14. Song H Y, Lei J J, Li C Q. Plant heat stress response and identification and evaluation of heat resistance[J]. China Vegetables, 1998, (1): 50-52.

15. Wang X L. Resistance identification of 19 watermelon materials to physiological race 2 of Fusarium oxysporum f. sp. niveum and evaluation of their quality. Yangling: Northwest A&F University, 2020.

16. Xu K. Screening and identification of fusarium wilt-resistant and low-temperature-tolerant rootstocks for protected watermelon[D]. Shaanxi: Northwest A&F University, 2021.

17. Martyn R D, Bruton B D. An initial survey of the United States for races of Fusarium oxysporum f. sp. niveum. Hortscience, 1989, 24: 696-698.

18. Chen, R. and Dubovyk, V. GERMINATION OF PUMPKIN SEEDS

UNDER CD STRESS. Bulletin of Sumy National Agrarian University. The series: Agronomy and Biology. 2025, 58, 4 (Mar. 2025), 3-8. DOI: https://doi.org/10.32782/agrobio.2024.4.1.

SECTION 4

TRANSCRIPTOMIC ANALYSIS OF RESISTANT AND SUSCEPTIBLE PUMPKIN PARENTS IN RESPONSE TO *FUSARIUM* WILT AND ROOT-KNOT NEMATODE INFECTION

Transcriptomics is a major approach for studying gene expression. Through transcriptomic analysis, the activation or inhibition of disease resistance-related genes and metabolic pathways can be revealed, leading to a deeper understanding of the plant immune response process [1]. Fusarium wilt and root-knot nematode are highly destructive soil-borne diseases, and grafted seedlings are commonly used for their control in production. At present, some scholars have conducted transcriptome studies under fusarium wilt and root-knot nematode stress in different crops [2], but there are few reports on transcriptomic analysis of cucurbit crops infected by Fusarium oxysporum and Meloidogyne incognita.

To understand the changes in early defense-related substances in resistant and susceptible pumpkin parents after infection by Fusarium oxysporum and root-knot nematode, RNA-seq technology was used in this study. The selected resistant pumpkin parent Hetou a2 and susceptible parent Lingchuan C1 were used as materials, and treated with Fusarium oxysporum infection (48 h, 96 h) and root-knot nematode infection (24 h, 48 h), respectively. Through transcriptome sequencing and bioinformatics analysis, differentially expressed genes and core metabolic pathways between resistant and susceptible parents were identified, and the early molecular mechanism of pumpkin in response to infection by the two soil-borne

diseases was elucidated. This study provides a theoretical basis and technical support for the cloning, functional verification and molecular breeding of resistance genes to fusarium wilt and root-knot nematode in pumpkin.

4.1 Materials and Methods

4.1.1 Experimental Materials

The dual-resistant pumpkin parent Hetou a2 and dual-susceptible pumpkin parent Lingchuan C1 were used as experimental materials, provided by the Pumpkin Research Group, College of Horticulture and Landscape Architecture, Henan Institute of Science and Technology. Pathogen: Fusarium oxysporum f. sp. Cucumerinum. Nematode: Meloidogyne incognita, both were provided by the Institute of Vegetables and Flowers, Chinese Academy of Agricultural Sciences.

4.1.2 Experimental Methods

4.1.2.1 Collection of Pathogen and Nematode

The methods were the same as those described in Section 3, 3.1.2.

4.1.2.2 Seedling Raising and Inoculation

Healthy and plump seeds of the dual-resistant pumpkin parent Hetou a2 and dual-susceptible parent Lingchuan C1 were selected. The inoculation procedures were the same as those described in Section 3, 3.1.2. Seedling leaves were collected at 48 h and 96 h after inoculation with Fusarium oxysporum, and seedling roots were collected at 24 h and 48 h after inoculation with root-knot nematode. Both inoculated treatments and controls were set with three biological replicates. Resistant control groups: K1, K2; Susceptible control groups: K3, K4; Resistant fusarium wilt treatment groups (48 h, 96 h): KB1, KB2; Susceptible fusarium wilt treatment

groups (48 h, 96 h): GB1, GB2; Resistant root-knot nematode treatment groups (24 h, 48 h): KC1, KC2; Susceptible root-knot nematode treatment groups (24 h, 48 h): GC1, GC2. At each sampling time point, 6 plants were collected for each sample with three replicates. All samples were immediately frozen in liquid nitrogen and stored at -80 °C until use. All samples were sent to Biomarker Technologies Corporation (Beijing) for transcriptome sequencing and subsequent data processing and analysis.

4.1.2.3 Transcriptome Sequencing and Bioinformatics Analysis

The experimental pipeline of RNA-seq included sample quality control, library construction, library quality inspection, and on-machine sequencing.

4.1.2.3.1 Sample Quality Control

To ensure qualified samples for transcriptome sequencing, Biomarker used advanced molecular biological equipment to detect the purity, concentration, and integrity of the extracted total RNA with strict quality control. The quality assessment methods for total RNA were as follows: (1) NanoDrop 2000 spectrophotometer: used to detect the purity and concentration of RNA; (2) Agilent 2100 / LabChip GX: used to accurately detect the integrity of RNA.

4.1.2.3.2 Library Construction

After passing quality control, library construction was performed with the main procedures as follows: (1) Eukaryotic mRNA was enriched using magnetic beads with Oligo(dT); (2) Fragmentation Buffer was added to fragment the mRNA randomly; (3) Using the fragmented mRNA as a template, the first-strand and second-strand cDNA were synthesized, followed by cDNA purification; (4) The

purified double-stranded cDNA was subjected to end repair, A-tailing, and ligation of sequencing adapters, and then fragment size selection was performed using AMPure XP beads; (5) Finally, the cDNA library was obtained by PCR enrichment.

4.1.2.3.3 Library Quality Control

After library construction, initial quantification was performed using a Qubit 3.0 fluorometer, with a required concentration above 1 ng/μL. The insert fragment size was then detected using a Qsep400 high-throughput analysis system. When the insert fragment met the expected size, the effective concentration of the library (> 2 nM) was accurately quantified by q-PCR to ensure library quality.

4.1.2.3.4 On-Machine Sequencing

After passing library quality control, sequencing was performed on the Illumina NovaSeq 6000 platform in the PE150 mode.

4.1.2.3.5 Analysis Pipeline

After sequencing, data analysis was performed using the bioinformatics pipeline provided by the Biomarker Cloud Platform (BMKCloud, www.biocloud.net). Raw sequencing data were filtered to obtain clean data, which were then aligned to the designated reference genome to obtain mapped data. Subsequent analyses included library quality assessment, structural-level analysis, differential expression analysis, gene functional annotation, and functional enrichment.

4.1.2.4 Analysis of Transcriptome Sequencing Data

The genome sequence of Cucurbita moschata was used as the reference genome for sequencing. Raw data were filtered to remove redundant sequences and

low-quality reads, yielding high-quality clean data. Clean reads were rapidly and accurately mapped to the reference genome using HISAT2 [3] to obtain positional information on the reference genome. The aligned reads were then assembled using StringTie [4] to reconstruct the transcriptome for subsequent analysis.

4.1.2.4.1 Sequencing Data Quality Control

The cDNA library was sequenced using the Illumina high-throughput sequencing platform, generating large quantities of high-quality data (raw data). Most base quality scores reached or exceeded Q30.

4.1.2.4.2 Sequencing Quality Control

Before data analysis, strict quality control was performed to ensure high-quality reads for accurate downstream analysis. The filtering steps were as follows: (1) Remove reads containing adapter sequences; (2) Remove low-quality reads (reads in which the proportion of N exceeded 10%; reads in which bases with quality score Q ≤ 10 accounted for more than 50% of the total read length). High-quality clean data were obtained after the above quality control procedures.

4.1.2.4.3 Base Quality Score Statistics

The base quality score (Q-score) is an integer mapping of the base-calling error probability. The commonly used Phred quality score formula [5] is (1):

$$Q = -10 \times log_{10}P \quad (1)$$

Where: P represents the probability of base-calling error.

The corresponding relationships between Q-score and base recognition accuracy are listed in Table 4.1.

Table 4.1 Correspondence between base quality score and base-calling error probability

Q-score	Incorrect base recognition	Correct base recognition rate
Q10	1/10	90%
Q20	1/100	99%
Q30	1/1000	99.9%
Q40	1/10000	99.99%

4.1.2.4.4 Unigene Functional Annotation

The assembled transcripts were aligned against public databases (COG, GO, KEGG, KOG, Pfam, SWISSPROT, eggNOG, and NR) using BLAST. Gene Ontology (GO) is a biological ontology language that annotates gene products and proteins from three aspects: biological process, molecular function, and cellular component. KEGG is a database integrating genomic, chemical, and systemic functional information, among which the KEGG Pathway database focuses on molecular interactions and regulatory networks. Gene similarity alignments were mainly based on the BLAST algorithm [6]. Unigene sequences were aligned against NR [8], Swiss-Prot [9], GO [10], COG [11], KOG [12], KEGG [13], and eggNOG databases using BLAST [7] software. KOBAS 2.0 [14] was used to obtain KEGG Orthology results of unigenes in KEGG. After predicting the amino acid sequences of unigenes, the HMMER software (Eddy et al., 1998) was used to align against the Pfam [15] database to obtain unigene annotation information. TransDecoder software was used to predict the coding sequences and corresponding amino acid sequences of unigenes.

Reads from 36 samples were aligned to the unigene library using Bowtie [16]. Based on the alignment results, expression levels were estimated using RSEM [17]. The expression abundance of unigenes was represented by FPKM values. FPKM (Fragments Per Kilobase of transcript per Million mapped reads) [18] represents the number of reads per kilobase of transcript per million mapped reads, and is a standard method for estimating gene expression levels in transcriptome analysis. Gene expression calculated by FPKM is not affected by gene length or sequencing depth, allowing direct comparison of gene expression differences among samples. The FPKM formula is (2):

$$FPKM = cDNA\ Fragments\ Mapped\ Fragments(Millions) \times transcriptLength(kb) \quad (2)$$

Where:

cDNA Fragments: number of cDNA fragments mapped to a transcript;

Mapped Fragments (Millions): total number of mapped fragments (in 10^6 units);

Transcript Length (kb): length of the transcript (in 10^3 bases).

Differential expression analysis among different samples was performed using DESeq [19] to identify differentially expressed gene sets between samples at different stages. The screening thresholds were P-value < 0.01 and fold change (FC) ≥ 2. FC represents the expression ratio between inoculated samples and blank controls at different time points. Functional annotation was performed for the screened differentially expressed genes (DEGs). Based on the annotation results, GO functional enrichment and KEGG metabolic pathway enrichment analyses were conducted for DEGs.

4.2 Results and Analysis

4.2.1 Sequencing Data Statistics

After filtering and quality control of the raw data, 254.55 Gb of clean data were obtained. The clean data for each sample reached 6.41 Gb, and the percentage of Q30 bases in all samples was not less than 97.14%, indicating high reliability (Table 4.2).

A total of 33,673 unigenes were assembled from the clean reads, with an N50 of 1,968 bp and a total length of 49,822,917 bp. The longest unigene was 16,728 bp, the shortest was 96 bp, and the average length was 1,479.61 bp (Figure 4.1). In terms of unigene length distribution, the number of sequences longer than 2,000 bp was the largest (8,076). Combined with key indices including an N50 value of 1,968 bp and an average length of 1,479.61 bp, the results indicated that the unigenes obtained in this sequencing and assembly had high integrity and a high proportion of long fragments, which could provide a reliable foundation for subsequent functional analysis.

Table 4.2 Evaluation of sample sequencing data

Samples	Read Number	Base Number	GC Content	%≥Q30
K1-1	21761865	6507782698	45.34	97.91
K1-2	21664347	6480025633	45.16	98.21
K1-3	24689864	7385145888	45.31	97.75
K2-1	21835200	6530477701	45.03	98.24
K2-2	21425740	6411775102	44.99	97.56
K2-3	23807521	7125046186	45.28	97.66
K3-1	24035712	7192241776	44.94	98.17
K3-2	21719074	6492437916	44.65	98.01
K3-3	26758547	8004800049	45.03	97.51
K4-1	24460404	7322740438	44.94	98.15
K4-2	21589634	6455213657	45.15	97.85
K4-3	23315237	6971615749	45.1	97.36
KB1-1	23020625	6889173029	44.97	97.85
KB1-2	28663136	8578820240	45.26	98.21
KB1-3	22418438	6703660739	44.98	97.82
KB2-1	28664285	8569088773	45.43	97.44
KB2-2	22303097	6669039646	45.29	98.33
KB2-3	23595754	7063352452	45.29	98.11
GB1-1	22250116	6660495067	45.68	97.66
GB1-2	23249234	6954852563	45.56	97.74
GB1-3	22995259	6880438389	45.42	97.79
GB2-1	23374784	7001317909	45.57	97.94
GB2-2	23383644	6996418339	45.38	98.18
GB2-3	22567697	6717787619	44.03	97.14
KC1-1	23193410	6934265700	44.74	98.42
KC1-2	23903701	7150875643	44.81	98.37
KC1-3	23457074	7013846482	44.93	98.41
KC2-1	22592350	6760062642	44.83	98.18

KC2-2	22934347	6862926764	44.74	98.18
KC2-3	24611080	7372023999	45.03	98.27
GC1-1	25485594	7626892507	44.65	98.19
GC1-2	23364238	6983597184	44.82	98.47
GC1-3	23731626	7102205552	44.69	98.32
GC2-1	25213140	7542741515	44.83	98.36
GC2-2	23508507	7031063284	44.79	98.33
GC2-3	25441462	7610160519	44.73	98.18

Note: %≥Q30: Percentage of bases with quality value ≥ 30 in clean data.

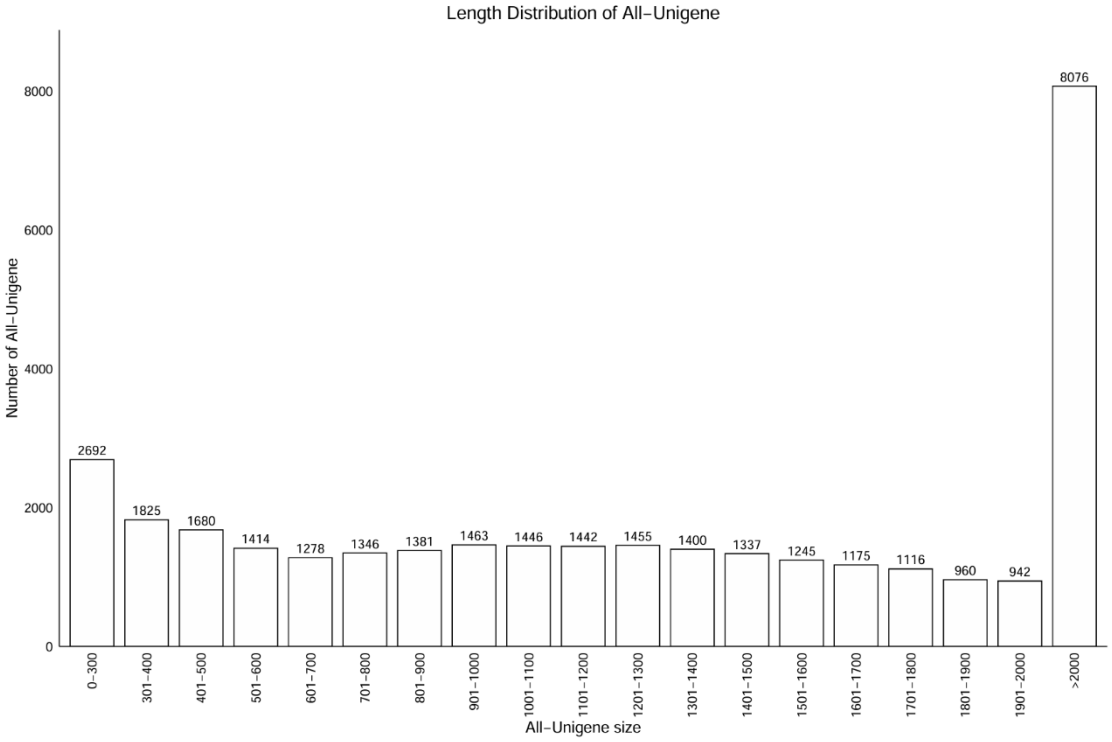

Figure 4.1. Length distribution graph of de novo Unigenes of infected Cucurbita moschata

4.2.2 Functional Annotation of Unigenes

The unigenes were aligned against public databases (COG, GO, KEGG, KOG, Pfam, SWISSPROT, eggNOG, and NR). The results showed that 28,977 unigenes were annotated, and 506 new genes were identified. 9,447 unigenes were annotated in the COG database, accounting for 32.60%; 24,125 unigenes were annotated in the

GO database, accounting for 71.60%; 20,277 unigenes were annotated in the KEGG database, accounting for 60.20%; 15,469 unigenes were annotated in the KOG database, accounting for 45.90%; 23,930 unigenes were annotated in the Pfam database, accounting for 71.10%; 21,261 unigenes were annotated in the SWISSPROT database, accounting for 63.10%; 24,629 unigenes were annotated in the eggNOG database, accounting for 73.10%; 28,899 unigenes were annotated in the NR database, accounting for 85.80%. Among them, 5,884 unigenes were annotated in all eight databases (Figure 4.2). Of the 28,899 unigenes annotated in the NR database: 25,107 unigenes (86.88%) were mapped to the Cucurbita moschata genome; 1,020 unigenes (3.53%) were mapped to the Cucurbita pepo genome; 613 unigenes (2.12%) were mapped to the Cucurbita maxima genome; 532 unigenes (1.84%) were mapped to the Cucumis melo genome; 456 unigenes (1.58%) were mapped to the Cucumis sativus genome (Figure 4.3).

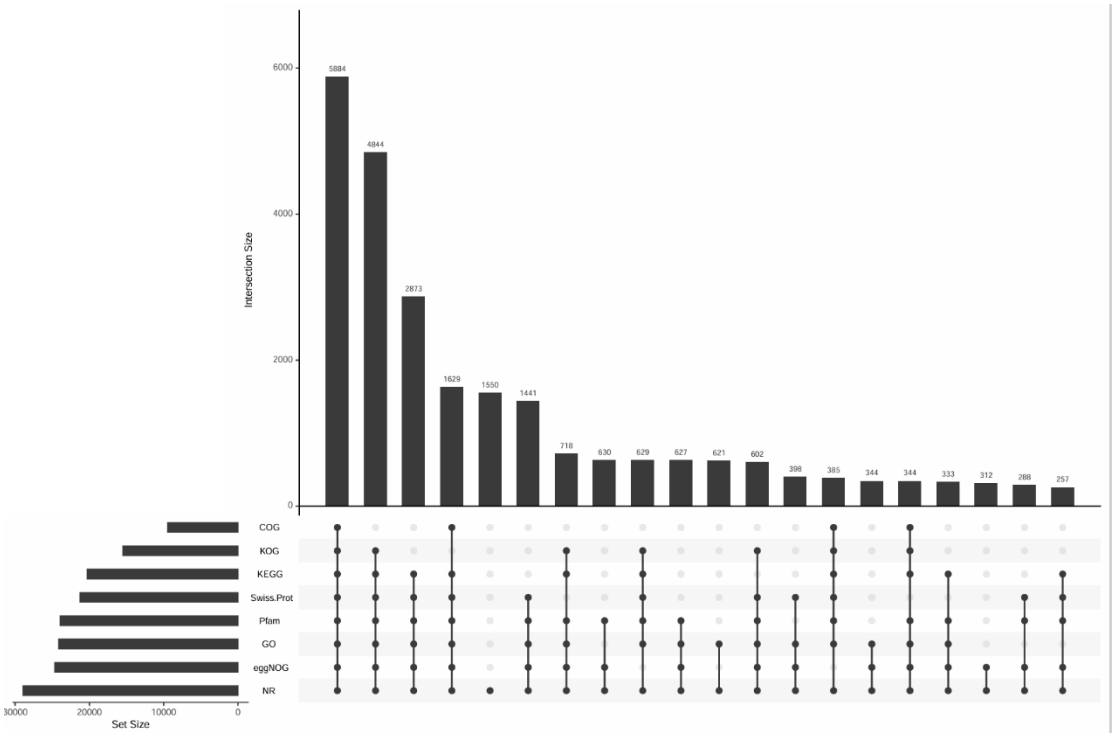

Figure 4.2. Upset plot of unigenes annotated in COG, GO, KEGG, KOG,

Pfam, SWISSPROT, eggNOG, and NR databases in pumpkin.

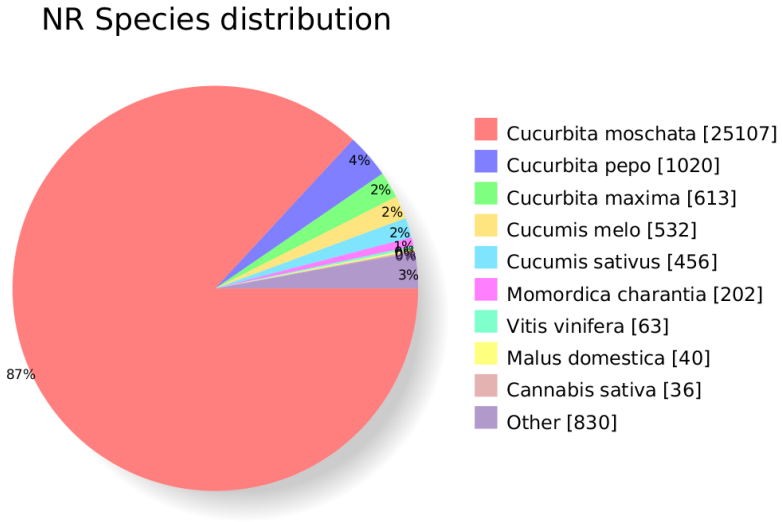

Figure 4.3. Species distribution of pumpkin sequences aligned against the NR database.

4.2.3 Gene Expression Level Analysis

The FPKM values of protein-coding genes detected by transcriptome sequencing spanned six orders of magnitude from 10^{-2} to 10^{4} [20], indicating high sensitivity of the detection (Figure 4.4).

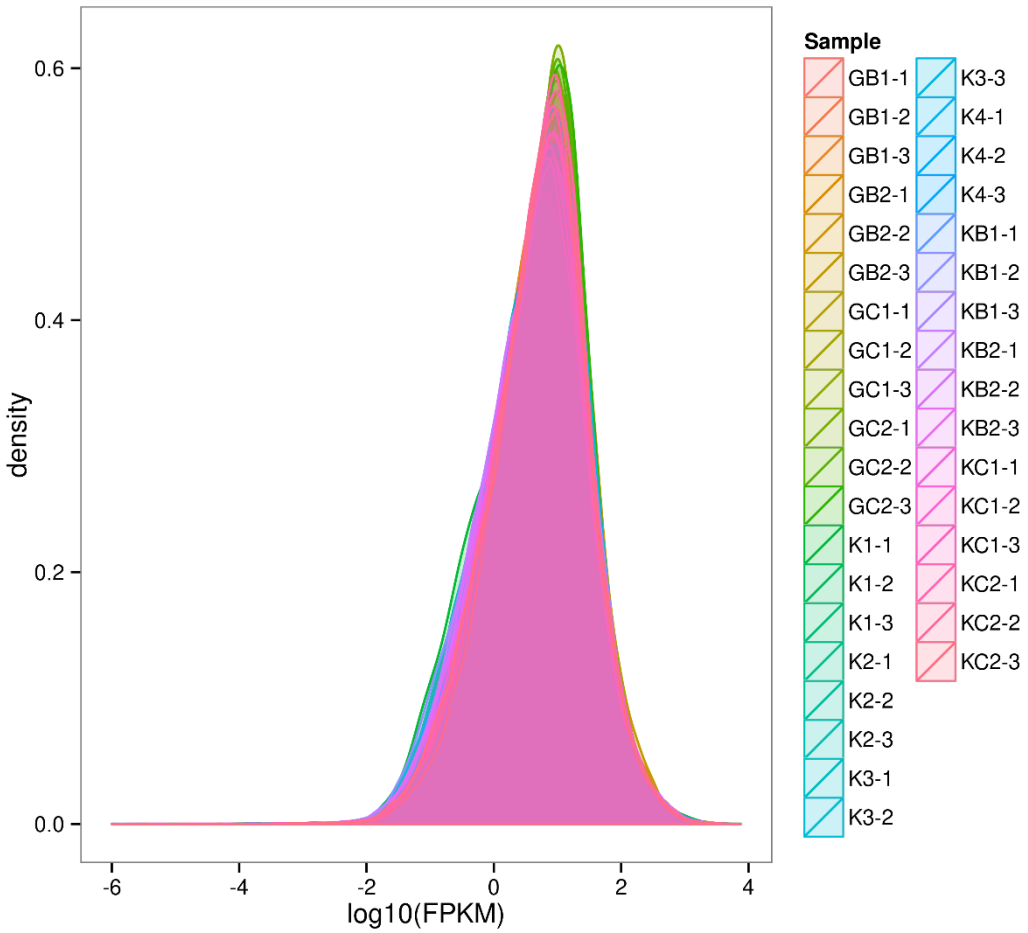

Figure 4.4. Alignment of FPKM density distribution in all samples

Note: The abscissa represents the logarithmic value of FPKM, and the ordinate represents the probability density. Curves of different colors represent different samples.

4.2.4 Analysis of Differentially Expressed Genes

By aligning the sequencing reads to the sequences in the Unigene library, the expression abundance information of Unigenes in the corresponding samples was obtained. According to the differences in gene expression levels between resistant and susceptible varieties in the inoculated treatment groups (Fusarium oxysporum and root-knot nematode) and the control groups, differentially expressed genes (DEGs) were screened based on the criteria of p-adjust < 0.05 and |log2FC| > 2.

The data were divided into 20 comparison groups for DEG analysis: K1_vs_K2, K3_vs_K4, KB1_vs_KB2, GB1_vs_GB2, KC1_vs_KC2, GC1_vs_GC2, K1_vs_K3, K1_vs_KB1, K1_vs_KC1, K3_vs_GB1, K3_vs_GC1, KB1_vs_GB1, KC1_vs_GC1, K2_vs_K4, K2_vs_KB2, K2_vs_KC2, K4_vs_GB2, K4_vs_GC2, KB2_vs_GB2, KC2_vs_GC2. The scatter distribution of DEG expression levels is shown in (Figure 4.5). The number of up-regulated and down-regulated genes varied among different treatment groups. Combined with the phenotypic characteristic map (Figure 4.6) and the distribution map of DEG numbers (Figure 4.7): Resistant treatment groups (KB1/KB2/KC1/KC2): The number of up-regulated genes was significantly higher than that of down-regulated genes in most groups, indicating that resistant materials mainly initiate defense by activating gene expression. Susceptible treatment groups (GB1/GB2/GC1/GC2): The number of down-regulated genes was higher than up-regulated genes in the late-stage treatment groups, suggesting that the normal physiological functions of susceptible materials were severely disturbed, leading to disordered gene expression regulation. Control groups (K1/K2/K3/K4): The number of up-regulated genes was higher than down-regulated genes, but the total number of DEGs was much lower than that in treatment groups, indicating small differences in basal expression. The large differences among treatment groups were mainly induced by stress.

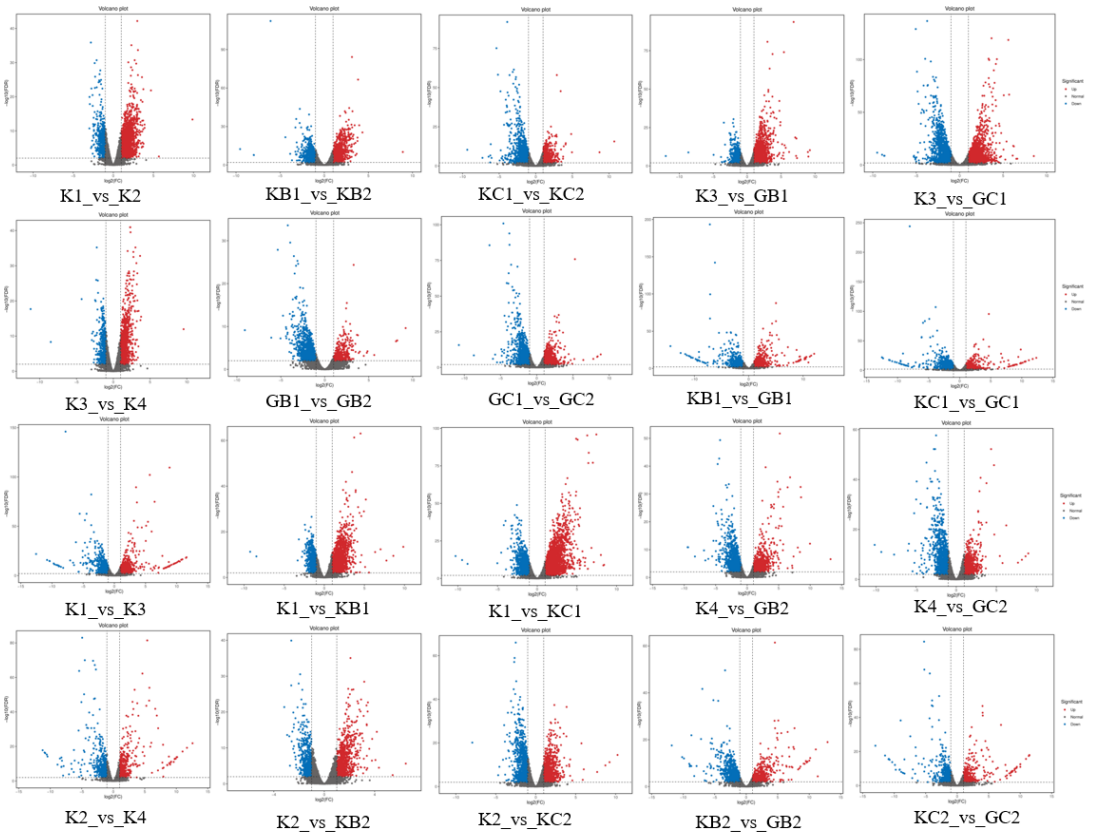

Figure 4.5. Scatter distribution diagram of differentially expressed genes in different pumpkin treatment groups

Note: Red represents up-regulation, blue represents no change, green represents down-regulation.

Figure 4.6. Phenotypic characteristics of pumpkin under different treatments

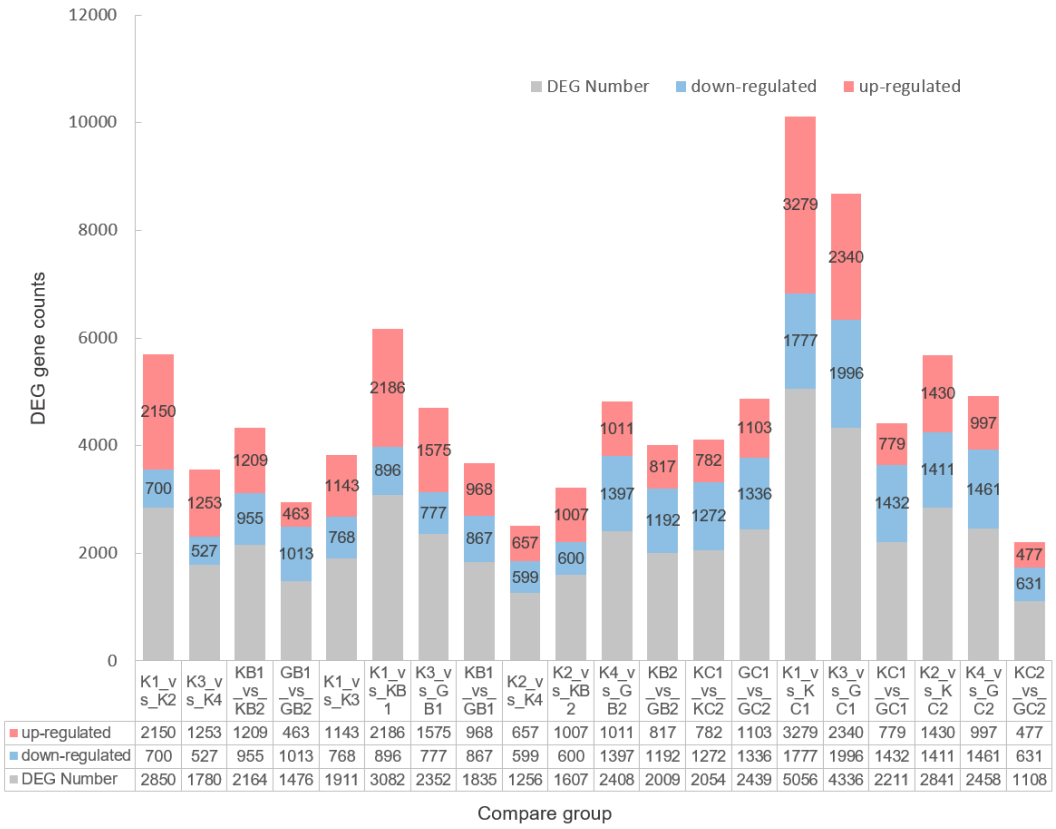

	K1_vs_K2	K3_vs_K4	KB1_vs_KB2	GB1_vs_GB2	K1_vs_K3	K1_vs_KB1	K3_vs_GB1	KB1_vs_GB1	K2_vs_K4	K2_vs_KB2	K4_vs_GB2	KB2_vs_GB2	KC1_vs_KC2	GC1_vs_GC2	K1_vs_KC1	K3_vs_GC1	KC1_vs_GC1	K2_vs_KC2	K4_vs_GC2	KC2_vs_GC2
up-regulated	2150	1253	1209	463	1143	2186	1575	968	657	1007	1011	817	782	1103	3279	2340	779	1430	997	477
down-regulated	700	527	955	1013	768	896	777	867	599	600	1397	1192	1272	1336	1777	1996	1432	1411	1461	631
DEG Number	2850	1780	2164	1476	1911	3082	2352	1835	1256	1607	2408	2009	2054	2439	5056	4336	2211	2841	2458	1108

Figure 4.7. Distribution of the number of differentially expressed genes in different treatment groups

Note: Red represents up-regulation, blue represents down-regulation.

4.2.5 GO Enrichment Analysis of Differentially Expressed Genes

GO enrichment analysis (Figure 4.8) showed that the functional enrichment patterns of differentially expressed genes among different comparison groups were generally conserved and highly consistent. In biological process (BP), DEGs were significantly enriched in 23 GO terms, among which cellular process, metabolic process, biological regulation, and response to stimulus were the core enriched terms, indicating that the basic life activities and defense regulatory networks of pumpkin were highly conserved in response to the two biotic stresses. In cellular component (CC), DEGs were mainly located in cellular anatomical entity, intracellular, and

protein-containing complex, which were closely related to core functions such as cellular metabolism and signal transduction. In molecular function (MF), DEGs were mainly enriched in binding, catalytic activity, transcription regulator activity, and transporter activity, suggesting that differentially expressed genes mainly participated in disease and nematode resistance responses by regulating molecular binding, enzymatic reactions, and transcriptional regulation. Notably, resistant materials showed higher enrichment of relevant functional terms at the early stress stage (48 h after Fusarium infection, 24 h after root-knot nematode infection), and the regulation tended to be stable over time. In susceptible materials, a large number of genes were down-regulated at the late stress stage (96 h after Fusarium infection, 48 h after root-knot nematode infection), with more disordered functional regulation. These results indicated that the resistance differences between resistant and susceptible materials were closely related to the timing, intensity, and stability of stress responses.

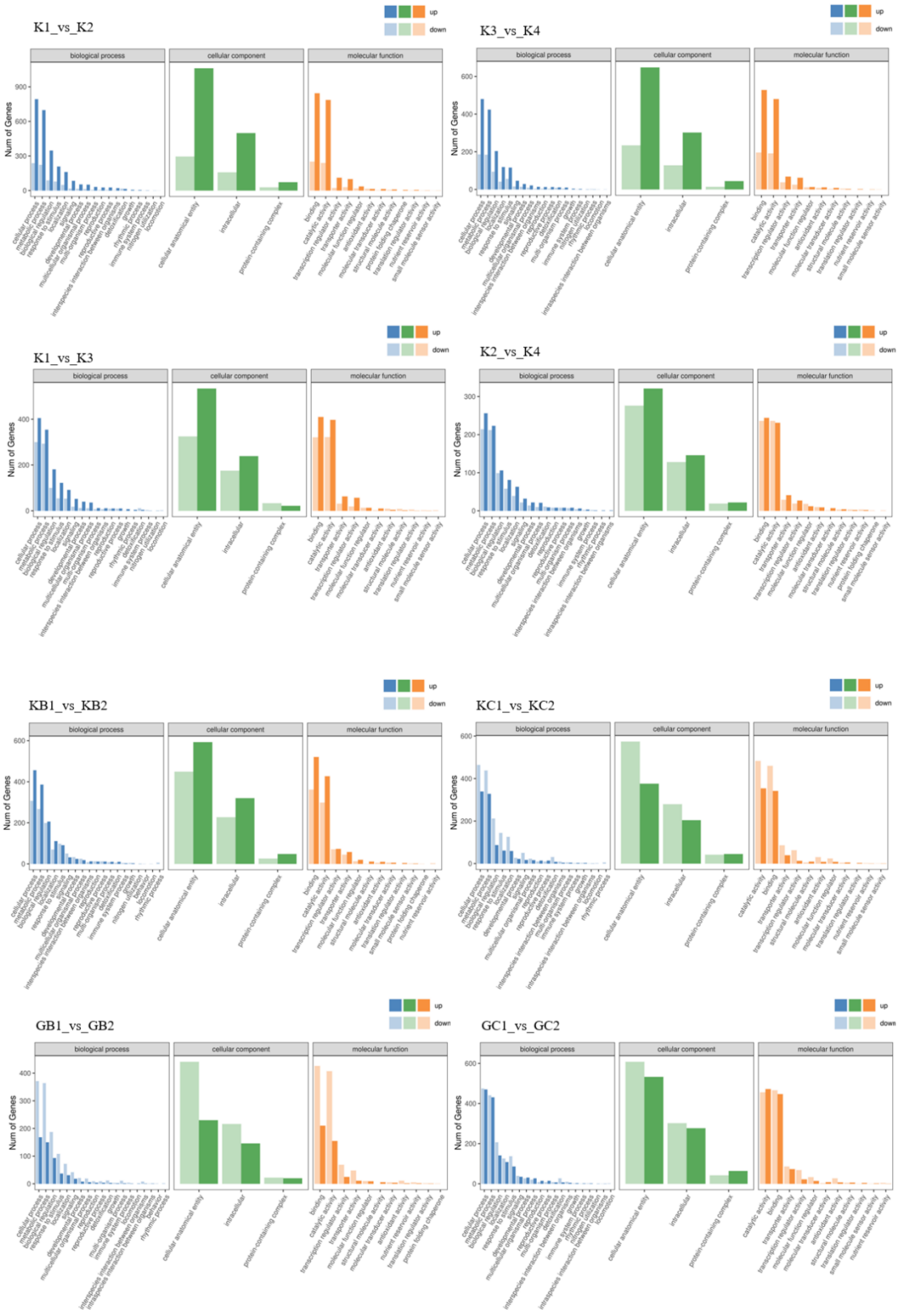
K1_vs_K2
K3_vs_K4
K1_vs_K3
K2_vs_K4
KB1_vs_KB2
KC1_vs_KC2
GB1_vs_GB2
GC1_vs_GC2
up
down
biological process
cellular component
molecular function
Num of Genes

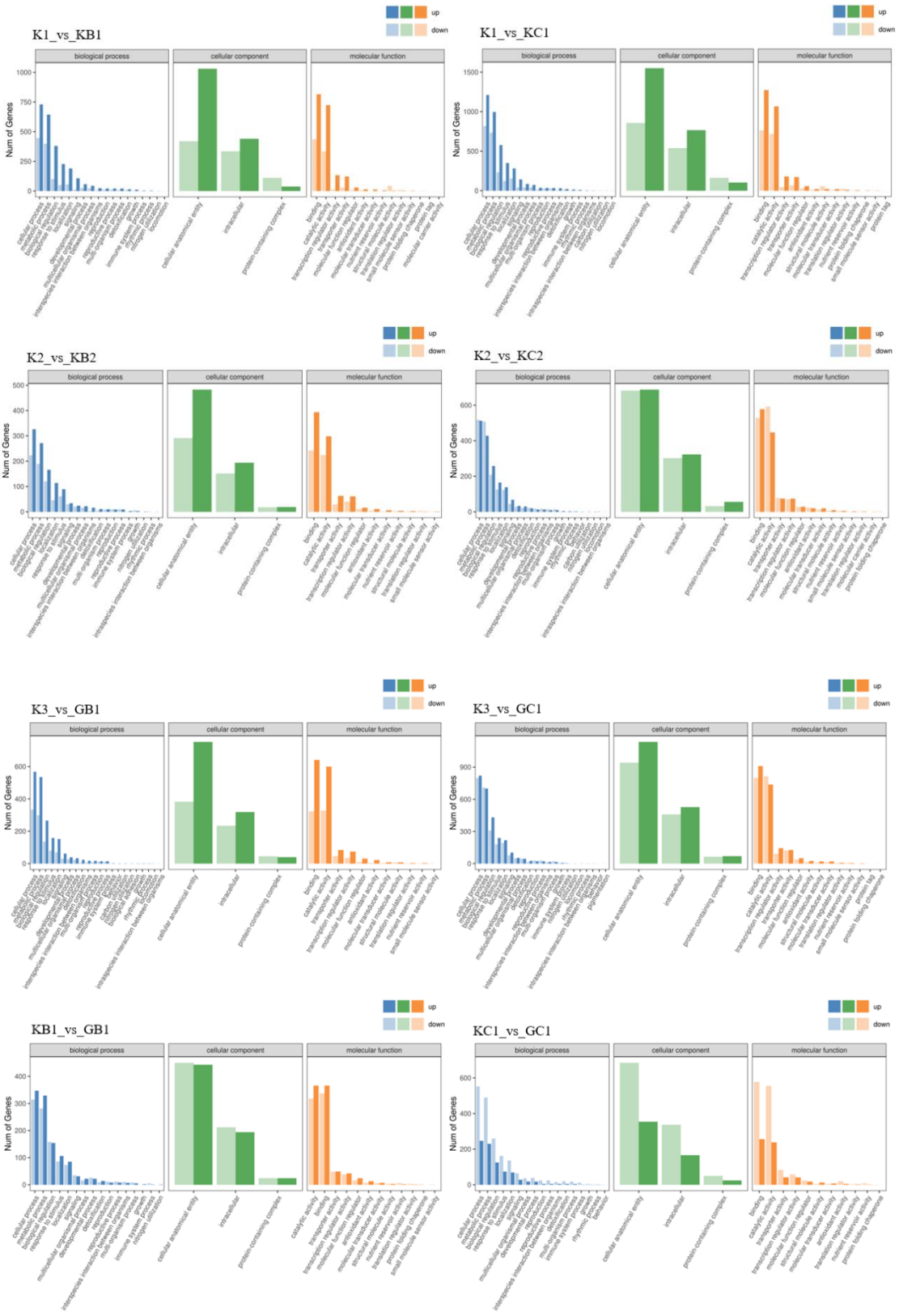
K1_vs_KB1
K1_vs_KC1
K2_vs_KB2
K2_vs_KC2
K3_vs_GB1
K3_vs_GC1
KB1_vs_GB1
KC1_vs_GC1
up
down
Num of Genes
biological process
cellular component
molecular function

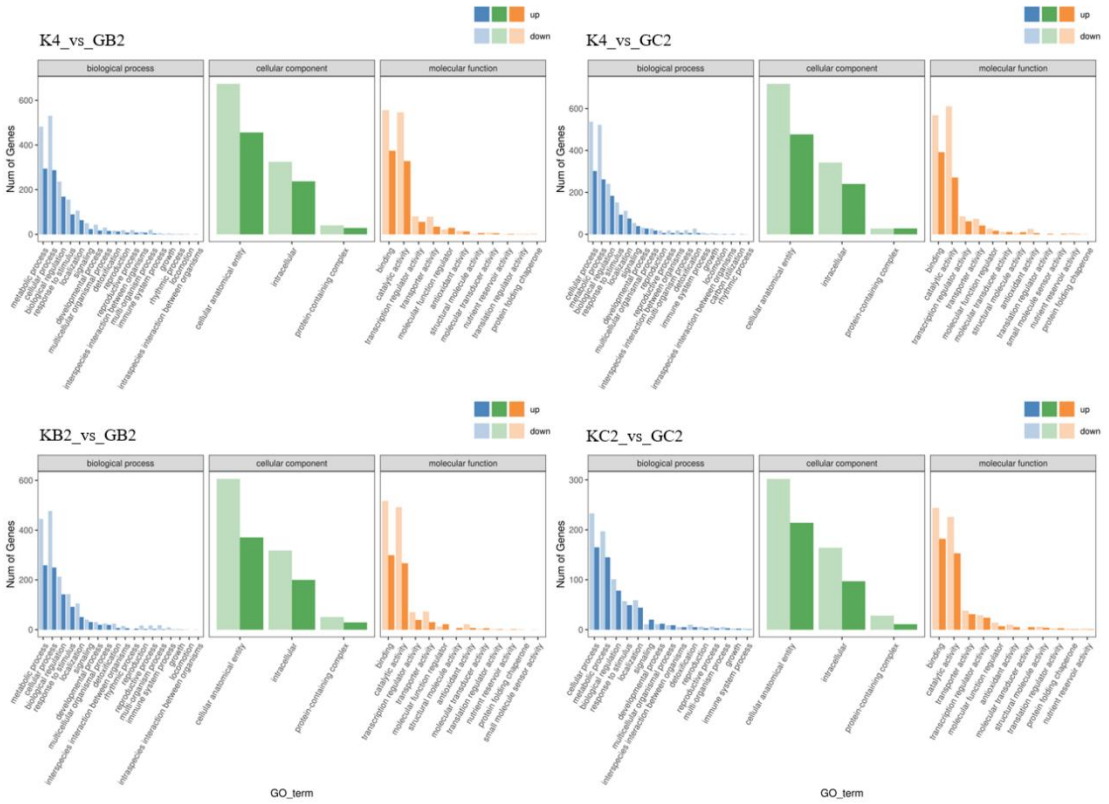

Figure 4.8. Significant GO function analysis of differentially expressed genes in each treatment group

4.2.6 KEGG Metabolic Pathway Analysis of Differentially Expressed Genes

KEGG enrichment analysis (Figure 4.9) showed that under infection by Fusarium oxysporum and root-knot nematode, the differentially expressed genes (DEGs) of different comparison groups exhibited highly consistent core characteristics in metabolic pathway enrichment, as well as specificity related to stress type and resistance difference. DEGs in all groups were significantly enriched in defense and metabolic pathways including Plant-pathogen interaction, MAPK signaling pathway-plant, Plant hormone signal transduction, Phenylpropanoid biosynthesis, and alpha-Linolenic acid metabolism, indicating that the core defense regulatory network of pumpkin was conserved in response to the two biotic stresses.

Under Fusarium oxysporum infection, antioxidant and secondary metabolic pathways such as Glutathione metabolism and Phenylalanine metabolism were more prominently enriched. Under root-knot nematode infection, basic metabolic pathways such as Carbon metabolism and Biosynthesis of amino acids, as well as membrane lipid-related pathways such as Biosynthesis of unsaturated fatty acids, were more significantly enriched, reflecting different infection strategies of different pathogens. At the early stress stage (48 h after Fusarium infection, 24 h after root-knot nematode infection), resistant materials showed higher enrichment and more precise regulation of core defense pathways. At the late stress stage (96 h after Fusarium infection, 48 h after root-knot nematode infection), susceptible materials showed disorder in more basic metabolic pathways and decreased enrichment of defense pathways, indicating that resistance differences were closely related to the timing, regulatory stability, and activation intensity of core pathways in stress responses.

K1_vs_K2

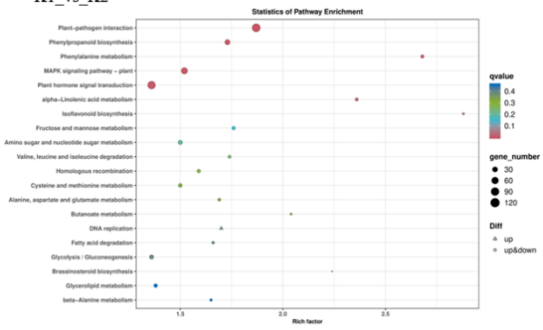

K3_vs_K4

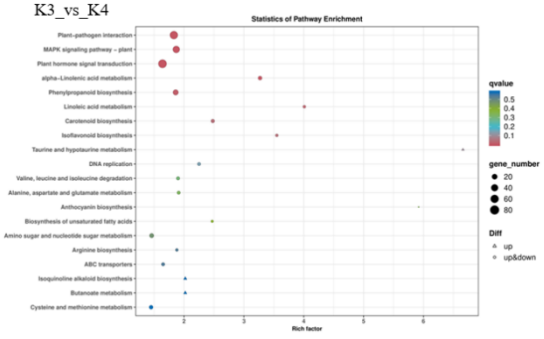

K1_vs_K3

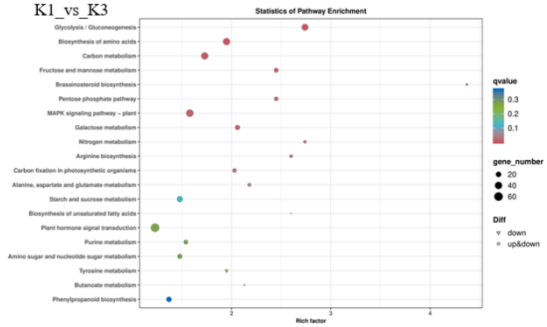

K2_vs_K4

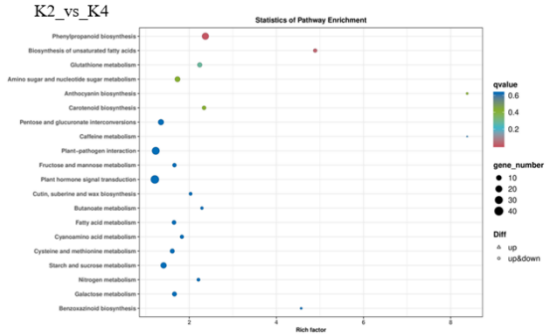

KB1_vs_KB2

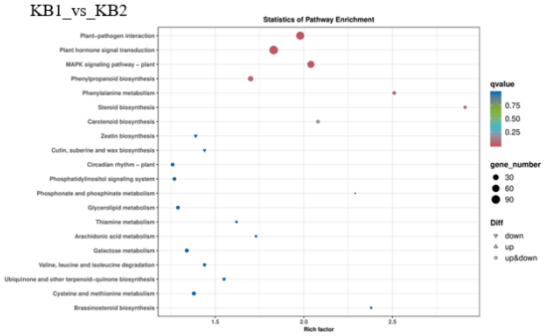

KC1_vs_KC2

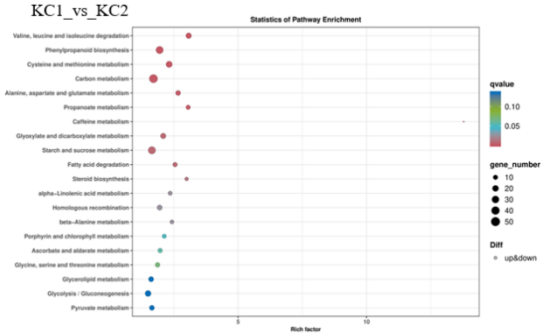

GB1_vs_GB2

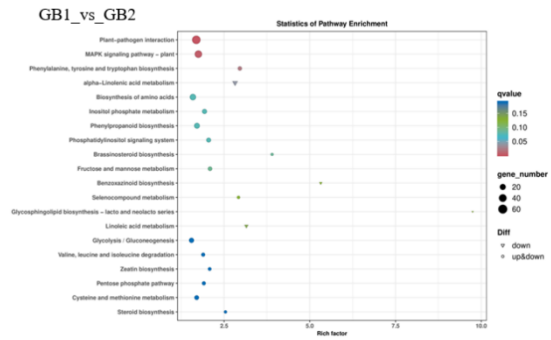

GC1_vs_GC2

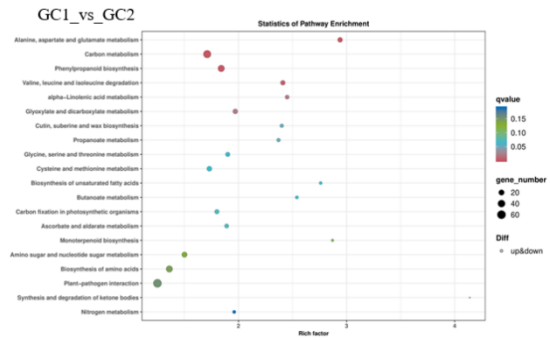

K1_vs_KB1

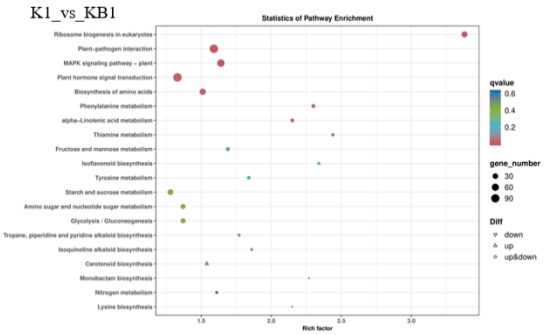

K1_vs_KC1

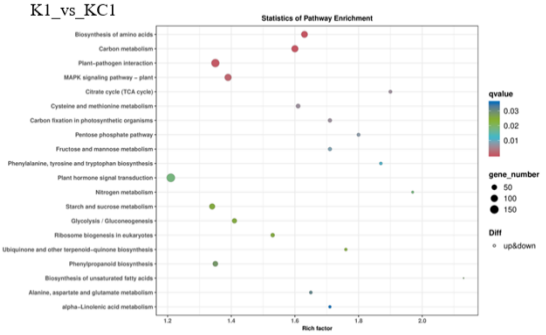

K2_vs_KB2

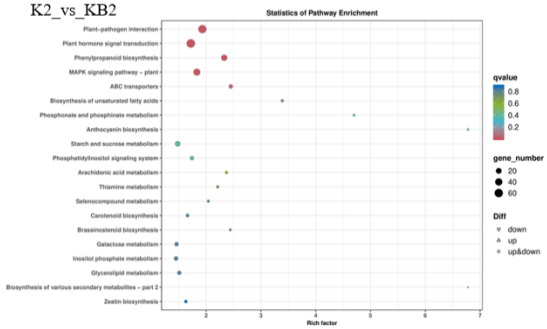

K2_vs_KC2

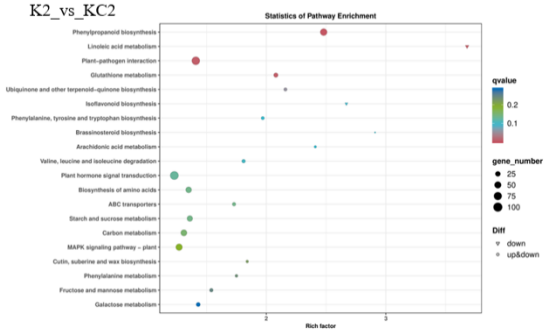

K3_vs_GB1

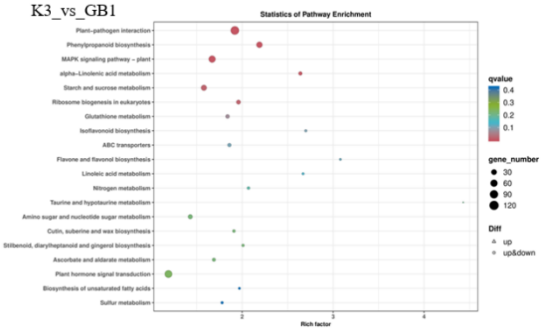

K3_vs_GC1

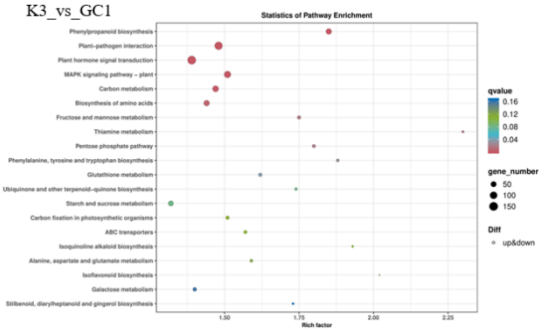

KB1_vs_GB1

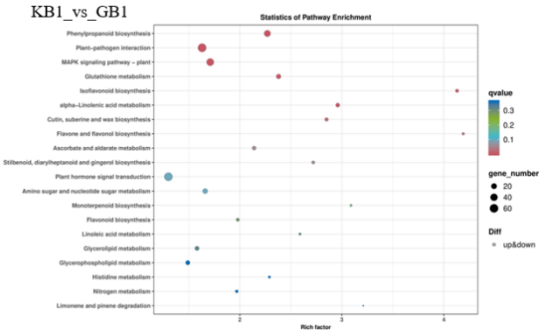

KC1_vs_GC1

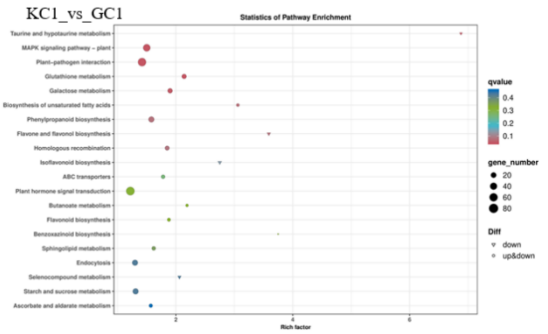

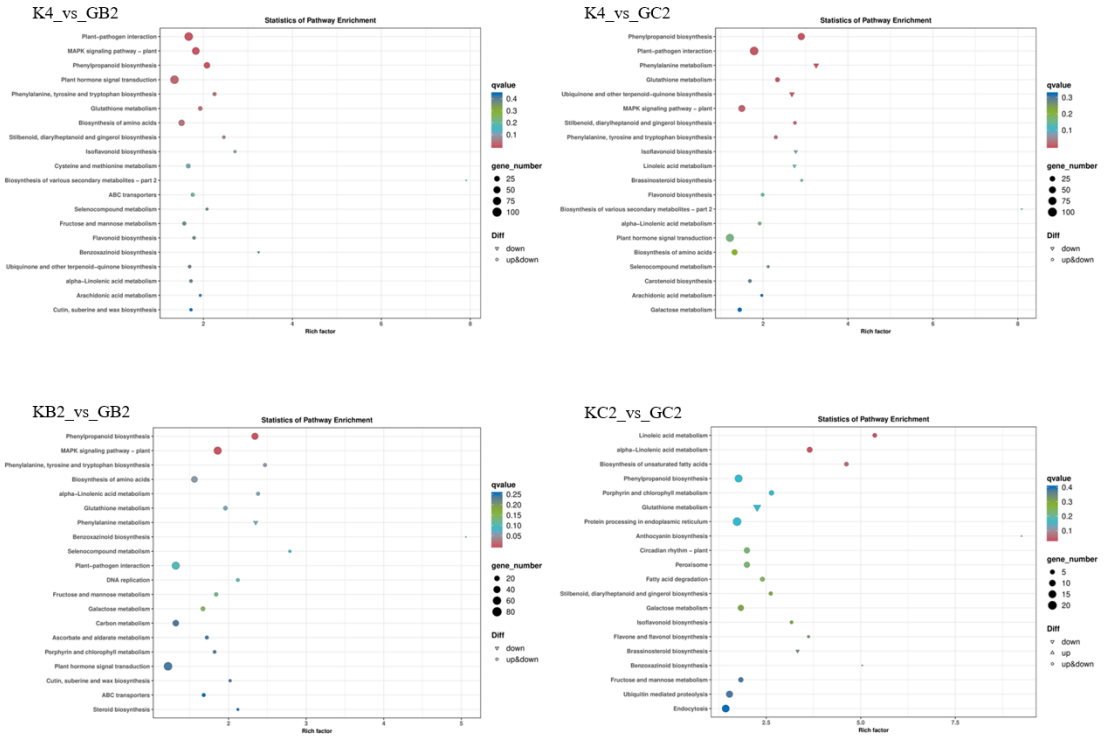

Figure 4.9. Top 20 bubble plots of KEGG enrichment for DEGs in each treatment group

Note: The X-axis represents the enrichment score. Larger bubbles indicate more DEGs included in the term. The color of the bubble represents the enrichment *p*-value: smaller *p*-value indicates higher significance.

4.2.7 Expression Pattern Analysis of Core Immune Pathways and Key Genes

Analysis of the plant–pathogen interaction pathway (ko04626) and core genes showed that the heatmap (Figure 4.10-A) revealed significant differentiation in the overall expression pattern of this pathway between resistant and susceptible pumpkin materials. After treatment with fusarium wilt and root-knot nematode stress, a large number of differentially expressed genes in this pathway showed a significant up-regulation trend in resistant materials, while susceptible materials mainly

exhibited gene down-regulation. Further cluster analysis showed that samples under the same stress type and time point clustered closely, confirming good experimental repeatability and high data reliability.

To identify core regulatory nodes in the pathway, the expression characteristics of three key immune genes, *RBOH (CmoCh04G007610), PR1 (CmoCh01G015070)*, and *FLS2 (CmoCh18G008180)*, were further validated (Figure 4.10-B). The results showed that: *RBOH*, a respiratory burst oxidase homolog gene involved in both the MAPK signaling pathway and plant–pathogen interaction pathway, was specifically and highly expressed in resistant materials under both stresses, serving as a broad-spectrum key regulatory gene for pumpkin resistance to biotic stress. The expression patterns of *PR1* (receptor tyrosine kinase CEPR1) and *FLS2* (LRR receptor kinase) showed stress-specific differentiation. *PR1* was significantly more highly expressed in susceptible materials under root-knot nematode treatment. *FLS2* was sharply up-regulated in resistant materials under fusarium wilt stress. These results indicated that pumpkin defends against different pathogens through a pattern dominated by broad-spectrum resistance genes and coordinated by stress-specific genes. *RBOH*, *PR1*, and *FLS2* play distinct regulatory roles in signal transduction, pathogen recognition, and stress response, respectively, and jointly constitute the molecular basis of disease resistance in pumpkin. This provides key candidate genes and theoretical support for further dissecting the stress resistance mechanism and molecular breeding of pumpkin.

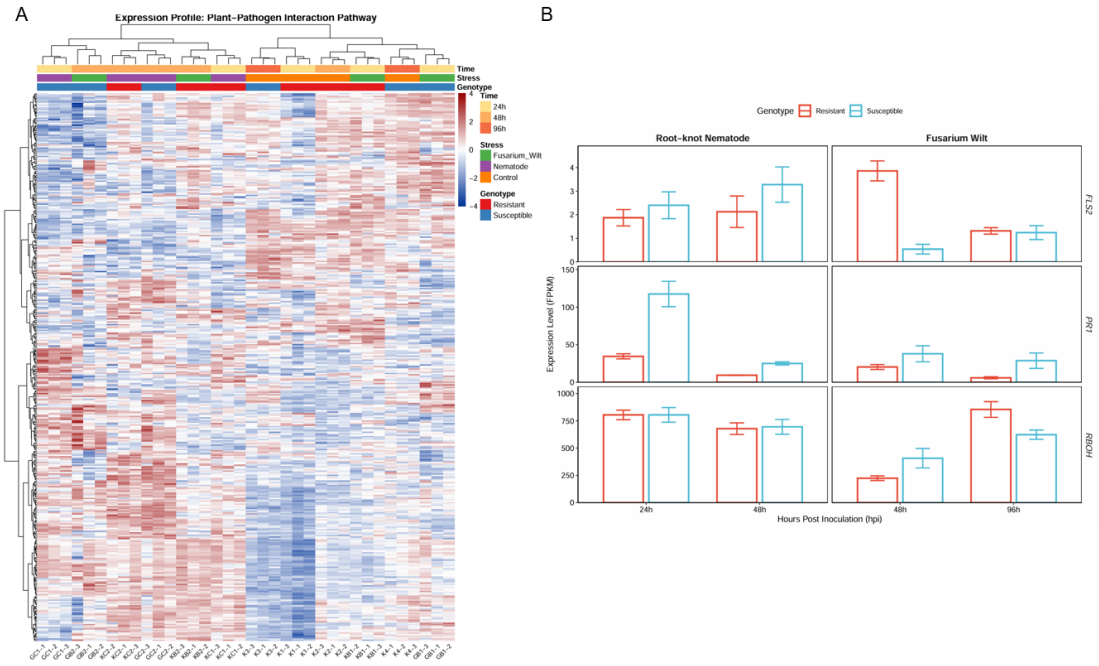

Figure 4.10. Analysis of the plant–pathogen interaction pathway and expression patterns of core genes

(A) Heatmap of gene expression in the plant–pathogen interaction pathway.

Rows represent differentially expressed genes in the pathway; columns represent different treated samples. The color bars at the top indicate the time point (Time), stress type (Stress), and genotype (Genotype) of samples. Color changes from blue to red indicate increasing gene expression levels (row-standardized values).

(B) Expression levels of core immune genes under different stresses.

The figure shows the mean FPKM values (± SD) of three core immune genes *RBOH*, *PR1*, and *FLS2* in resistant and susceptible pumpkin materials under root-knot nematode and fusarium wilt stresses.

4.2.8 WGCNA Analysis of Differentially Expressed Genes

4.2.8.1 Global Module Construction and Trait Association

To systematically dissect the molecular regulatory mechanism of pumpkin in response to *Fusarium* oxysporum, root-knot nematode infection, and disease resistance, weighted gene co-expression network analysis (WGCNA) was performed based on transcriptome sequencing data to construct a global gene co-expression network. A total of 13,299 differentially expressed genes were combined from *Fusarium* and nematode samples. After filtering out low-expression and low-variation genes, 10,000 genes were finally selected for WGCNA construction. When the optimal soft threshold $\beta = 12$, R^2 approached 0.8 and the average connectivity tended to 0, indicating that this power value could generate a qualified scale-free network (Figure 4.11). Meanwhile, a hierarchical clustering tree was constructed. Using the dynamic tree cut algorithm, genes with significantly synergistic expression patterns were clustered into independent co-expression modules, and 33 differentially expressed co-expression modules were finally obtained (Figure 4.12). The modules showed reasonable size distribution, with the number of genes ranging from 44 to 1,263. The largest module was ME1 and the smallest was ME32 (Figure 4.13).

To screen core co-expression modules closely associated with target traits, the correlations between module eigengenes and three key traits (disease resistance, *Fusarium* infection, and nematode infection) were further analyzed (Figure 4.12-B). Using the screening criteria of absolute correlation $|r| \geq 0.6$ and $p < 0.05$, 6 specific

co-expression modules significantly associated with target traits were identified. ME17 showed an extremely strong positive correlation with disease resistance (r = 0.98, p < 5e-25). ME9 showed an extremely strong negative correlation with disease resistance (r = -0.89, p < 4e-13). Both modules jointly participate in the bidirectional regulation of plant disease resistance. ME20 was strongly positively correlated with *Fusarium* infection (r = 0.70, p < 3e-06). ME26 was strongly negatively correlated with *Fusarium* infection (r = -0.76, p < 7e-08), representing specific functional modules in response to *Fusarium* infection. ME5 was strongly positively correlated with nematode infection (r = 0.69, p < 3e-06). ME23 was strongly negatively correlated with nematode infection (r = -0.65, p < 2e-05), mediating specific responses to root-knot nematode infection.

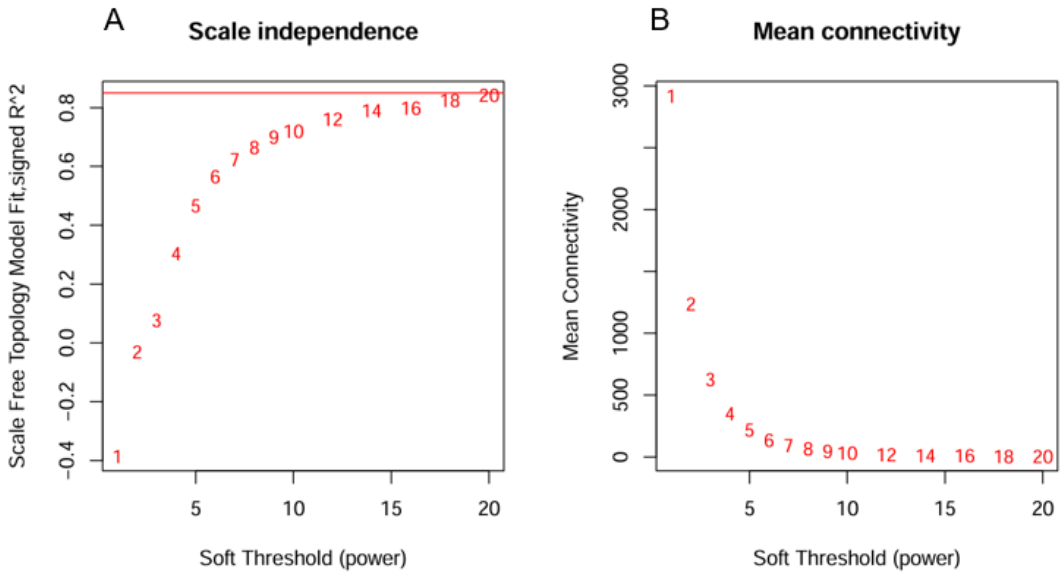

Figure 4.11. Determination of soft threshold power value

(A) Scale-free network model diagram; (B) Network average connectivity.

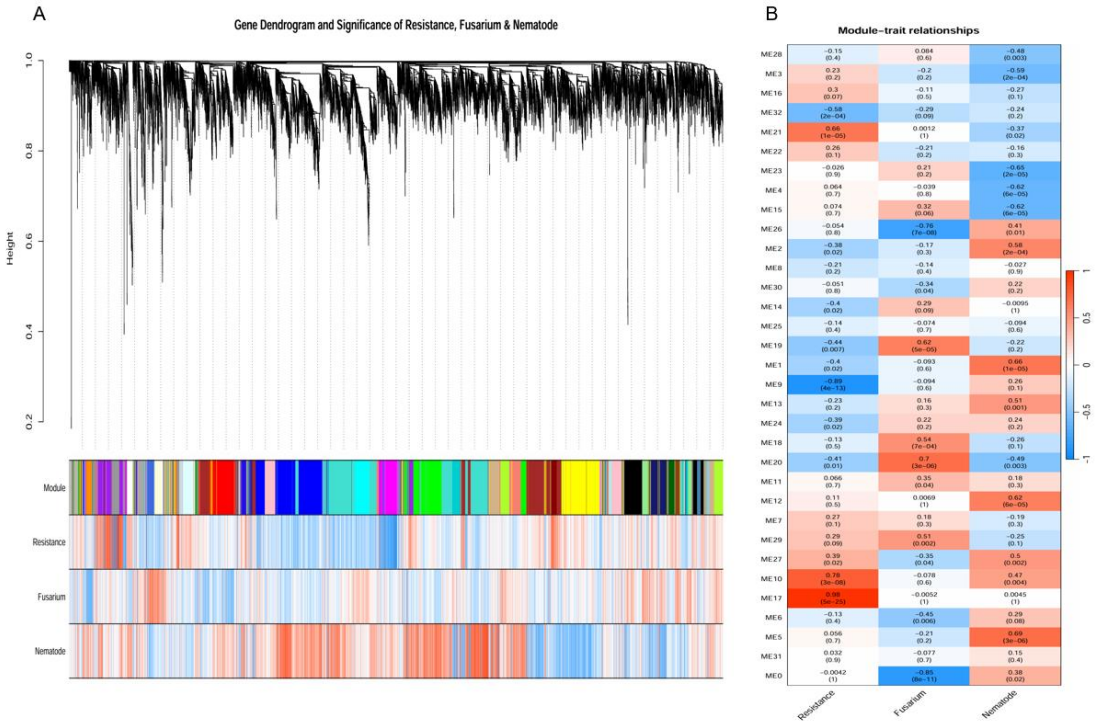

Figure 4.12. Weighted gene co-expression network analysis

(A) Hierarchical clustering tree and module division diagram;

(B) Correlation heatmap between co-expressed gene modules and traits.

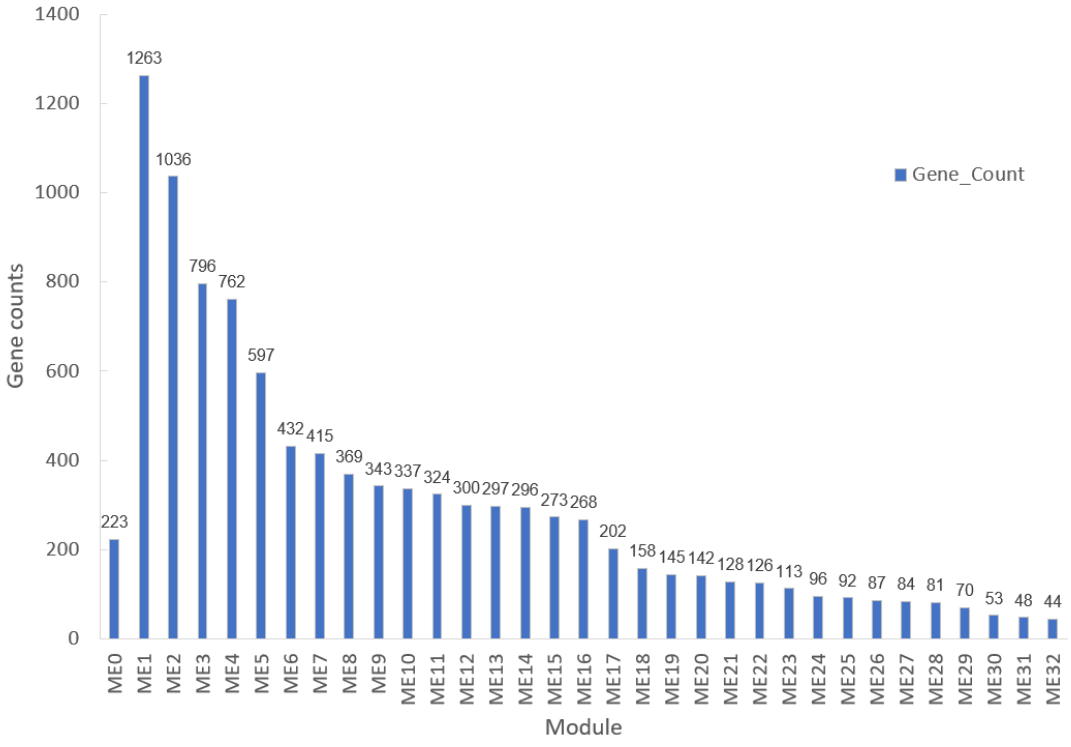

Figure 4.13. Distribution of gene number in each module

4.2.8.2 Detailed Analysis of Core Modules

4.2.8.2.1 Resistance-Related Modules: ME17 (+), ME9 (−)

Module-trait association analysis showed that ME17 was extremely significantly positively correlated with plant resistance ($r = 0.98$, $p < 5e\text{-}25$), and ME9 was extremely significantly negatively correlated with resistance ($r = -0.89$, $p < 4e\text{-}13$). Further tests on the expression differences of module eigengenes (Figure 4.14-A, 4.14-B) showed that the eigengene expression of ME17 was significantly higher in resistant samples than in susceptible samples ($P < 5.41e\text{-}25$), while the eigengene of ME9 was markedly up-regulated in susceptible samples ($P < 6.94e\text{-}10$). Their expression patterns were consistent with module-trait correlation results, indicating that ME17 positively regulates resistance, while ME9 negatively regulates resistance. On this basis, the overall expression patterns of genes within the modules were analyzed (Figure 4.14-C, 4.14-D). Genes in ME17 and ME9 both showed co-expression trends highly consistent with the module eigengenes, further confirming the stability and reliability of module expression. GO/KEGG enrichment analysis (Figure 4.14-E, 4.14-F) revealed that: ME17 was significantly enriched in disease resistance-related pathways, including PR protein synthesis, ROS scavenging, and salicylic acid signal transduction, serving as a key module involved in resistance activation. ME9 was mainly enriched in processes related to cell growth and gibberellin signaling pathways, suggesting that plants may coordinate and allocate resources between defense responses and growth/development under biotic stress.

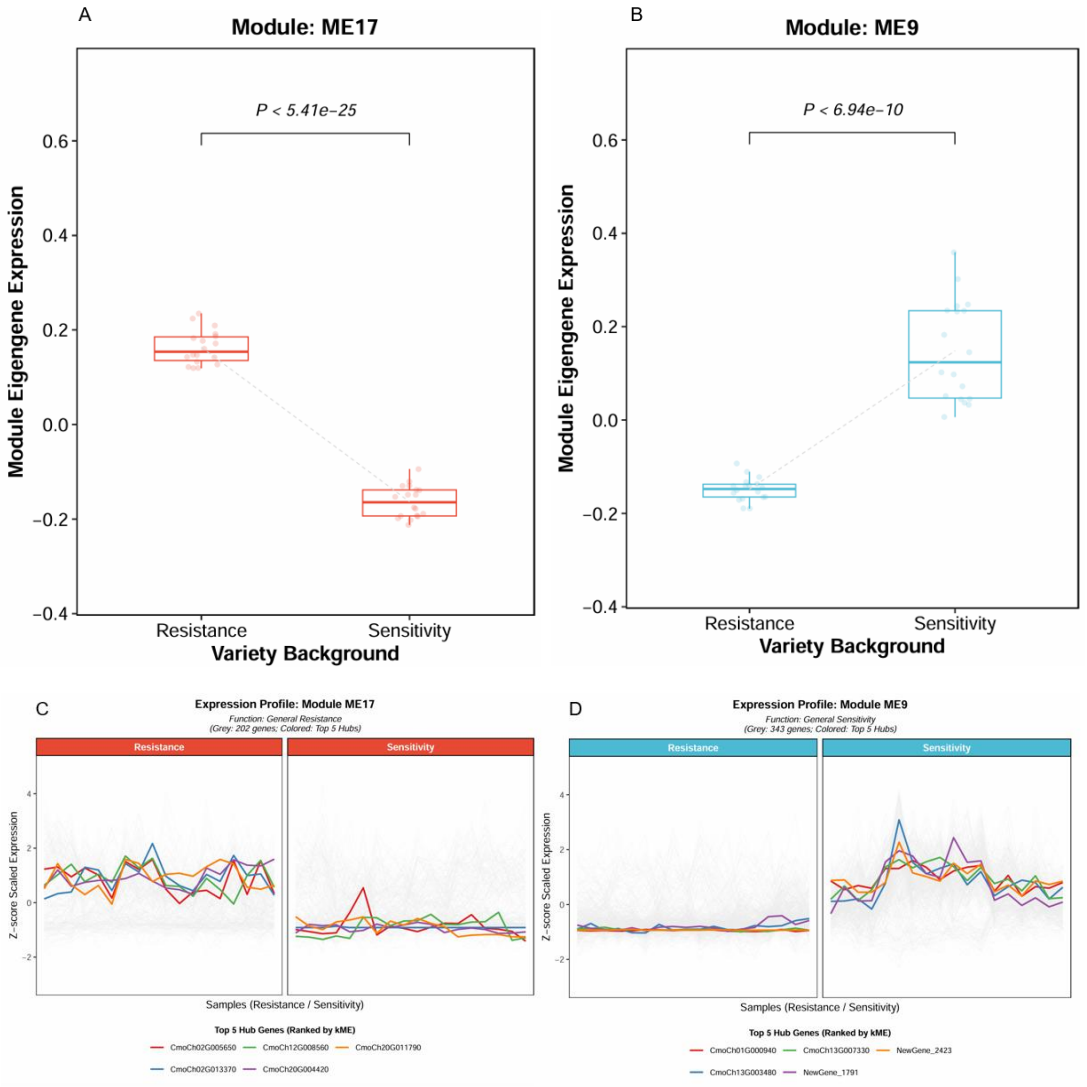
A
Module: ME17
P < 5.41e−25
Module Eigengene Expression
0.6
0.4
0.2
0.0
−0.2
−0.4
Resistance
Sensitivity
Variety Background
B
Module: ME9
P < 6.94e−10
Module Eigengene Expression
0.6
0.4
0.2
0.0
−0.2
−0.4
Resistance
Sensitivity
Variety Background
C
Expression Profile: Module ME17
Function: General Resistance
(Grey: 202 genes; Colored: Top 5 Hubs)
Resistance
Sensitivity
Z-score Scaled Expression
Samples (Resistance / Sensitivity)
Top 5 Hub Genes (Ranked by kME)
CmoCh02G005650
CmoCh12G008560
CmoCh20G011790
CmoCh02G013370
CmoCh20G004420
D
Expression Profile: Module ME9
Function: General Sensitivity
(Grey: 343 genes; Colored: Top 5 Hubs)
Resistance
Sensitivity
Z-score Scaled Expression
Samples (Resistance / Sensitivity)
Top 5 Hub Genes (Ranked by kME)
CmoCh01G000940
CmoCh13G007330
NewGene_2423
CmoCh13G003480
NewGene_1791

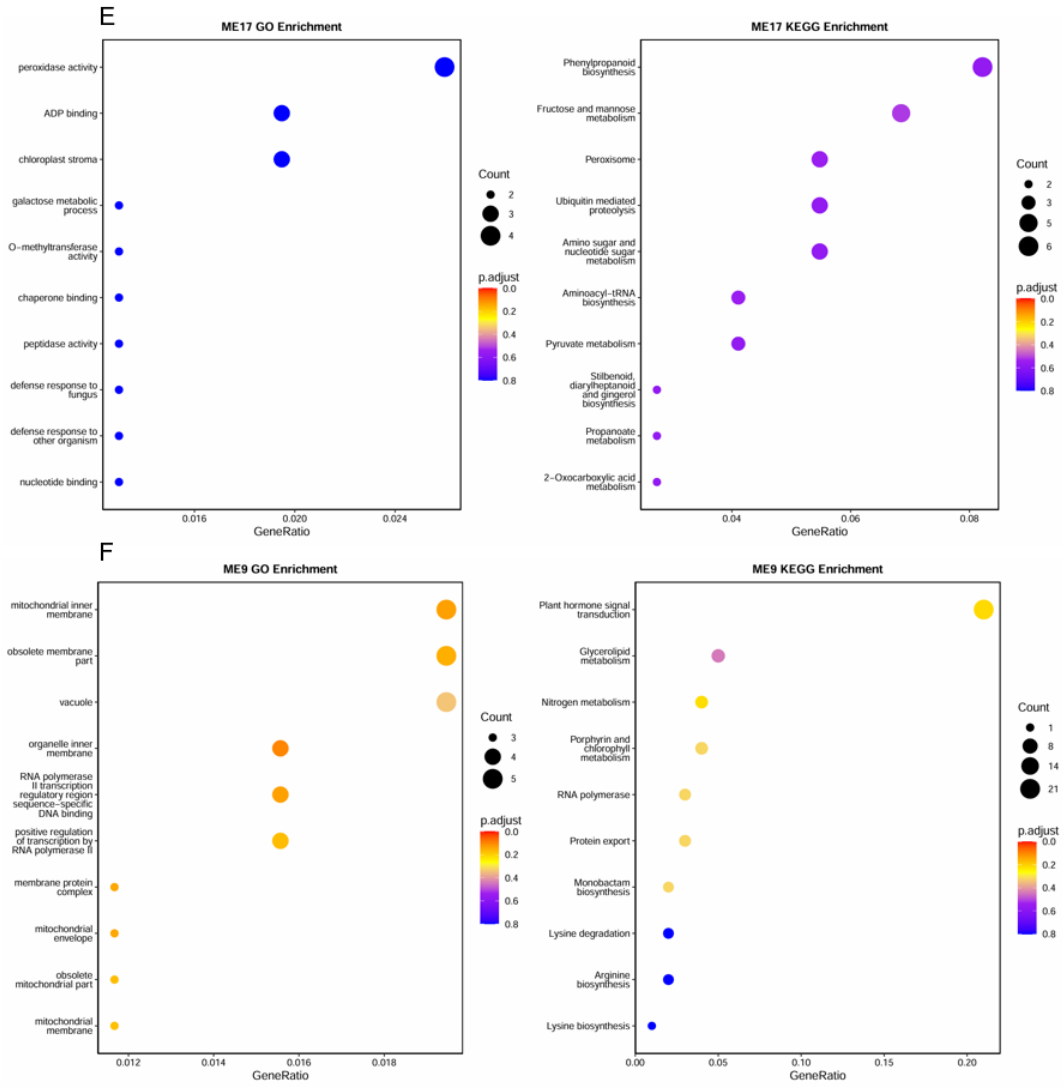

Figure 4.14. Expression patterns and functional enrichment analysis of ME17 and ME9 modules

A–B: Boxplots of module eigengene expression for ME17 (A) and ME9 (B) in high-resistance and low-resistance samples;

C–D: Heatmaps of gene expression in ME17 (C) and ME9 (D) modules. Samples were grouped by high-resistance and low-resistance;

E–F: Bubble plots of GO/KEGG enrichment analysis for genes in ME17 (E) and ME9 (F) modules.

4.2.8.2.2 Fusarium-Specific Response Modules: ME20 (+), ME26 (−)

For the specific response to fusarium wilt stress, module-trait association analysis showed that ME20 was significantly positively correlated with plant fusarium wilt resistance ($r = 0.32$, $p < 0.017$), while ME26 showed no significant correlation with fusarium wilt resistance ($P > 0.05$). Further tests on the expression differences of module eigengenes (Figure 4.15-A, 4.15-B) showed that the eigengene expression of ME20 was significantly higher in resistant samples than in susceptible samples ($P < 0.017$), whereas the eigengene of ME26 showed no significant expression difference between resistant and susceptible samples ($P > 0.05$). Their expression patterns were consistent with module-trait correlation results, indicating that ME20 may positively regulate fusarium wilt-specific resistance, while ME26 showed no significant regulatory association with fusarium wilt resistance in this study. On this basis, the overall expression patterns of genes within the modules were analyzed (Figure 4.15-C, 4.15-D). Genes in ME20 showed a co-expression trend highly consistent with the module eigengene, further confirming the stability and reliability of module expression. Genes in ME26 showed relatively dispersed expression patterns, which was consistent with its lack of significant association with resistance. GO/KEGG enrichment analysis (Figure 4.15-E, 4.15-F) revealed that: ME20 was significantly enriched in pathways closely related to fusarium wilt resistance, including plant–pathogen interaction, phenylpropanoid metabolism, and response to biotic stress, serving as a key module involved in the activation of fusarium wilt-specific resistance. ME26 was mainly enriched in basic metabolic processes such as starch and sucrose metabolism and amino acid

metabolism, suggesting that it is more likely involved in basic physiological functions rather than specific resistance regulation.

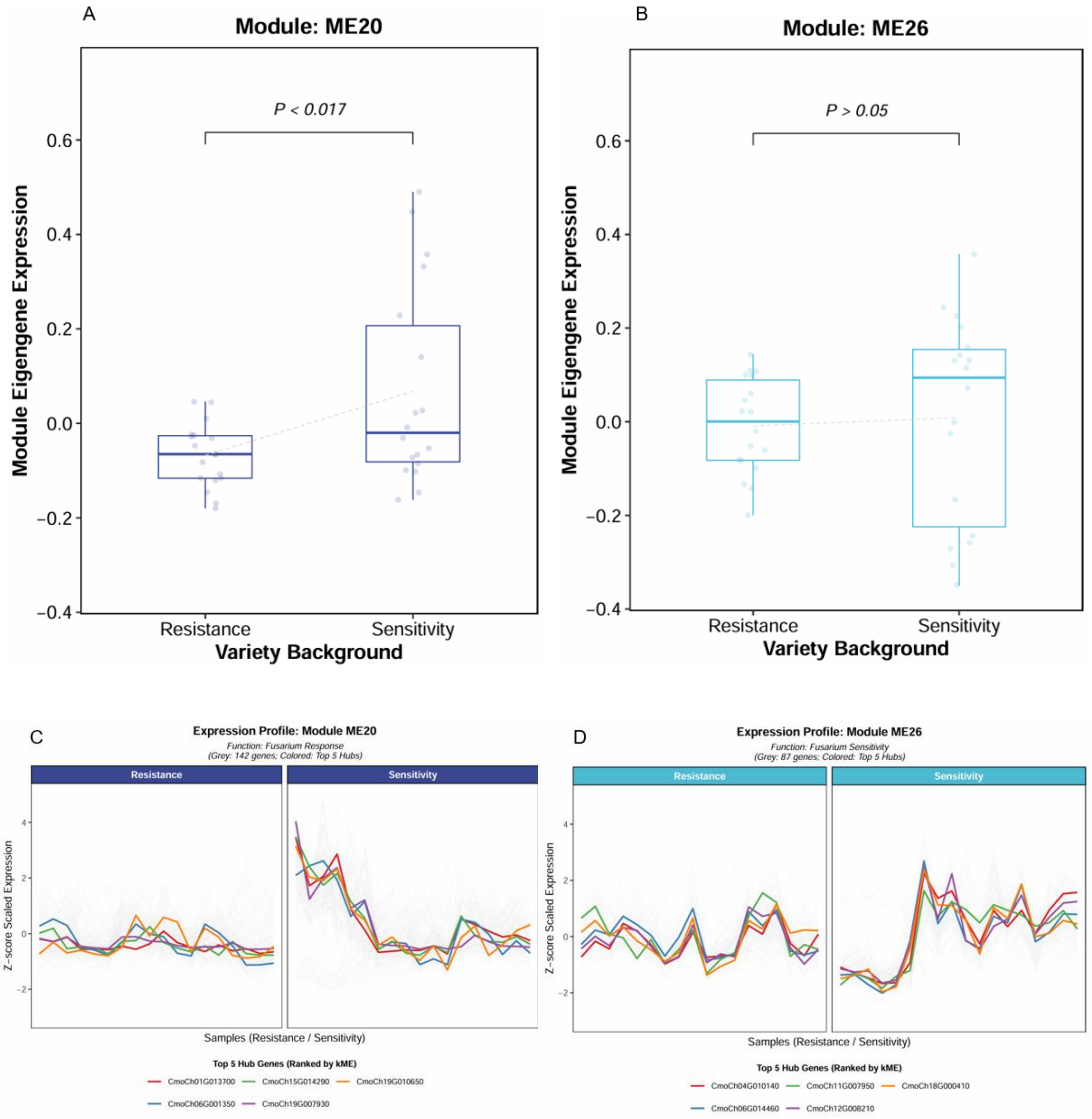

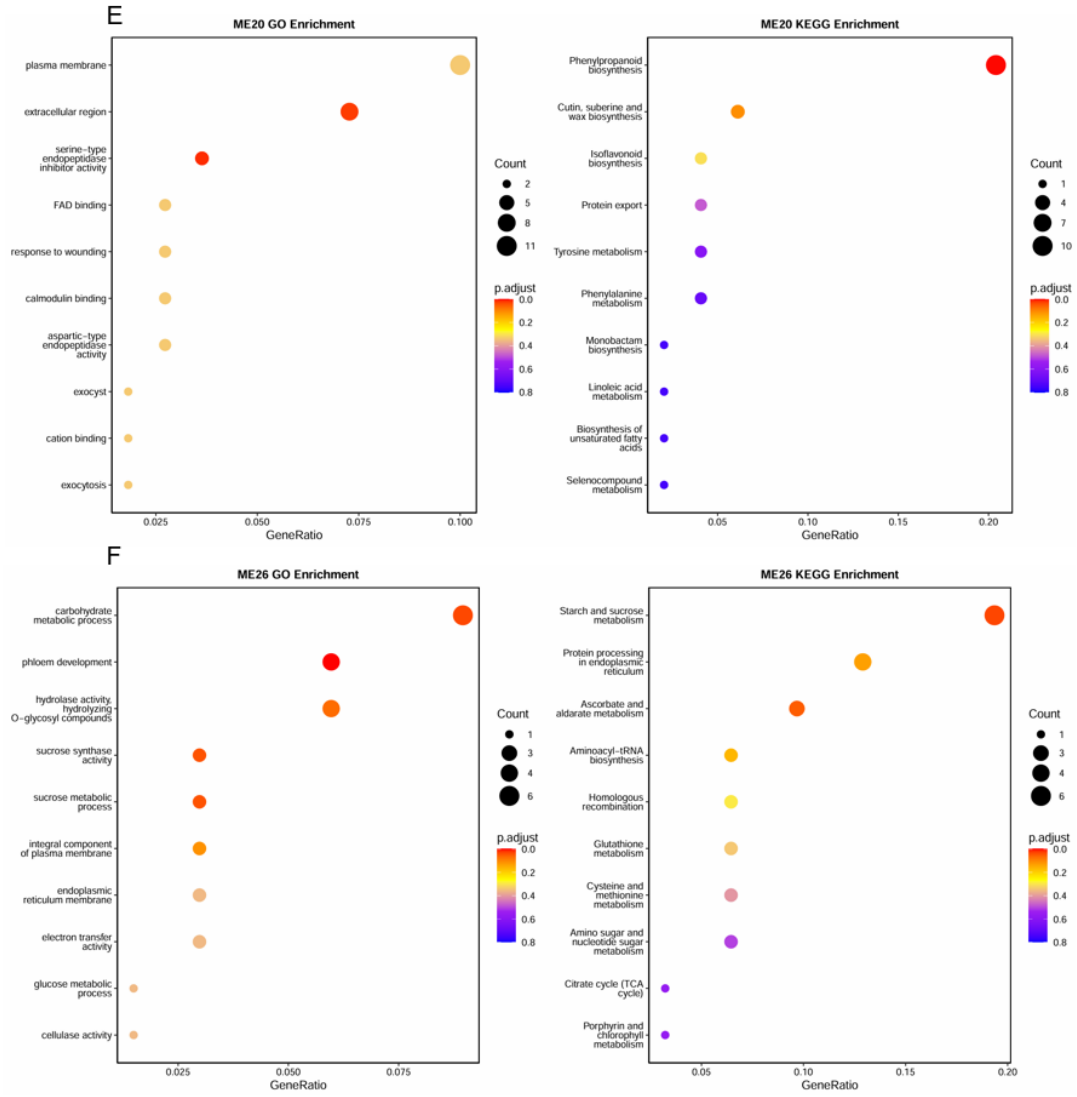

Figure 4.15. Expression patterns and functional enrichment analysis of ME20 and ME26 modules

A–B: Boxplots of module eigengene expression for ME20 (A) and ME26 (B) in high-resistance and low-resistance samples;

C–D: Heatmaps of gene expression in ME20 (C) and ME26 (D) modules. Samples were grouped by high-resistance and low-resistance;

E–F: Bubble plots of GO/KEGG enrichment analysis for genes in ME20 (E) and ME26 (F) modules.

4.2.8.2.3 Root-Knot Nematode-Specific Response Modules: ME5 (+), ME23 (−)

For the specific response to root-knot nematode stress, module-trait association analysis showed that ME5 had no significant correlation with plant root-knot nematode resistance ($P > 0.05$), and ME23 also showed no significant correlation with root-knot nematode resistance ($P > 0.05$). Further tests on the expression differences of module eigengenes (Figure 4.16-A, 4.16-B) showed that the eigengene of ME5 exhibited no significant expression difference between resistant and susceptible samples ($P > 0.05$), and the eigengene of ME23 also showed no significant difference between resistant and susceptible samples ($P > 0.05$). Their expression patterns were consistent with the module-trait correlation results. ME5 and ME23 showed no significant regulatory association with root-knot nematode resistance in this study. On this basis, the overall expression patterns of genes within the modules were analyzed (Figure 4.16-C, 4.16-D). Genes in both ME5 and ME23 showed relatively dispersed expression patterns, without highly consistent co-expression trends with the module eigengenes, which was consistent with their lack of significant association with resistance. GO/KEGG enrichment analysis (Figure 4.16-E, 4.16-F) revealed that: ME5 was significantly enriched in processes including plant–pathogen interaction, RNA transport, and base excision repair, suggesting that it may participate in the regulation of plant basal immunity and general stress responses. ME23 was mainly enriched in basic physiological processes such as homologous recombination, cell cycle, and amino acid metabolism, indicating that it is more involved in plant growth, development, and basal metabolism rather than

specific root-knot nematode resistance responses.

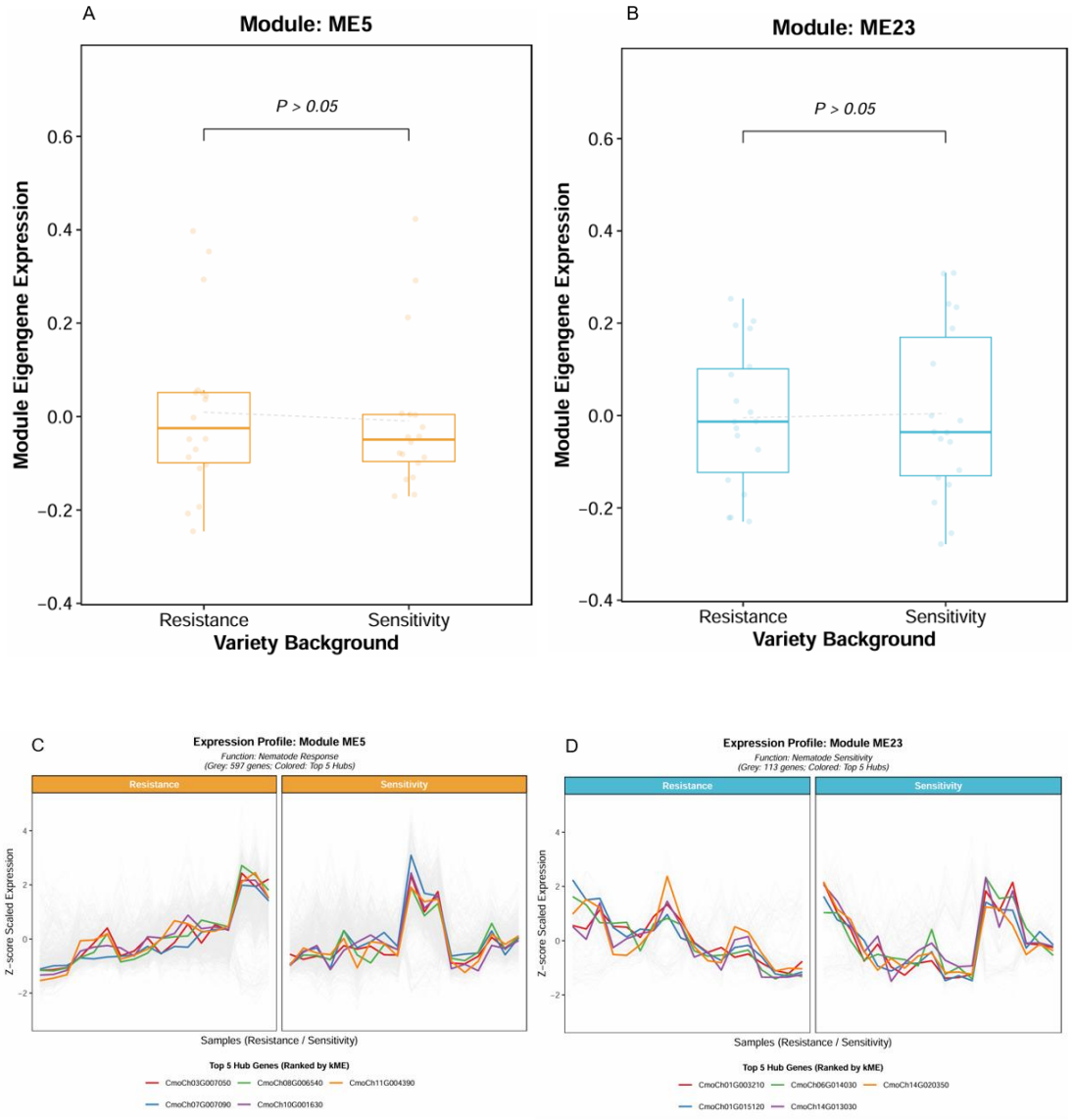

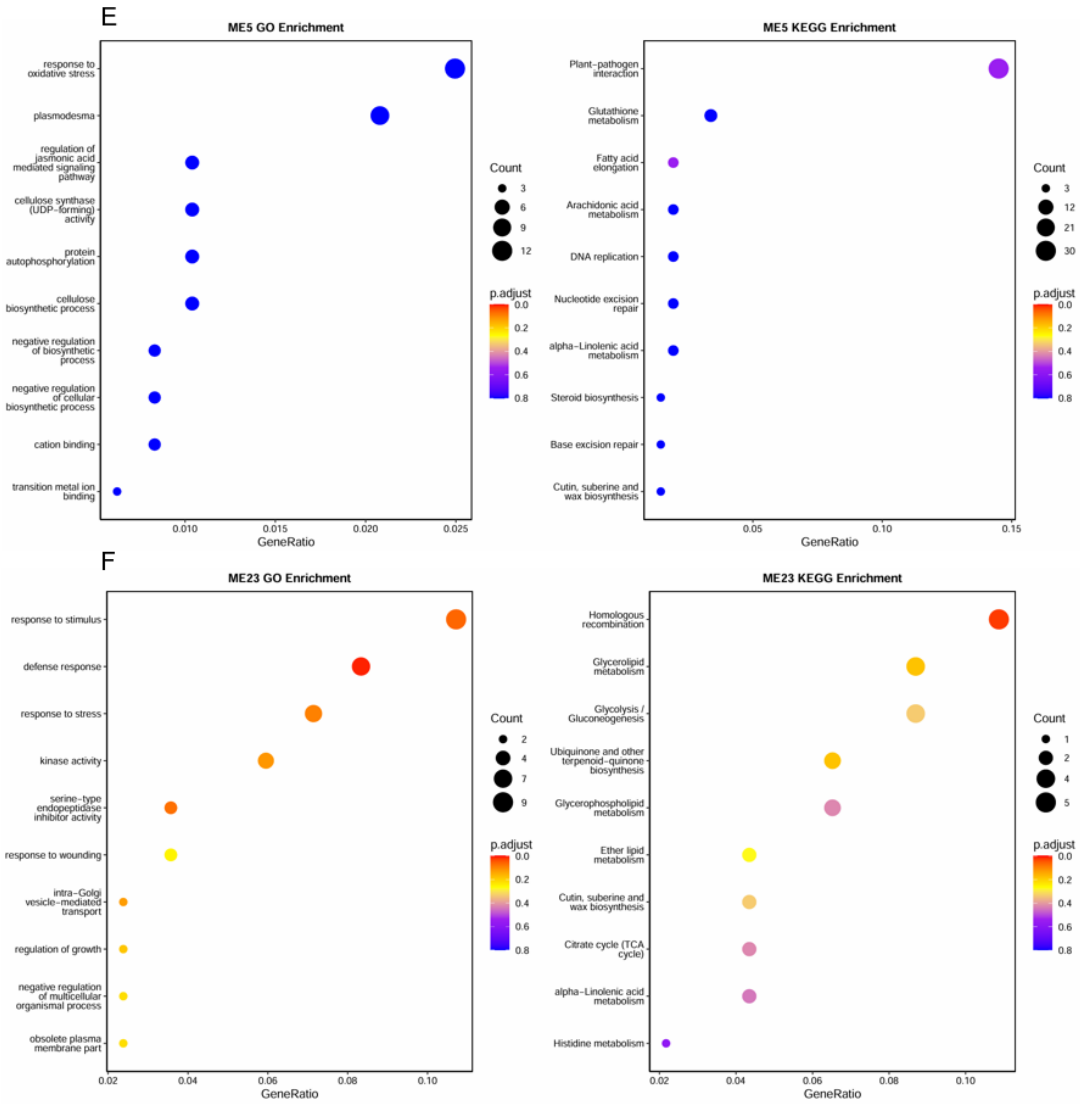

Figure 4.16. Expression patterns and functional enrichment analysis of ME5 and ME23 modules

A–B: Boxplots of module eigengene expression for ME5 (A) and ME23 (B) in high-resistance and low-resistance samples;

C–D: Heatmaps of gene expression in ME5 (C) and ME23 (D) modules. Samples were grouped by high-resistance and low-resistance;

E–F: Bubble plots of GO/KEGG enrichment analysis for genes in ME5 (E) and ME23 (F) modules.

4.2.8.2 Cross-Module Comparison and Global Validation

Comparative analysis of gene composition among the three core positively correlated disease-resistance modules (ME17, ME20, ME5) was performed. Venn diagram results (Figure 4.17-A) showed that the number of shared genes among the three modules was 0, and the proportion of unique genes in each module was 100%, indicating that plant resistance responses to different pathogens (general resistance, *Fusarium*, root-knot nematode) are highly pathogen-specific. Correlation heatmap of eigengenes from the six core modules (Figure 4.17-B) showed significant positive correlations among modules of the same type and significant negative correlations among modules of different types, confirming that the regulatory pattern of positive activation and negative inhibition is conserved in plant disease resistance responses. GO/KEGG enrichment analyses were performed on unique genes of the three positively correlated modules (Figure 4.17-C, 4.17-D). The results showed that: Unique genes in ME17 were significantly enriched in broad-spectrum defense pathways such as PR protein synthesis and salicylic acid signal transduction. Unique genes in ME20 were significantly enriched in *Fusarium*-specific resistance pathways such as phenylpropanoid metabolism and plant–pathogen interaction. Unique genes in ME5 were significantly enriched in root-knot nematode-specific response pathways such as RNA transport and base excision repair. These results indicate that when plants respond to different pathogenic stresses, conserved basal defense mechanisms coexist with specific response mechanisms activated against particular diseases.

A

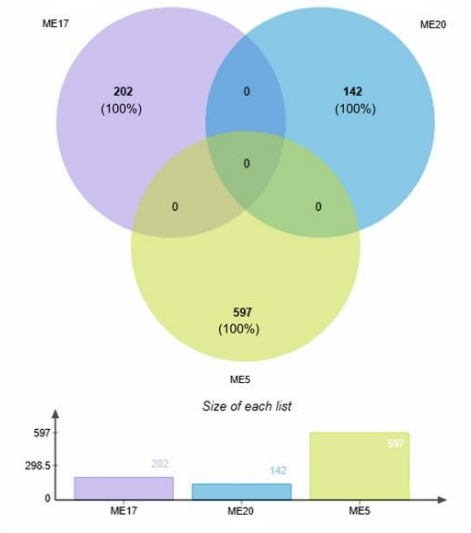
ME17
ME20
202
(100%)
0
142
(100%)
0
0
0
597
(100%)
ME5
Size of each list
597
298.5
0
202
142
597
ME17
ME20
ME5

B

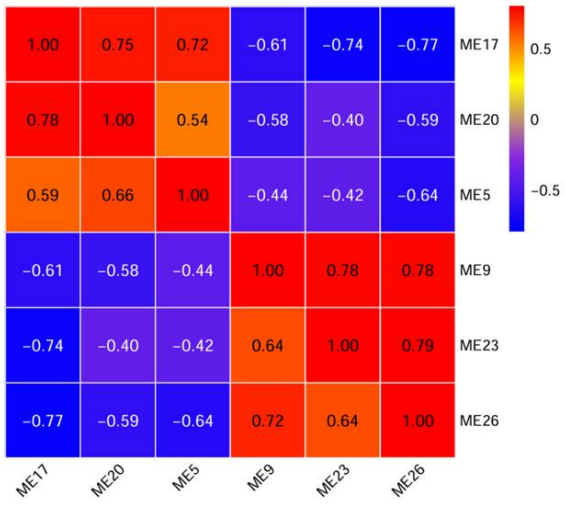
1.00 0.75 0.72 −0.61 −0.74 −0.77 ME17
0.78 1.00 0.54 −0.58 −0.40 −0.59 ME20
0.59 0.66 1.00 −0.44 −0.42 −0.64 ME5
−0.61 −0.58 −0.44 1.00 0.78 0.78 ME9
−0.74 −0.40 −0.42 0.64 1.00 0.79 ME23
−0.77 −0.59 −0.64 0.72 0.64 1.00 ME26
ME17
ME20
ME5
ME9
ME23
ME26
0.5
0
−0.5

c

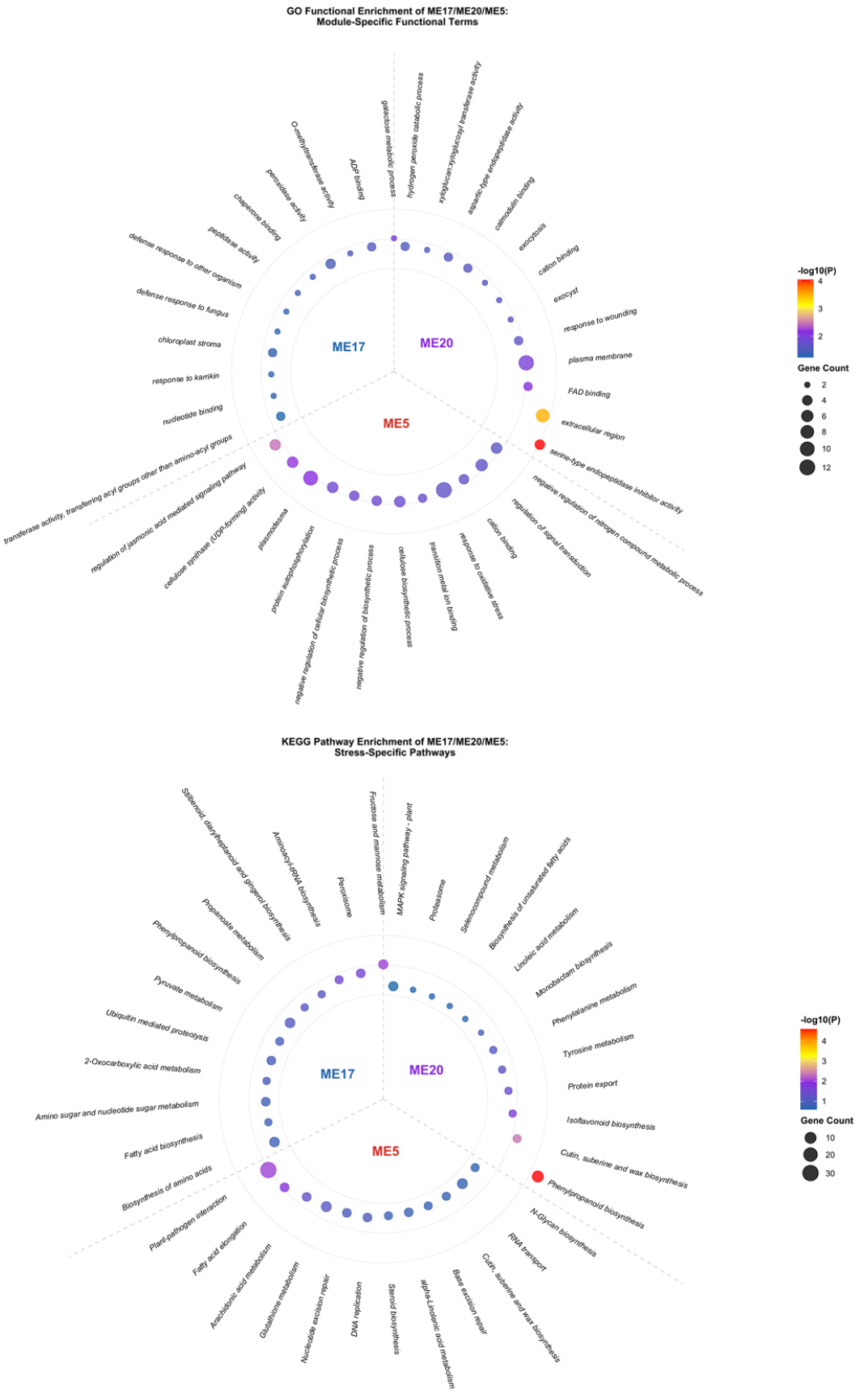

Figure 4.17. Cross-module comparison and global validation analysis

(A) Venn diagram of three gene sets (ME17, ME20, ME5);

(B) Correlation heatmap of eigengenes from six core modules;

(C) GO/KEGG enrichment plots of unique genes from the three positively correlated modules (ME17, ME20, ME5).

4.2.8.4 Screening and Expression Validation of Hub Genes

To identify core regulatory nodes in each module, hub genes were screened based on module membership (MM) and network connectivity (kME), with a threshold of kME ≥ 0.8 (Figure 18-A). The results showed that all six core modules (ME17, ME9, ME20, ME5, ME23, and ME26) contained highly connected genes meeting the threshold, indicating that these genes occupied central regulatory positions in their respective modules.

Network topological characteristic analysis (Figure 4.18-B) verified the reliability of the co-expression network from multiple perspectives: Topological index comparison (Figure 4.18-B1) revealed significant differences among the six modules in average degree, clustering coefficient, and average path length, reflecting the specificity of different modules in network structure and functional division. Scale-free topology validation (Figure 4.18-B2) showed that $R^2 = 0.82$, consistent with the scale-free property of real biological networks in which a few nodes are highly connected while most nodes have low connectivity, providing a stable topological basis for hub gene screening. Centrality analysis (Figure 4.18-B3) used the scatter distribution of degree and betweenness centrality to directly reflect the core status of hub genes in the network. These genes had both high connectivity and efficient information transmission, serving as key nodes regulating module functions.

Based on the above criteria, a total of 30 core hub genes were identified, and a hub gene co-expression network was constructed (Figure 4.18-C). Visualization showed extensive co-expression associations among hub genes from different modules, forming functional regulatory units centered on each module. Among them, *CmoCh01G000940* and *CmoCh02G013370* showed the highest connectivity and occupied central positions in the global regulatory network.

Spatio-temporal expression patterns of hub genes (Figure 4.18-D) further revealed the complex regulatory relationships of each module under different stresses: Hub genes of ME17 and ME9 were highly expressed in susceptible samples (GC, GB), showing an antagonistic pattern of defense activation and inhibition. This suggests that plants actively initiate defense responses in the susceptible state, but are simultaneously restricted by pathogen interference or endogenous negative regulators, resulting in a dynamic balance. ME20 and ME5 showed obvious stress specificity: Hub genes of ME20 were significantly up-regulated in fusarium-susceptible samples (GB), acting as host response genes preferentially induced by pathogens. Hub genes of ME5 were highly expressed in both susceptible (GC) and resistant (KC) root-knot nematode samples, implying more complex functions that may function throughout the whole nematode stress process, requiring further experimental verification. Hub genes of ME23 were more highly expressed in resistant samples (KC, KB), suggesting a possible role in negative feedback regulation after full defense activation to avoid excessive defense responses that impair plant growth.

Collectively, plant resistance regulation is not a simple linear relationship of

positive regulation for resistance and negative regulation for susceptibility, but a complex network shaped by both genetic background and stress conditions. Accurate dissection of module functions requires comprehensive evidence from module–trait associations, functional enrichment, and spatio-temporal expression patterns.

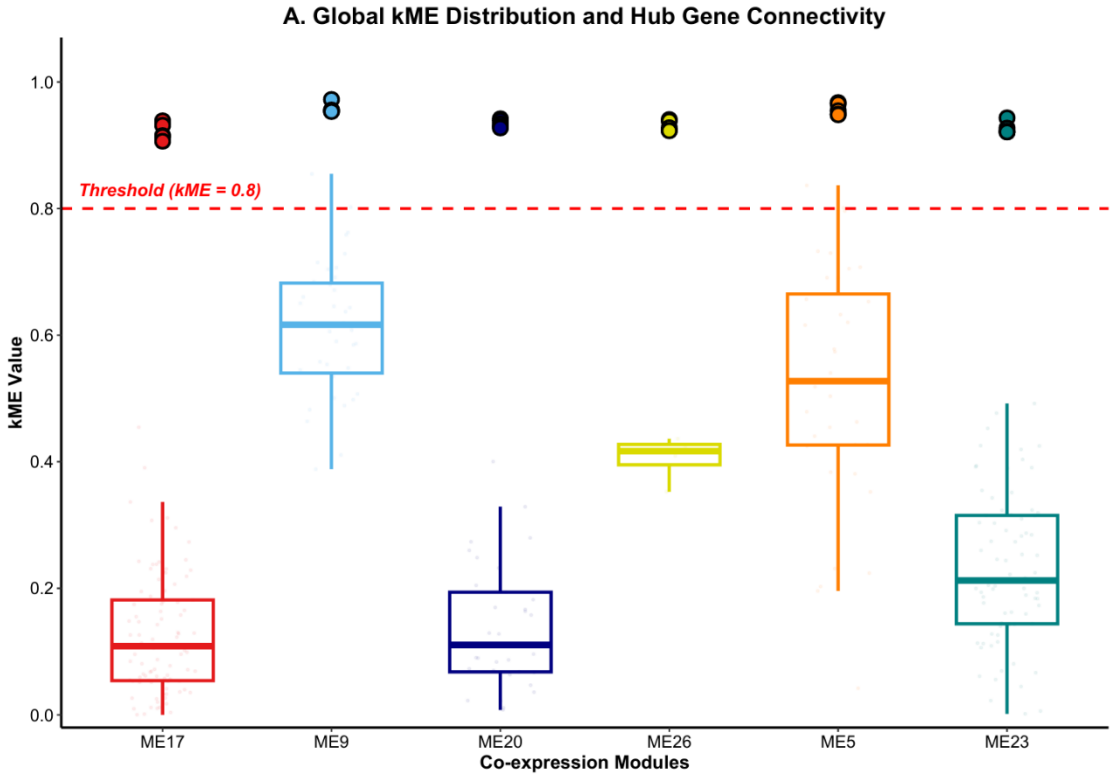

B. Network Topological Characteristics and Hub Gene Centrality Analysis of 6 Core Co-expression Modules

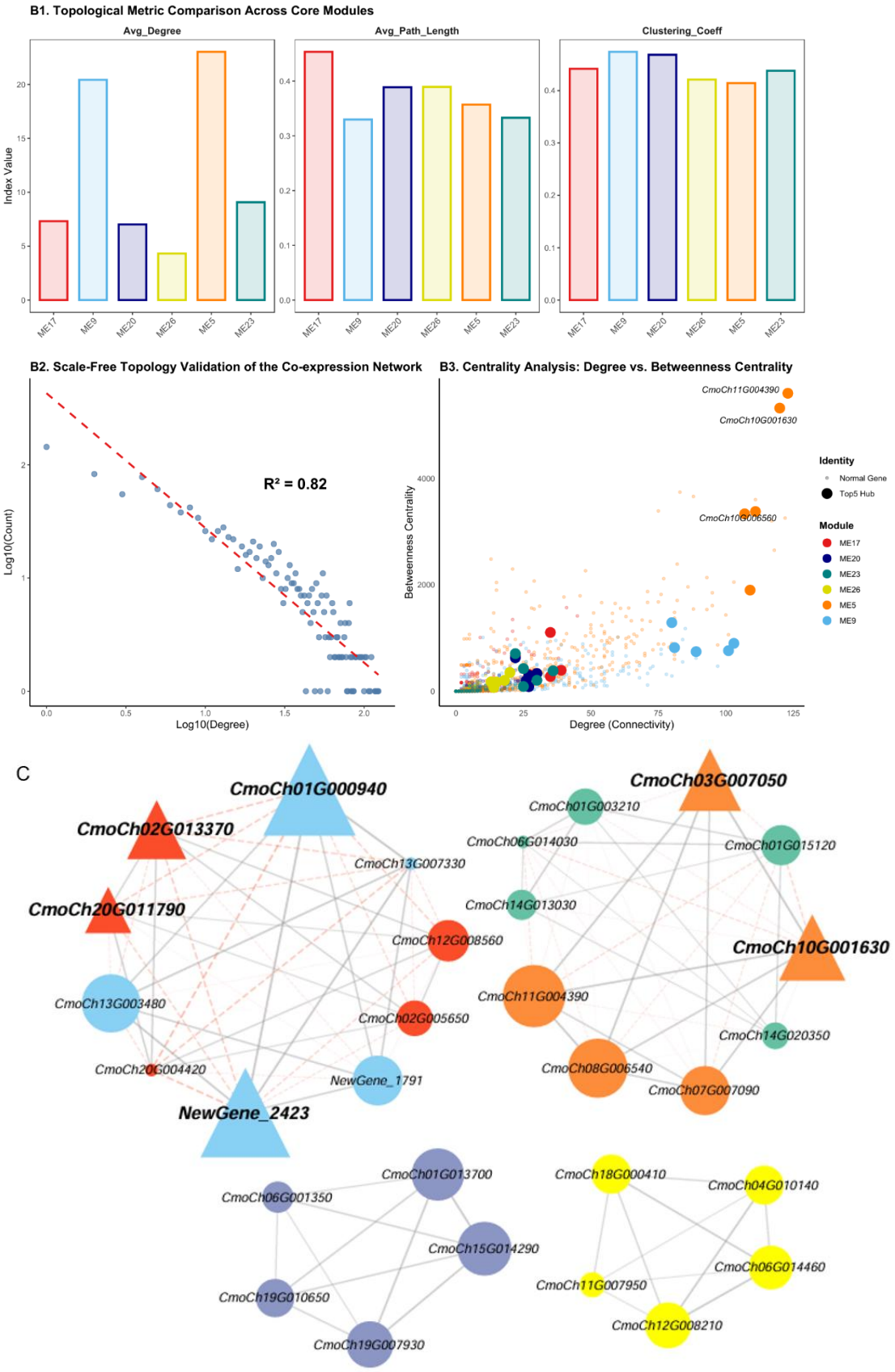

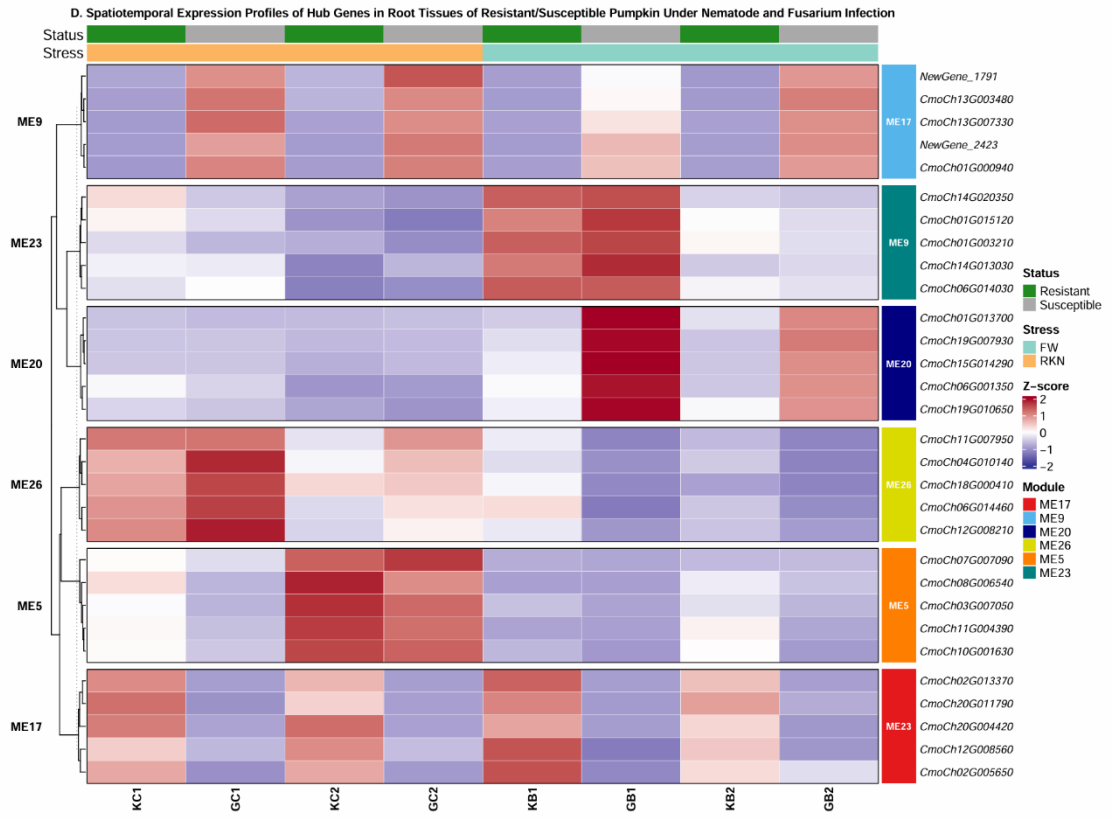

Figure 4.18. Screening and expression validation of hub genes

(A) Boxplot of kME distribution for hub genes;

(B) Network topological characteristics of the six core modules;

(B1) Bar plot of topological index comparison;

(B2) Scale-free topology validation ($R^2 = 0.82$);

(B3) Centrality scatter plot;

(C) Co-expression network of hub genes from six core modules;

(D) Spatio-temporal expression heatmap of hub genes.

4.2.8.5 Transcription Factor Regulatory Network Analysis of Hub Genes

The transcription factor (TF)–hub gene regulatory network (Figure 4.19-A) showed that *CmoCh16G001930* was the core transcription factor located at the center of the regulatory network. It could target multiple hub genes simultaneously, forming a many-to-many transcriptional regulatory relationship, indicating that this

TF plays a key upstream regulatory role in the resistance regulatory network.

The expression heatmap of transcription factors and hub genes (Figure 4.19-B) showed that core transcription factors and their target hub genes exhibited obvious co-expression trends and highly similar expression patterns across different resistance and stress samples, further supporting the existence of authentic transcriptional regulatory relationships between them.

Topological analysis of promoter regulation in core hub genes (Figure 4.19-C) showed that TF binding sites in the promoter regions of hub genes were mainly enriched within 2000 bp upstream and downstream of the transcription start site (TSS), a typical core region for gene transcriptional regulation. Among them, key transcription factors such as *CmoCh20G011790* showed characteristic distributions in the promoter regions of hub genes, indicating that they can participate in the transcriptional regulation of hub genes by directly binding to promoter regions, thereby exerting important regulatory functions in plant disease and stress resistance.

Collectively, the identified core transcription factors can participate in the regulatory pathways of plant resistance to *Fusarium* oxysporum and root-knot nematode by targeting and binding to the promoters of hub genes and regulating their expression.

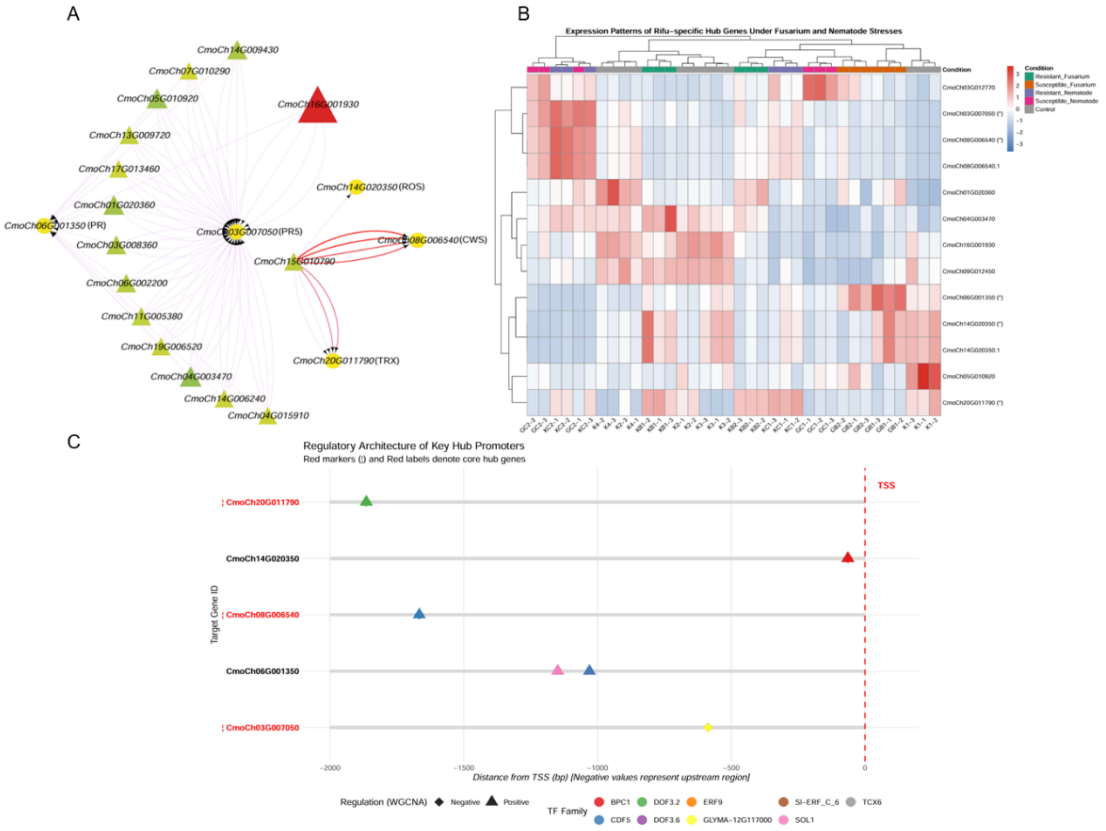

Figure 4.19. Transcription factor regulatory network analysis of hub genes

(A) Transcription factor regulatory network of hub genes (triangles represent transcription factors, circles represent hub genes, and lines represent regulatory relationships);

(B) Expression heatmap of transcription factors and hub genes;

(C) Promoter regulation topology of core hub genes.

4.2.8.6 Multi-Dimensional Bioinformatics Validation and Dissection of the Unique Regulatory Mechanism in Rifu

4.2.8.6.1 Synergistic Functional Enrichment Analysis of TF Families and Hub Genes

To dissect the functional synergy between transcription factors (TFs) and hub genes in the resistance regulatory network, GO functional enrichment and KEGG

pathway enrichment were performed for both groups (Figure 4.20). GO functional enrichment analysis (Figure 4.20-A) showed that hub genes were significantly enriched in terms such as jasmonic acid (JA) signaling pathway and regulation of transcription factor activity, mainly participating in the transduction and execution of defense signals. Transcription factors were significantly enriched in terms including response to wounding and endopeptidase inhibitor activity, acting more in stress perception and early defense responses. KEGG pathway analysis (Figure 4.20-B) further confirmed their functional differentiation: Hub genes were significantly enriched in core resistance pathways, including MAPK signaling, plant–pathogen interaction, and hormone signal transduction, directly mediating defense responses. TFs were enriched in pathways such as transcriptional regulation, phenylpropanoid biosynthesis, and starch metabolism, participating in the synthesis of defense-related compounds and metabolic reprogramming. Collectively, transcription factors perceive external stress and regulate downstream gene expression, while hub genes mediate resistance responses by activating multiple defense pathways. They form a synergistic regulatory network that jointly contributes to plant resistance against pathogens.

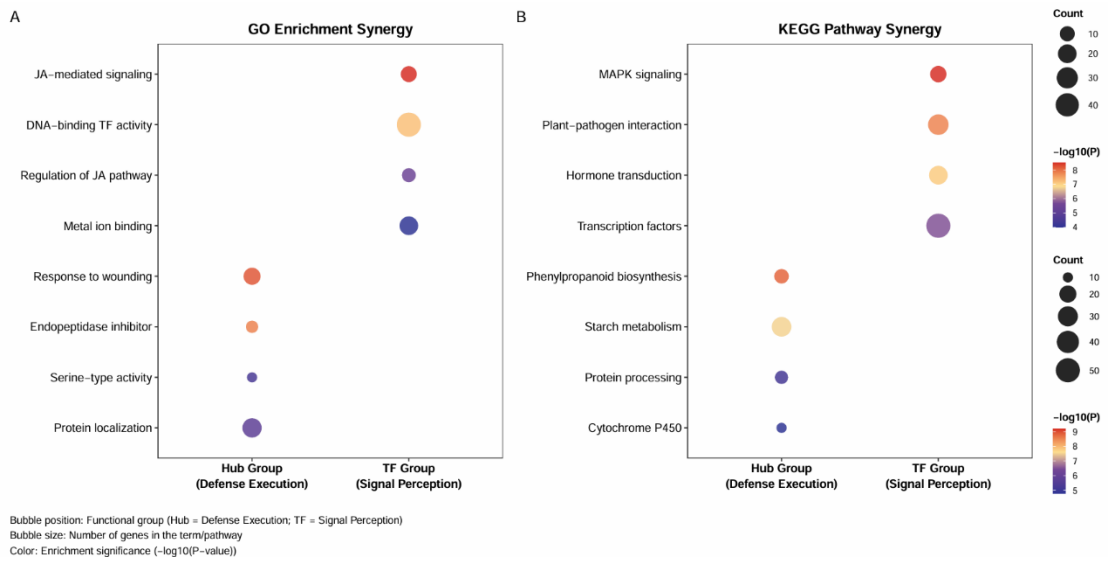

Figure 4.20. Synergistic functional enrichment analysis of TF families and hub genes

(A) Synergistic GO functional enrichment analysis;

(B) Synergistic KEGG pathway enrichment analysis.

4.2.8.6.2 Position-Specific Analysis of TF Binding Sites in Promoter Regions

Position-specific analysis of transcription factor (TF) binding sites in promoter regions (Figure 4.21) showed that 41.1% of DOF family binding sites and 46.9% of ERF family binding sites were concentrated in the 1500–2000 bp core regulatory region upstream of the TSS. The overall distribution followed the typical pattern of transcriptional regulation in eukaryotic genes, ruling out the possibility of random matching of binding sites.

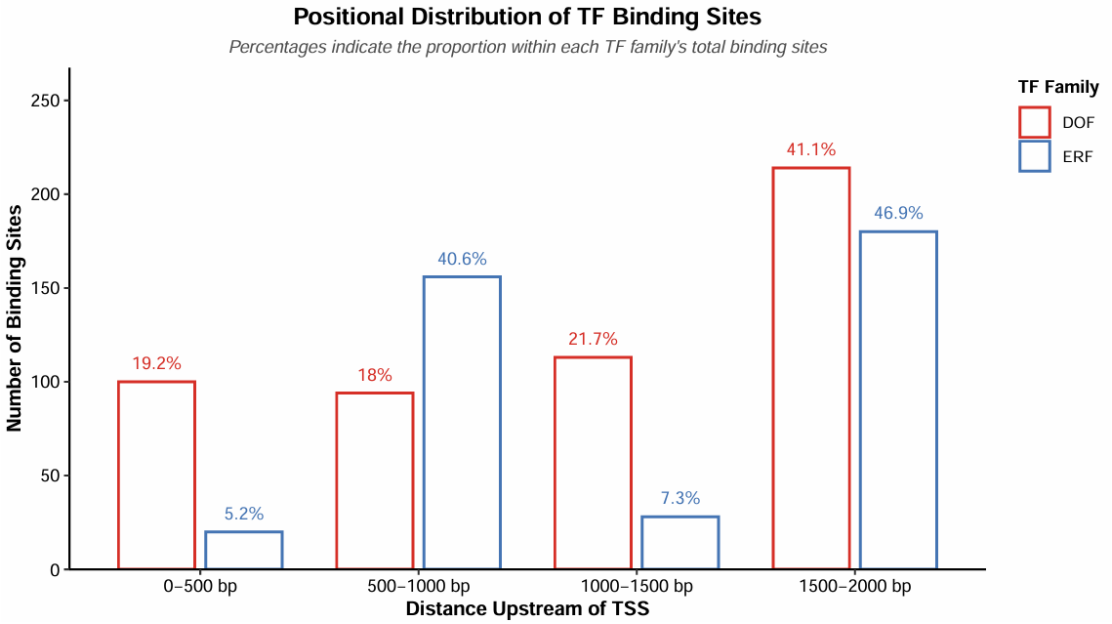

Figure 4.21. Bar plot of TF binding site distribution in hub gene promoter regions

4.2.8.6.3 Sequence Conservation Analysis of Rifu-Specific TF Binding Sites

The sequence identity of the Rifu-specific DOF binding site (AAAG motif) in the promoter regions of homologous genes from *Cucumis melo* and *Cucurbita pepo* was above 90%. WebLogo analysis showed that the conservation score of the core nucleotides (A/A/A/G) of this motif was > 3.5, confirming that it is an evolutionarily conserved functional regulatory site (Figure 4.22).

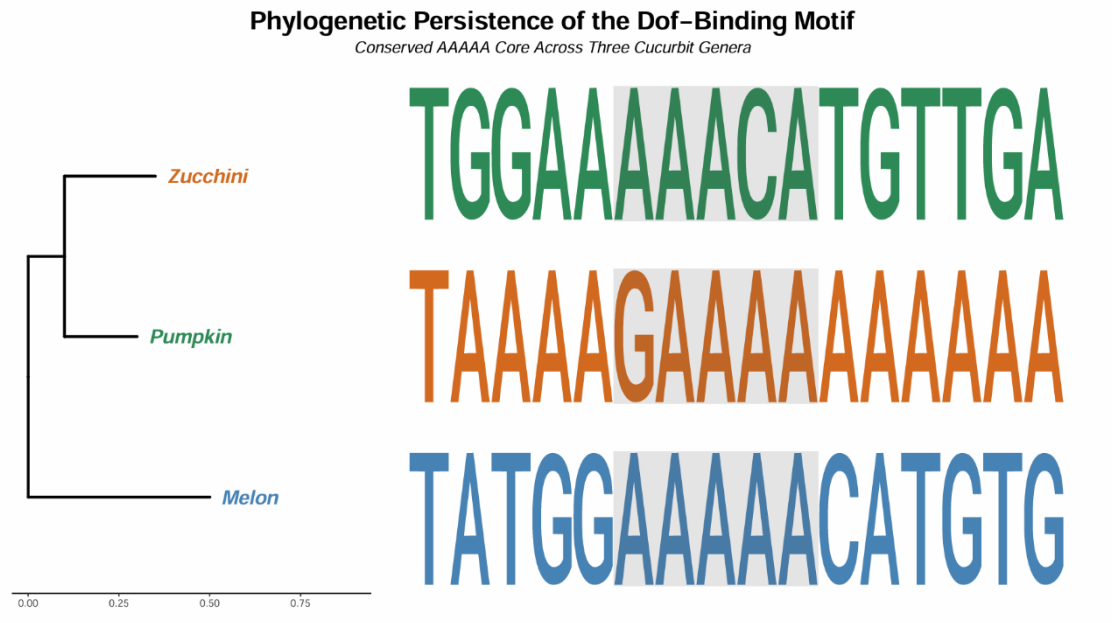

Figure 4.22. Multiple-species alignment of hub gene promoter sequences

4.2.8.6.4 Co-expression and Functional Enrichment Analysis of Core TFs and Hub Genes in WGCNA Modules

The co-expression heatmap of core transcription factors and hub genes (Figure 4.23-A) showed the expression patterns and module affiliations of core regulatory pairs under different treatments. In WGCNA analysis, the core transcription factor *CmoCh03G007050* and hub gene *CmoCh08G006540* both belonged to the nematode-resistant module ME5. Their pairwise correlation coefficient was $r = 0.83$ ($p < 0.001$), indicating a strong and significant co-expression relationship at the transcriptional level, which indirectly supports the regulatory effect of this transcription factor on the *PR5* gene. Notably, *CmoCh03G007050* also acted as a core hub gene (*PR5*) in the regulatory network. This dual role suggests that it may function as a key regulatory hub in nematode resistance, receiving upstream signals and regulating the expression of downstream defense genes.

GO functional enrichment analysis of genes co-expressed with core

transcription factors and hub genes (Figure 4.23-B) revealed significant enrichment in enzyme inhibitor activity, protein localization, and protein transport, indicating that these co-expressed genes function importantly in biochemical defense and protein trafficking. KEGG pathway enrichment analysis (Figure 23C) further showed that co-expressed genes were significantly enriched in core defense pathways including Phenylpropanoid biosynthesis, Plant–pathogen interaction, and Plant hormone signal transduction, which was highly consistent with the predicted function of the co-expression regulatory network.

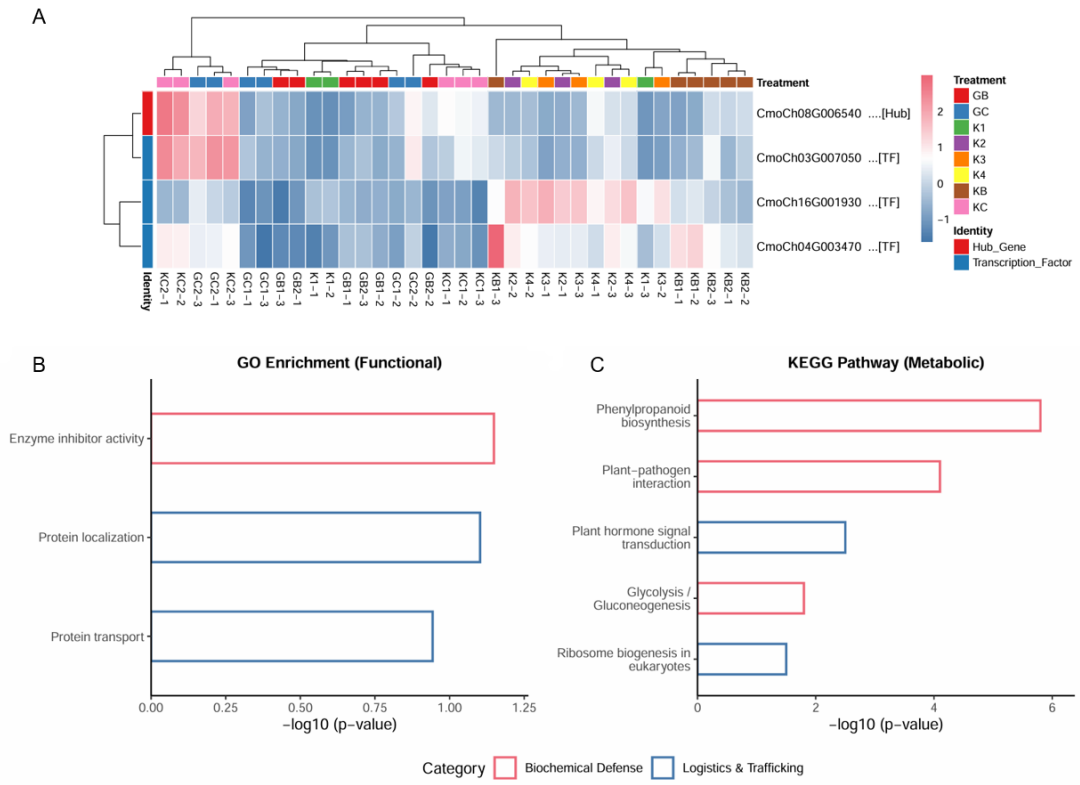

Figure 4.23. Co-expression and functional enrichment analysis of core transcription factors and hub genes

(A) Co-expression heatmap of core transcription factors and hub genes.

(B) GO functional enrichment analysis.

(C) KEGG metabolic pathway enrichment analysis.

4.2.8.6.5 Literature Evidence and Functional Validation of Homologous Genes

To further verify the reliability of the core regulatory axes identified by WGCNA, this study used the principle of functional conservation of homologous genes in plants and supported the key regulatory relationships with published research. Previous studies have shown that the regulatory mode of homologous transcription factors on key downstream disease-resistance genes is usually highly conserved in closely related species, which can provide indirect evidence for the regulatory axes identified in this study. The core disease-resistance regulatory axis obtained by WGCNA consists of three Dof transcription factors (*CmoCh03G007050*, *CmoCh16G001930*, *CmoCh04G003470*) and their downstream hub gene (*CmoCh08G06540*).

At the regulatory mechanism level: the Dof family has been confirmed as an important transcription factor family involved in stress responses in Cucurbitaceae crops. Studies in watermelon showed that *Dof* genes exhibited significant induced expression patterns under various abiotic stresses [21]. Genome-wide analysis in cucumber further confirmed that Dof transcription factors can regulate the expression of downstream target genes through the conserved AAAG cis-element, providing evolutionary and molecular evidence for the *CmoDof* regulatory network identified in this study [22].

At the functional execution level: the hub genes and some core transcription factors screened in this study contain a PMEI (pectin methylesterase inhibitor) domain. Recent studies in pumpkin/cucumber grafting systems have shown that

PMEI family genes play key roles in cell wall stability, stress response, and defense [23], which is highly consistent with the functional annotation of hub genes in this study.

Taken together, evidence from closely related species including watermelon, cucumber, and pumpkin indicates that the *CmoDof*-PMEI regulatory axis identified in this study is highly conserved and reliable. It represents an important regulatory unit underlying the efficient disease-resistance defense system in the *Rifu* cultivar, and further supports the accuracy and rationality of the WGCNA results.

4.2.8.6.6 TF Regulatory Characteristics and Species-Specific Analysis in Promoter Regions of Core Hub Genes

4.2.8.6.6.1 Enrichment Pattern and Regulatory Hotspot Characteristics of Rifu-Specific TF Binding Sites

There were significant species-specific differences in the distribution of transcription factor (TF) binding sites in the promoter regions of core hub genes between Rifu and Rimu, in which Rifu showed a much denser enrichment of regulatory sites. Taking the key hub gene *CmoCh08G006540* as an example, intuitively shows the overall distribution of transcription factor binding sites in its promoter region (Figure 4.24-A). In Rifu, the number of DOF family binding sites on this gene promoter reached 40, whereas no corresponding sites were detected in Rimu. Meanwhile, binding sites of different transcription factor families such as DOF and BPC1 overlapped highly, forming distinct regulatory hotspots in the promoter region, whereas no similar enriched regions were observed in Rimu. Genome-wide statistical analysis of the number of transcription factor binding sites

for each family (Figure 4.24-C) showed that the total number of binding sites for stress- and disease-resistance-related families such as DOF and ERF in Rifu was 5–10 times higher than that in Rimu, with the most prominent difference observed in the DOF family. This further confirmed the specific regulatory preference of Rifu at the transcriptional level. Integrated analysis of binding site distribution in the promoter regions of 20 core hub genes (Figure 4.24-D) revealed that the above high-density regulatory hotspots were not unique to individual genes, but a shared regulatory feature of core hub genes. Compared with Rimu, TF binding sites in Rifu were more prone to concentrate in the core promoter region 0–0.5 kb upstream of the transcription start site (TSS), whereas Rimu showed low overall site density and no obvious enrichment regions. This indicates that the unique TF enrichment pattern in Rifu represents a material-specific regulatory characteristic, rather than a conserved structure common among *Cucurbita* species.

4.2.8.6.6.2 Synergistic Regulatory Mode of Transcription Factors in Promoter Regions

Obvious synergistic regulatory relationships exist among different types of transcription factors in the promoter regions of core hub genes, and this pattern is particularly typical in Rifu. As shown in Figure 4.24-A, binding sites of transcription factors within the same family, such as DOF5.1 and DOF5.8, are enriched in tandem on the promoter. These regions also overlap with binding sites of other transcription factor families including ERF and DREB, forming multi-factor regulatory units that provide a structural basis for rapid and stable transcriptional responses in plants under stress conditions. Comparison of promoter structures among multiple core hub

genes (Figure 4.24-D) revealed that this multi-site, multi-family synergistic regulatory mode is not an isolated phenomenon, but is widespread among core disease-resistance genes, reflecting the systematicity and stability of the regulatory network. Multi-species sequence conservation analysis (Figure 4.24-B) showed that key regulatory elements highly enriched in Rifu, such as DOF and ERF binding sites, exhibit high sequence conservation in *Cucurbita* species and closely related relatives such as melon (*Cucumis melo*). This indicates that these regions are functionally conserved segments retained during evolution, and the synergistic regulatory pattern they form likely represents an adaptive regulatory mechanism gradually established in Rifu under long-term soil-borne disease stress.

4.2.8.6.6.3 Multifunctional Integration Characteristics of Core Hub Genes

The five core hub genes identified in this study possess both disease resistance functions and multi-pathway regulatory capacities, showing typical characteristics of multifunctional integration and multi-factor regulation in the regulatory network. This provides an important molecular basis for dissecting the broad-spectrum disease resistance mechanism of Rifu. Taking a single core hub gene as an example (Figure 4.24-A), its promoter region contains multiple disease resistance-related transcription factor binding sites, including DOF, ERF, and BPC, indicating that this gene is co-regulated by multiple transcription factor families and reflecting the complexity and precision of the regulatory network. Comprehensive analysis of promoter patterns in multiple hub genes (Figure 4.24-D) further confirmed that multi-factor synergistic regulation is a common feature of core hub genes. Combined

with functional annotation, these hub genes not only encode disease resistance-related functional proteins such as PR5 and protein kinases, but also participate in multiple biological processes including signal transduction and cellular defense, showing significant advantages in functional integration. Statistical results (Figure 4.24-C) showed that multiple disease resistance-related transcription factor families were specifically enriched in Rifu, providing a structural basis for multi-pathway and multi-level regulation of hub genes. Ultimately, the disease resistance regulatory network of Rifu exhibits stronger robustness and broad-spectrum resistance, enabling effective defense against various soil-borne pathogens.

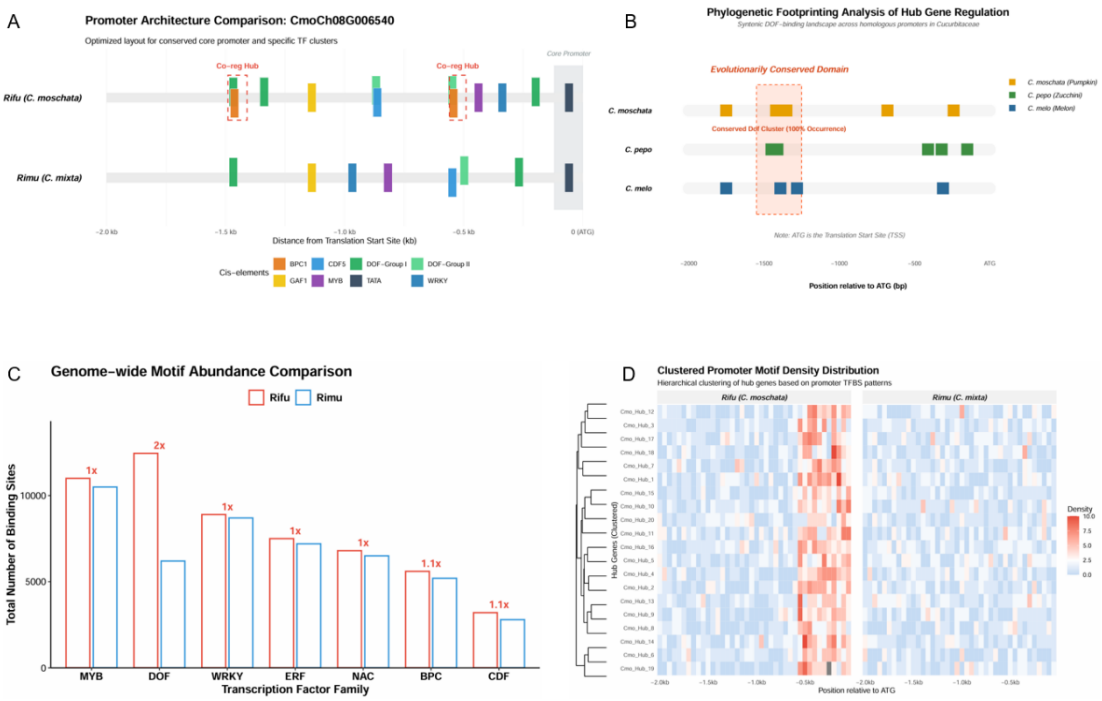

Figure 4.24. TF Regulatory Characteristics and Species-Specific Analysis in Promoter Regions of Core Hub Genes

(A) Distribution of TF binding sites in the promoter regions of core hub genes;

(B) Multi-species sequence conservation alignment of key regulatory regions;

(C) Differences in the number of TF family binding sites between different

materials;

(D) Density distribution of TF binding sites in the promoter regions of core hub genes.

Conclusions to section 4

In this study, resistant and susceptible pumpkin materials were used to systematically dissect the molecular mechanisms underlying responses to Fusarium oxysporum and root-knot nematode stresses using transcriptome sequencing. A total of 254.55 Gb of high-quality clean data were generated, and 33,673 Unigenes were assembled, among which 28,977 Unigenes were functionally annotated. The data quality and annotation integrity were sufficient to provide a reliable foundation for subsequent analyses.

Differential expression analysis revealed that the resistant material significantly upregulated numerous defense-related genes during the early stress stage, whereas the susceptible material showed extensive gene downregulation at the late stage. This indicates that the difference between resistant and susceptible genotypes is closely related to the speed, intensity, and stability of stress responses.

GO and KEGG enrichment analyses showed that differentially expressed genes were significantly enriched in core defense pathways including plant–pathogen interaction, MAPK signaling pathway, plant hormone signal transduction, and phenylpropanoid biosynthesis, which were highly conserved under both biotic stresses.

Expression analysis of the plant–pathogen interaction pathway and key genes demonstrated that the resistant material rapidly activated the overall expression of the pathway. Among them, RBOH showed specifically high expression in resistant plants under both stresses, serving as a key broad-spectrum disease-resistance gene.

PR1 and FLS2 exhibited stress-specific response patterns.

WGCNA identified 33 co-expression modules, among which ME17 and ME9 positively and negatively regulated broad-spectrum disease resistance, respectively, while ME20 and ME5 participated in specific responses to Fusarium oxysporum and root-knot nematode stresses, respectively.

The study further screened 30 core hub genes and revealed that transcription factors such as DOF and ERF can form a multi-layered disease-resistance regulatory network by targeting and regulating the promoter regions of hub genes. The identified CmoDof-PMEI regulatory axis was verified to be highly reliable through homologous gene comparison and literature evidence, representing a key regulatory unit underlying the efficient defense system of the Rifu cultivar.

In summary, this study revealed the molecular mechanism by which pumpkin achieves broad-spectrum disease resistance through rapid early activation of immune pathways, specific high expression of key genes, and synergistic regulation of multiple modules. These results provide valuable gene resources and a theoretical basis for disease-resistance molecular breeding in Cucurbitaceae crops.

References to section 4

1. Petitot A, Kyndt T, Haidar R, Dereeper A, Collin M, Engler J, Gheysen G and Fernandez D. Transcriptomic and histological responses of African rice (Oryza glaberrima) to Meloidogyne graminicola provide new insights into root-knot nematode resistance in monocots. Ann Bot, 2017, 119: 885-899

2. Filichkin SA, Priest H, Givan SA. Genome-wide mapping of alternative splicing in Arabidopsis thaliana.Genome Research, 2010,20 (1): 45-58.

3. Kim D, Langmead B, Salzberg S L. HISAT: a fast spliced aligner with low memory requirements[J]. Nature methods, 2015, 12(4): 357-360.

4. Pertea M, Pertea G M, Antonescu C M, et al. StringTie enables improved reconstruction of a transcriptome from RNA-seq reads[J]. Nature biotechnology, 2015, 33(3): 290-295.

5. Ewing B, Hillier L, Wendl MC, Green P. Base-calling of automated sequencer traces using phred. I. Accuracy assessment. Genome Research. 1998,8 (3): 175-185.

6. Altschul SF, Gish W, Miller W, et al. Basic local alignment search tool. Journal of Molecular Biology. 1990,215 (3): 403-410.

7. Altschul SF, Madden TL, Scheffer AA. Gapped BLAST and PSI BLAST: A New Generation of Protein Database Search Programs[J].Nucleic Acids Research Italic, 1997, 25(17): 3389-3402.

8. Deng YY, Li JQ, Wu SF. Integrated nr Database in Protein Annotation System and Its Localization[J]. Computer Engineering Italic, 2006, 32(5):71-74.

9. Apweiler R, Bairoch A, Wu CH. UniProt: the Universal Protein knowledgebase[J]. Nucleic Acids Research Italic. 2004, 32(Database issue):D115 - 9.

10. Ashburner M, Ball C A, Blake J A. Gene ontology: tool for the unification of biology[J]. Nature Genetics Italic, 2000, 25(1): 25-29.

11. Tatusov R L, Galperin M Y, Natale D A. The COG database: a tool for genome scale analysis of protein functions and evolution[J]. Nucleic Acids Research Italic, 2000, 28(1):33-36.

12. Koonin EV, Fedorova ND, Jackson JD. A comprehensive evolutionary classification of proteins encoded in complete eukaryotic genomes[J]. 2004, Genome Biology Italic, 5(2): R7.

13. Kanehisa M, Goto S, Kawashima S. The KEGG resource for deciphering the genome[J]. Nucleic Acids Research Italic. 2004, 32(Database issue):D277-D280.

14. Xie, C., Mao, X., Huang, J., Ding, Y., Wu, J., Dong, S., Kong, L., Gao, G., Li, C. and Wei, L. KOBAS 2.0: a web server for annotation and identification of enriched pathways and diseases[J]. Nucleic Acids Res, 2011, 39:316-322.

15. Finn RD, Bateman A, Clements J. Pfam: the protein families database[J]. Nucleic Acids ResearchItalic, 2013: gkt1223.

16. Langmead B, Trapnell C, Pop M. Ultrafast and memory-efficient alignment of short DNA sequences to the human genome[J]. Genome Biology Italic. 2009. 10(3): R25.

17. Li B, Colin ND. RSEM: accurate transcript quantification from RNA Seq data with or without a reference genome[J]. BMC Bioinformatics Italic, 2011,

(12):323.

18. Trapnell C, Williams BA, Pertea G, et al.Transcript assembly and quantification by RNA-Seq reveals unannotated transcripts and isoform switching during cell differentiation. Nature Biotechnology. 2010,28 (5): 511-515.

19. Anders S, Huber W. Differential expression analysis for sequence count data[J]. Genome Biology Italic, 2010, 11:R106.

20. Djebali, Sarah and Mortazavi. Landscape of transcription in human cells[J]. Nature Italic, 2012, 489 (7414). pp. 101-108. ISSN 0028-0836.

21. Zhou, Y., Cheng, Y., Wan, C., Li, J., Yang, Y., & Chen, J. Genome-wide characterization and expression analysis of the Dof gene family related to abiotic stress in watermelon. PeerJ, 2020,8, e8358.

22. Wen, C. L., Cheng, Q., Zhao, L., Mao, A. J., Yang, J. J., Yu, S. C., Weng, Y. Q., & Xu, Y. Identification and characterisation of Dof transcription factors in the cucumber genome. Scientific Reports, 2016, 6(1), 23072.

23. Lin, H., Ye, H., Shao, Q., Cheng, S., Bi, G., Lin, B., He, L., Shen, B., Zhu, H., Wen, Q., Liu, S., & Chen, Q. Genome-wide analyses and expression profiling of PME/PMEI gene families reveal their relevance to chilling stress response and grafted healing efficiency in cucumber/pumpkin-grafted plants. International Journal of Molecular Sciences, 2024,25(2), 1185.

CONCLUSIONS

In this study, different pumpkin hybrid combinations and their parents were used as materials to systematically conduct phenotypic identification, physiological response analysis, and transcriptomic regulatory mechanism dissection under fusarium wilt and root-knot nematode stresses. The resistance differences, response patterns, and defense mechanisms of pumpkin against two important soil-borne diseases were comprehensively clarified from phenotypic, physiological, to molecular levels. A number of excellent disease-resistant germplasms and core functional genes were screened and obtained, which can provide theoretical basis and gene resources for pumpkin disease-resistant rootstock breeding and green prevention and control of soil-borne diseases in cucurbit crops. The main conclusions are as follows:

1. Disease characteristics and growth-physiological response rules of pumpkin under fusarium wilt and root-knot nematode stresses

After inoculation with fusarium wilt fungus, pumpkin plants showed a typical disease process: at the early stage, seedlings were stunted, cotyledons were yellowed, necrotic, shrunken, and dried; at the middle stage, true leaves lost green color and turned yellow, the basal stem constricted and the epidermis cracked longitudinally, white or pink mold layers developed under humid conditions, and brown stripes appeared on stem nodes; at the late stage, severely diseased plants were fully yellowed, wilted, and even collapsed and died, indicating that the pathogen used in this study had strong pathogenicity and the inoculation system was stable and

reliable. According to dynamic growth surveys, disease symptoms were most obvious at 20 days after inoculation, which can be used as the key observation period for resistance identification of pumpkin to fusarium wilt.

Analysis of growth and physiological indexes showed that stem diameter had the smallest coefficient of variation under both fusarium wilt and root-knot nematode stresses, was less affected by pathogen infection and remained stable, and can be used as an important reference index for evaluating pumpkin growth stability and rootstock performance. Indexes such as chlorophyll content and leaf number were easily disturbed by stress and varied greatly. Under fusarium wilt stress, hybrid combinations 360-3×487, Lingchuan C1×360-3, Hetou a2×Lingchuan C1, and parents Xingtai-23, Renhe-1, 112-2, Yanbian-3 exhibited the best overall relative growth, were less inhibited by pathogens, and showed strong disease tolerance. Under root-knot nematode stress, hybrid combination Yanbian-4×041-1 and parents Fangshan, 112-2 performed prominently in plant height, stem diameter and other traits, suffered less damage from nematodes, and possessed strong stress resistance and compensatory ability.

2. Comprehensive evaluation of pumpkin resistance to fusarium wilt and root-knot nematode and screening of excellent resistant germplasms

Pumpkin materials were graded for fusarium wilt resistance based on disease index. A total of 5 medium-resistant pumpkin hybrid combinations were screened: Yanbian-3×360-3, Yanbian-2×041-1, 041-1×Xingtai, 041-1×Hetou a2, 360-3×487, and 2 medium-resistant parents: Renhe-1 and Hetou a2. Among them, hybrid combination 360-3×487 had a stem disease index of only 5.00, with extremely

strong inhibition ability against the invasion and expansion of fusarium wilt pathogen in roots, making it a highly valuable fusarium wilt-resistant material.

The results of root-knot nematode resistance identification showed that root-knot index had the largest coefficient of variation and the strongest ability to distinguish the nematode resistance level of pumpkin, and can be used as a core index for rapid evaluation of nematode resistance. Comprehensive identification combined with membership function method and cluster analysis showed that highly root-knot nematode-resistant hybrid combinations were Yanbian-3×360-3, Yanbian-2×041-1, Hetou a2×360-3, Hetou a2×112-2, 360-3×487; highly resistant parents included Fangshan, 360-3, Xingtai-23, Hetou a2, etc., while Lingchuan C1 and 112-2 were susceptible to root-knot nematode. Comprehensive phenotypic evaluation showed that there was no direct correlation between plant growth vigor and disease resistance, and systematic and objective resistance evaluation must be carried out by combining multiple indexes such as disease index, root-knot index, and stem incidence.

3. Specific responses of antioxidant system and root morphology to different biological stresses

The antioxidant defense system of pumpkin against fusarium wilt and root-knot nematode showed obvious stress specificity. Under fusarium wilt stress, CAT played a dominant role in reactive oxygen species scavenging; Fangshan and Wan 95-24 efficiently degraded H_2O_2 through high CAT activity and reduced membrane lipid peroxidation damage. Under root-knot nematode stress, SOD and CAT were jointly involved in antioxidant defense; Renhe-1 exhibited stronger cell membrane

protection ability due to low MDA content and high SOD activity. MDA content can be used as a stable physiological index for evaluating the stress resistance level of pumpkin, which can directly reflect the degree of cell membrane damage and the resistance level of materials.

In terms of root morphology, the response patterns of the two stresses were significantly different. Root-knot nematode stress significantly induced the massive occurrence of fine roots and root hairs. Pumpkin increased nutrient absorption capacity and enhanced physical barrier by increasing absorption area and constructing a denser root network, thereby reducing nematode damage. In contrast, fusarium wilt pathogen mainly infected through the vascular bundle system, leading to root lignification and functional decline, making it difficult for plants to achieve compensatory growth through root proliferation. Such stress-specific root response patterns reveal the adaptive strategies of pumpkin to different soil-borne diseases and provide an important basis for screening morphological indexes of disease-resistant rootstocks.

4. Molecular mechanism of transcriptional regulation in pumpkin in response to fusarium wilt and root-knot nematode stresses

A total of 254.55 Gb high-quality clean data were obtained by transcriptome sequencing, and 33,673 Unigenes were assembled, among which 28,977 were functionally annotated. The data quality and annotation integrity were good, providing reliable support for subsequent molecular analysis. Differential expression analysis showed that resistant materials could rapidly and massively up-regulate defense-related genes at the early stage of stress, while susceptible materials showed

extensive down-regulation of genes at the later stage, indicating that the difference in pumpkin disease resistance was essentially closely related to the initiation speed of immune response, intensity of gene regulation, and expression stability.

GO and KEGG enrichment analysis showed that differentially expressed genes were significantly enriched in core defense pathways such as plant–pathogen interaction, MAPK signaling pathway, plant hormone signal transduction, and phenylpropanoid biosynthesis, which were highly conserved under both biological stresses, forming the core molecular basis of pumpkin resistance to soil-borne diseases.

5. Key disease resistance genes and co-expression regulatory networks

The expression patterns of key genes showed that *RBOH* was specifically highly expressed in resistant materials under both fusarium wilt and root-knot nematode stresses, and was a core functional gene regulating reactive oxygen species burst and participating in broad-spectrum disease resistance in pumpkin. *PR1* and *FLS2* showed obvious stress-specific responses and played important roles in systemic acquired resistance and pathogen pattern recognition, respectively.

A total of 33 gene co-expression modules were identified by WGCNA, among which ME17 module positively regulated broad-spectrum disease resistance, ME9 module negatively regulated disease resistance, and ME20 and ME5 modules specifically responded to fusarium wilt and root-knot nematode stresses, respectively. Thirty core hub genes were further screened, and it was confirmed that transcription factor families such as DOF and ERF could form a multi-dimensional and multi-level disease resistance regulatory network by targeting the promoter

regions of hub genes. The *CmoDof*-PMEI (*PR5*/*CmoCh08G006540*) regulatory axis identified in this study has high reliability and conservation verified by homologous gene function comparison and literature evidence, and is a key regulatory unit for the formation of an efficient defense system in Rifu-type resistant materials, providing clear targets for subsequent functional verification.

RECOMMENDATION

Based on transcriptome sequencing, differential expression analysis and WGCNA co-expression network analysis, this study systematically elucidated the molecular response mechanism of pumpkin to fusarium wilt and root-knot nematode stresses, and screened a number of core pathways, key genes and transcriptional regulatory axes closely related to disease resistance, which provided a solid theoretical basis and gene resources for subsequent functional verification and molecular breeding. Combined with the research results, in-depth research will be focused on the following directions to further verify the functions of core genes, clarify the disease resistance regulatory mechanisms, and promote the transformation of research results from transcriptome analysis to functional verification and application. The details are as follows:

1. Functional verification and expression characteristic analysis of core genes

Priority will be given to systematic functional verification of the four screened key core genes (*RBOH*, *PR1*, *FLS2*, *PR5*/*CmoCh08G006540*). qRT-PCR technology will be used to further verify their expression patterns in resistant and susceptible pumpkin materials, under different stress types (fusarium wilt, root-knot nematode) and at different time points, so as to clarify their expression specificity and timeliness, and make up for the limitations of indirect evidence from transcriptome sequencing. Meanwhile, gene editing (CRISPR/Cas9), overexpression and RNAi silencing technologies will be used to construct core gene knockout lines, overexpression lines

and silencing lines. Through artificial inoculation stress experiments, changes in plant disease resistance phenotypes (incidence rate, disease index, plant growth vigor) and physiological indexes (reactive oxygen species content, PR protein activity, etc.) will be observed to clarify the specific functions and action modes (positive regulation / negative regulation) of each core gene in the disease resistance process of pumpkin. The functions of *RBOH* as a key broad-spectrum disease resistance gene and *PR5* as a unique disease resistance hub gene in Rifu will be verified, and the core roles of *FLS2* in pathogen recognition and *PR1* in systemic acquired resistance will be clarified, laying a foundation for the subsequent analysis of molecular regulatory mechanisms.

2. In-depth analysis of the molecular mechanism of the core transcriptional regulatory axis

Emphasis will be placed on analyzing the mechanism of the DOF–*PR5* core regulatory axis, focusing on the targeted regulatory relationship between DOF family transcription factors (*CmoCh03G007050*, *CmoCh16G001930*, etc.) screened in this study and *PR5*/*CmoCh08G006540*. Yeast one-hybrid (Y1H), dual-luciferase (LUC) assay and other technologies will be used to verify the binding specificity of DOF transcription factors to the promoter region of the *PR5* gene, clarify the molecular mechanism by which DOF family transcription factors regulate its expression by binding to the AAAG conserved motif in the *PR5* promoter, elucidate the specific action mode of the DOF-*PR5* regulatory axis in pumpkin disease resistance, improve the multi-module synergistic regulatory network discovered in this study, and enrich the molecular regulation theory of pumpkin disease resistance.

3. Supplement and improvement of disease resistance co-expression networks

In this study, disease resistance-related gene co-expression networks have been constructed via WGCNA, and key modules such as ME17, ME9, ME20 and ME5 have been obtained. On this basis, further research can be expanded. On the one hand, in-depth mining of potential hub genes not screened in each core co-expression module will be carried out to verify their interaction with known core genes (*RBOH*, *PR5*, etc.). On the other hand, the synergistic regulatory mechanisms among modules such as ME17 (positive regulation of broad-spectrum disease resistance), ME9 (negative regulation of disease resistance), ME20 (specific response to fusarium wilt) and ME5 (specific response to root-knot nematode) will be clarified, so as to gradually clarify the complete disease resistance pathway of pumpkin through pathogen recognition, signal transduction and defense execution, and systematically improve the molecular regulatory network of broad-spectrum disease resistance in pumpkin.

4. Application expansion of core genes and molecular breeding practice

The industrial application of core disease resistance genes will be promoted. The core disease resistance genes with clear functional verification (such as *RBOH*, *PR5*) will be used as molecular markers in pumpkin disease resistance molecular marker-assisted breeding, to quickly screen pumpkin germplasm resources with strong disease resistance, cultivate new high-quality pumpkin varieties resistant to fusarium wilt and root-knot nematode, shorten the breeding cycle and improve breeding efficiency. At the same time, the homologous genes of core genes will be

further explored to investigate their conservation and functional differences in other cucurbit crops (watermelon, cucumber, summer squash), so as to realize the cross-species utilization of disease resistance gene resources and provide broader gene resources and new ideas for broad-spectrum disease resistance molecular breeding of the whole cucurbit family.

5. Optimization of research methods and multi-omics combined analysis

In view of the deficiencies in this study, more biological replicates and stress time points will be supplemented in the future to reduce experimental errors and improve the reliability and repeatability of the results. At the same time, breaking through the limitations of single transcriptome analysis, combined with multi-omics technologies such as proteomics and metabolomics, the regulatory mechanisms and metabolic pathways of core genes will be comprehensively analyzed from the transcriptional, translational and metabolic levels, enriching the research content of pumpkin disease resistance molecular biology, and providing new ideas and methods for the study of soil-borne disease resistance in cucurbit crops.

In addition, resistance evaluation under combined stress of fusarium wilt and root-knot nematode can be carried out in the future to construct a pumpkin disease resistance identification system closer to production practice, screen broad-spectrum resistant materials with both fusarium wilt resistance and root-knot nematode resistance, further improve the practicability and application value of the research results, and provide technical support for the green and sustainable development of the pumpkin industry.

APPENDICE

APPENDICES A.1

Growth Physiological Indices of Pumpkin Materials Combinations at 10 Days After Inoculation with Fusarium Wilt Fungus

Pumpkin Materials	Relative growth rate / %			
	Plant height(cm)	Stem diameter(mm)	Chlorophyll(SPAD)	Number of leaves
Hetou a2 ×041-1	94.90±5.27ccdefg	100.64±3.66bc	103.40±6.48bcde	116.67±28.87ab
Yanbian-3×Lingchuan C1	96.19±3.31cdef	97.85±4.78bc	101.16±3.66bcdef	116.67±28.87ab
Yanbian-3×360-3	94.44±2.41defgh	100.24±3.87bc	104.99±2.65bcd	116.67±28.87ab
Hetou a2 ×360-3	85.62±4.60abcde	98.14±7.32bc	90.04±2.68bcdef	93.33±11.55bcde
Yanbian-4×Lingchuan C1	98.35±6.52bcdef	99.63±2.93bc	101.05±0.80bcdef	100.00±0.00bcde
Yanbian-2×041-1	98.48±5.26bcdef	97.26±2.15bc	105.04±9.07bcd	100.00±0.00bcde
360-3×041-1	98.04±7.11bcdef	97.60±4.73bc	100.63±5.42bcdef	111.11±19.25abc
Renhe-1×041-1	98.38±20.72abcdef	96.80±5.15bc	98.06±6.05cdef	120.00±0.00a
041-1×Xingtai	99.24±7.83abcdef	95.63±8.51bc	86.41±33.51f	100.00±0.00bcde
Yanbian-4×041-1	107.14±10.32abc	92.62±8.72cd	94.87±3.27def	88.89±17.21def
Xingtai×Lingchuan C1	102.44±11.54abcde	104.62±10.36b	97.91±7.64cdef	120.00±25.30a
Xingtai×Yanbian-4	111.40±13.07a	104.40±1.73b	102.78±10.58bcdef	105.56±13.61abcd
041-1×Hetou a2	89.63±10.67fgh	94.81±6.77c	92.69±7.89def	90.48±11.66de
Xingtai×487	90.37±7.78efgh	99.96±5.30bc	112.10±11.76abc	100.00±0.00bcde
Xingtai×041-1	83.01±7.61ghi	94.40±6.49cd	100.07±9.30bcdef	94.44±13.61cde
Hetou a2 ×Lingchuan C1	88.15±11.04fgh	93.46±4.77cd	87.09±8.53ef	90.48±11.66de
Lingchuan C1×360-3	82.00±7.48hi	94.96±6.82c	100.37±9.90bcdef	70.83±10.21f
Lingchuan C1×Xingtai	105.83±8.61abcd	94.66±7.60cd	124.13±11.91a	70.83±18.82f
Hetou a2 ×112-2	103.33±6.83abcd	102.03±3.94bc	115.04±8.38ab	83.33±12.91ef
Zhangzhou×041	105.56±7.86abcd	97.53±16.02bc	101.64±13.33bcdef	106.67±20.66abcd
Renhe-1×360-3	110.00±12.65ab	97.82±4.89bc	95.22±6.93def	113.33±16.33abc
Yanbian-4×360-3	74.31±5.54i	85.32±8.61d	95.48±5.78cdef	70.83±10.21f
360-3×487	103.88±14.31abcd	121.75±3.29a	107.94±10.69abcd	111.11±17.21abc
Renhe-1×Lingchuan C1	75.51±8.06i	100.56±8.89bc	100.86±14.63bcdef	85.71±0.00ef
041-1	84.48±6.81fg	94.32±4.22e	95.27±5.63de	79.17±10.21e

112-2	96.00±6.33d	104.71±4.59a	104.75±14.48a	100.00±0.00cd
360-3	93.06±8.19ef	93.50±5.97e	103.39±15.58bcd	91.67±12.91d
487	114.29±6.02c	95.79±4.72de	85.71±10.56e	100.00±0.00cd
Renhe-1	123.96±15.52b	115.18±3.96a	100.93±7.52bcd	155.56±27.22a
Hetou a2	99.12±6.15de	104.93±7.84bc	106.29±11.71bc	104.17±10.21cd
Yanbian-3	99.36±12.5de	111.02±7.90ab	124.03±14.65a	125.00±0.00b
Xingtai-23	155.56±14.34a	102.34±7.68c	95.83±8.07cde	108.33±12.91c
Lingchuan C1	76.39±11.08g	102.97±11.20c	93.59±11.06de	100.00±15.81cd
Fangshan	83.33±0.00g	104.85±0.00bc	93.83±0.00de	100.00±0.00cd
Wan 95-24	96.00±0.00de	106.41±0.00bc	107.35±0.00b	133.33±0.00b
Daziwang-24	100.00±0.00de	101.56±0.00cd	100.58±0.00bcd	100.00±0.00cd

APPENDICES A.2

Growth Physiological Indices of Pumpkin Materials Combinations at 20 Days After Inoculation with Fusarium Wilt Fungus

Pumpkin Materials	Relative growth rate / %			
	Plant height(cm)	Stem diameter(mm)	Chlorophyll(SPAD)	Number of leaves
Hetou a2 ×041-1	97.48±2.18ef	95.73±3.65defgh	100.37±2.67bc	94.44±9.62bcdef
Yanbian-3×Lingchuan C1	91.11±4.25fg	94.10±5.37efghi	90.94±2.10bcde	88.89±19.25def
Yanbian-3×360-3	98.61±2.41ef	100.31±7.03abcdef	102.04±5.15b	101.11±18.36bcd
Hetou a2 ×360-3	85.62±4.60gh	98.14±7.32bcdefg	90.04±2.68bcde	93.33±11.55cdef
Yanbian-4×Lingchuan C1	96.96±2.64ef	93.36±3.79efghi	97.54±5.88bcd	100.00±0.00bcde
Yanbian-2×041-1	97.58±5.74ef	99.90±5.91abcdefg	100.22±10.04bc	100.00±0.00bcde
360-3×041-1	92.62±2.63fg	96.89±3.2cdefgh	99.71±2.25bc	93.33±11.55cdef
Renhe-1×041-1	117.89±8.95bc	92.51±3.39fghi	90.06±8.71bcde	84.85±9.39ef
041-1×Xingtai	112.59±8.74cd	90.06±8.94ghi	83.62±11.45ef	103.33±15.06abcd
Yanbian-4×041-1	115.94±13.38cd	103.3±3.42abcde	88.09±6.98cde	93.94±7.42bcdef
Xingtai×Lingchuan C1	105.80±5.94de	106.61±8.28abc	92.51±6.54bcde	103.70±11.48abcd
Xingtai×Yanbian-4	127.93±12.64ab	101.83±6.90abcdef	92.77±4.28bcde	100.00±12.65bcde
041-1×Hetou a2	91.16±15.20fg	95.21±8.51defgh	90.62±13.74bcde	90.91±11.50cdef
Xingtai×487	84.85±8.50gh	108.66±9.07a	97.84±9.26bcd	90.91±11.50cdef

Xingtai×041-1	91.53±7.07fg	107.37±7.56ab	96.94±12.6bcd	90.91±0.00cdef
Hetou a2 ×Lingchuan C1	92.16±10.45fg	100.06±11.79abcdefg	90.47±11.72bcde	118.52±11.48a
Lingchuan C1×360-3	75.13±8.67h	104.80±6.34abcd	123.39±18.11a	106.67±10.33abc
Lingchuan C1×Xingtai	78.57±7.49h	86.93±8.69hij	87.51±6.04cdef	91.67±9.13cdef
Hetou a2 ×112-2	111.32±5.72cd	92.95±11.94fghi	74.56±2.35f	91.67±9.13cdef
Zhangzhou×041	130.83±10.21a	98.83±11.97abcdefg	93.96±11.28bcde	100.00±12.65bcde
Renhe-1×360-3	113.04±15.31cd	89.98±5.73ghi	85.05±7.47def	110.00±16.73ab
Yanbian-4×360-3	93.94±7.96fg	79.18±7.68j	93.42±16.29bcde	81.82±9.96f
360-3×487	131.29±9.10a	107.12±4.35ab	91.80±7.46bcde	106.06±13.69abc
Renhe-1×Lingchuan C1	92.73±10.97fg	84.96±8.66ij	96.95±10.62bcd	91.67±9.13cdef
041-1	98.33±3.50d	99.86±6.68cd	104.71±6.58ab	86.67±10.33de
112-2	96.00±11.06cd	104.71±5.34a	104.75±10.70abc	100.00±8.16cd
360-3	98.21±7.05d	94.14±14.10def	82.13±6.93de	96.67±15.06cd
487	95.37±8.18d	89.34±2.62fg	90.64±11.13cd	90.48±7.38cde
Renhe-1	142.42±13.69a	92.23±4.75efg	73.02±32.41e	123.33±15.06b
Hetou a2	102.56±15.13cd	78.47±4.35h	106.29±13.62a	96.67±15.06cd
Yanbian-3	78.17±6.80e	104.63±6.80bc	101.46±11.33abc	141.67±12.91a
Xingtai-23	127.38±10.51b	87.00±11.58g	81.80±8.47de	83.33±0.00e
Lingchuan C1	58.80±7.74f	98.10±6.70cde	82.60±5.88de	100.00±17.89c
Fangshan	0±0g	0±0i	0±0f	0±0f
Wan 95-24	118.75±0.00b	109.09±0.00b	107.89±0.00a	125.00±0.00b
Daziwang-24	107.14±0.00c	95.08±0.00def	92.25±0.00bcd	125.00±0.00b

APPENDICES A.3

Growth Physiological Indices of Pumpkin Materials Combinations at 30 Days After Inoculation with Fusarium Wilt Fungus

Pumpkin Materials	Relative growth rate / %			
	Plant height(cm)	Stem diameter(mm)	Chlorophyll(SPAD)	Number of leaves
Hetou a2 ×041-1	89.78±2.75ef	91.78±1.85defg	95.65±2.40bcd	91.07±7.78bcde
Yanbian-3×Lingchuan C1	86.91±1.86ef	90.55±1.12fg	93.84±3.48bcde	94.44±9.62bcd
Yanbian-3×360-3	92.15±3.77def	96.55±1.04bcdefg	101.61±12.95bc	106.67±11.55ab

Hetou a2 ×360-3	91.27±4.31def	93.78±1.30cdefg	94.13±15.26bcde	100.00±0.00abcd
Yanbian-4×Lingchuan C1	90.02±9.64ef	93.10±2.23defg	89.57±2.63cde	90.48±16.50cde
Yanbian-2×041-1	92.09±3.65def	93.90±0.22cdefg	102.88±17.00bc	101.11±18.36abcd
360-3×041-1	88.63±6.96ef	87.12±0.65gh	96.99±16.03bcd	94.44±9.62bcd
Renhe-1×041-1	84.57±6.38f	88.05±6.26gh	94.06±11.34bcde	86.11±6.80def
041-1×Xingtai	85.48±8.35f	90.76±10.84efg	104.63±13.93bc	91.67±9.13bcd
Yanbian-4×041-1	116.98±11.93b	96.16±9.84bcdefg	99.22±16.81bcd	106.06±13.69abc
Xingtai×Lingchuan C1	86.89±9.89ef	102.69±7.96abc	101.34±12.86bc	100.00±9.96abcd
Xingtai×Yanbian-4	102.26±9.92cd	105.5±7.34ab	99.82±2.12bcd	97.44±7.94abcd
041-1×Hetou a2	95.24±9.63def	98.67±9.31bcdef	88.51±18.45cde	103.03±9.39abc
Xingtai×487	92.59±10.51def	103.93±7.28ab	93.29±17.36bcde	97.22±6.80abcd
Xingtai×041-1	111.67±10.90bc	111.38±9.77a	100.28±11.02bcd	100.00±9.96abcd
Hetou a2 ×Lingchuan C1	91.23±11.53def	111.18±7.77a	78.37±7.72e	112.12±13.69a
Lingchuan C1×360-3	85.71±5.68f	111.54±8.98a	155.05±26.68a	102.78±12.55abc
Lingchuan C1×Xingtai	87.78±9.81ef	80.26±7.83h	88.15±10.83cde	75.56±10.89ef
Hetou a2 ×112-2	143.26±16.74a	91.99±6.68defg	91.88±11.31bcde	105.13±6.28abc
Zhangzhou×041	88.71±10.94ef	98.18±7.23bcdef	107.30±11.09b	86.11±6.80def
Renhe-1×360-3	116.98±6.31b	92.15±8.06defg	88.53±11.76cde	94.87±11.58bcd
Yanbian-4×360-3	88.89±10.04ef	80.25±8.52h	83.85±13.71de	73.81±5.83f
360-3×487	97.85±14.38de	100.94±5.84bcd	98.72±11.71bcd	100±25.28abcd
Renhe-1×Lingchuan C1	110.06±8.74bc	100.16±9.51bcde	90.79±8.92bcde	105.56±13.61abc
041-1	89.78±2.75ef	91.78±1.85defg	95.65±2.40bcd	91.07±7.78bcde
112-2	86.91±1.86ef	90.55±1.12fg	93.84±3.48bcde	94.44±9.62bcd
360-3	92.15±3.77def	96.55±1.04bcdefg	101.61±12.95bc	106.67±11.55ab
487	91.27±4.31def	93.78±1.30cdefg	94.13±15.26bcde	100.00±0.00abcd
Renhe-1	90.02±9.64ef	93.10±2.23defg	89.57±2.63cde	90.48±16.50cde
Hetou a2	92.09±3.65def	93.90±0.22cdefg	102.88±17.00bc	101.11±18.36abcd
Yanbian-3	88.63±6.96ef	87.12±0.65gh	96.99±16.03bcd	94.44±9.62bcd
Xingtai-23	84.57±6.38f	88.05±6.26gh	94.06±11.34bcde	86.11±6.80def
Lingchuan C1	85.48±8.35f	90.76±10.84efg	104.63±13.93bc	91.67±9.13bcd

Fangshan	116.98±11.93b	96.16±9.84bcdefg	99.22±16.81bcd	106.06±13.69abc
Wan 95-24	86.89±9.89ef	102.69±7.96abc	101.34±12.86bc	100.00±9.96abcd
Daziwang-24	102.26±9.92cd	105.5±7.34ab	99.82±2.12bcd	97.44±7.94abcd

APPENDICES A.4

Disease Index and Disease Resistance Grade of Pumpkin Materials at 30 Days After Inoculation with Fusarium Wilt Fungus

Pumpkin Materials	The number of the disease incidence about different level (leaf/stem)						Number of Diseased Plants	Total Number of Plants	Disease Index	Resist disease level
	0	1	2	3	4	5			leaf/stem	leaf/stem
Hetou a2 ×041-1	0	0	0	1	12	47	60	60	95.33±8.08a	HS
Yanbian-3×Lingchuan C1	0	0	0	29	31	0	60	60	87.92±8.04a	HS
Yanbian-3×360-3	0	0	0	5	41	14	60	60	83.00±4.58b	HS
Hetou a2 ×360-3	0	17	9	28	6	0	60	60	59.58±4.73c	S
Yanbian-4×Lingchuan C1	0	0	32	18	10	0	60	60	52.67±1.53c	MR
Yanbian-2×041-1	0	34	22	3	1	0	60	60	37.92±1.91d	MR
360-3×041-1	0	0	0	4	42	14	60	60	83.33±6.35b	S
Renhe-1×041-1	0	4	12	25	19	0	60	60	74.58±16.27ab	S
041-1×Xingtai	0	0	0	0	60	0	60	60	80.00±0.00b	S
Yanbian-4×041-1	0	4	23	32	1	0	60	60	62.92±4.73bc	S
Xingtai×Lingchuan C1	0	0	25	27	7	1	60	60	54.67±0.58c	MR
Xingtai×Yanbian-4	0	34	9	10	7	0	60	60	45.83±8.32d	MR
041-1×Hetou a2	0	0	0	10	32	18	60	60	82.67±2.89b	S
Xingtai×487	0	8	9	35	8	0	60	60	67.92±6.17bc	S
Xingtai×041-1	0	0	12	47	1	0	60	60	56.33±6.35fgh	S
Hetou a2 ×Lingchuan C1	0	26	13	21	0	0	60	60	47.92±21.45defg	MR
Lingchuan C1×360-3	0	0	34	26	0	0	60	60	48.67±5.69h	MR
Lingchuan C1×Xingtai	0	0	53	7	0	0	60	60	52.92±5.05cdef	MR
Hetou a2 ×112-2	0	0	33	25	2	0	60	60	49.67±4.04h	MR
Zhangzhou×041	0	6	14	40	0	0	60	60	64.17±18.76bcd	S

Renhe-1×360-3	0	0	12	48	0	0	60	60	56.00±3.46fgh	S
Yanbian-4×360-3	0	53	6	1	0	0	60	60	28.33±5.77hi	R
360-3×487	0	0	0	60	0	0	60	60	60.00±0.00fefg	S
Renhe-1×Lingchuan C1	0	40	20	0	0	0	60	60	33.33±8.78ghi	R
041-1	0	0	34	26	0	0	60	60	48.67±4.62h	MR
112-2	0	26	14	20	0	0	60	60	47.50±10.90defg	MR
360-3	0	0	6	54	0	0	60	60	58.00±3.46fgh	S
487	0	60	0	0	0	0	60	60	25.00±0.00i	R
Renhe-1	0	0	12	48	0	0	60	60	56.00±3.46fgh	S
Hetou a2	0	20	14	26	0	0	60	60	52.50±25.37cdef	MR
Yanbian-3	0	0	6	54	0	0	60	60	58.00±3.46fgh	S
Xingtai-23	0	13	34	13	0	0	60	60	50.00±7.50defg	MR
Lingchuan C1	0	0	0	40	6	14	60	60	71.33±19.63cd	S
Fangshan	0	12	21	20	7	0	60	60	59.17±8.87bcde	S
Wan 95-24	0	0	0	54	6	0	60	60	62.00±3.46defg	S
	0	40	14	6	0	0	60	60	35.83±9.46fghi	MR
Hetou a2 ×041-1	0	0	0	54	6	0	60	60	62.00±3.46defg	S
Yanbian-3×Lingchuan C1	0	26	13	21	0	0	60	60	47.92±14.05defg	MR
Yanbian-3×360-3	0	0	6	54	0	0	60	60	58.00±3.46fgh	S
Hetou a2 ×360-3	0	40	20	0	0	0	60	60	33.33±8.78ghi	R
Yanbian-4×Lingchuan C1	0	0	12	35	13	0	60	60	60.33±6.03efg	S
Yanbian-2×041-1	0	60	0	0	0	0	60	60	25.00±0.00i	R
360-3×041-1	0	0	6	34	20	0	60	60	64.67±10.07def	S
Renhe-1×041-1	0	20	40	0	0	0	60	60	41.67±14.43fghi	MR
041-1×Xingtai	0	0	20	40	0	0	60	60	53.33±7.02gh	MR
Yanbian-4×041-1	48	12	0	0	0	0	60	60	5.00±4.33j	HR
Xingtai×Lingchuan C1	0	0	0	34	26	0	60	60	68.67±4.62de	S
Xingtai×Yanbian-4	0	26	21	13	0	0	60	60	44.58±5.91efgh	MR
041-1×Hetou a2	0	0	0	33	27	0	60	60	69.00±3.46bc	S
Xingtai×487	0	19	20	21	0	0	60	60	50.83±0.72c	MR

Xingtai×041-1	0	0	0	46	14	0	60	60	64.67±4.04cd	S
Hetou a2 ×Lingchuan C1	0	0	7	53	0	0	60	60	72.08±5.05b	S
Lingchuan C1×360-3	0	0	0	46	14	0	60	60	64.67±4.04cd	S
Lingchuan C1×Xingtai	0	14	33	13	0	0	60	60	49.58±14.43c	MR
Hetou a2 ×112-2	0	0	0	60	0	0	60	60	60.00±0.00d	S
Zhangzhou×041	0	33	27	0	0	0	60	60	36.25±4.33d	MR
Renhe-1×360-3	0	0	46	14	0	0	60	60	44.67±4.04f	MR
Yanbian-4×360-3	0	14	32	13	0	0	60	60	48.75±9.01c	MR
360-3×487	0	0	26	34	0	0	60	60	51.33±7.51e	MR
Renhe-1×Lingchuan C1	0	40	20	0	0	0	60	60	33.33±8.13de	R
041-1	0	0	0	60	0	0	60	60	60.00±0.00d	S
112-2	0	33	27	0	0	0	60	60	36.25±4.33d	MR
360-3	0	0	0	27	33	0	60	60	71.00±3.46b	S
487	0	27	33	0	0	0	60	60	38.75±4.33d	MR
Renhe-1	0	0	0	46	14	0	60	60	64.67±4.04cd	S
Hetou a2	0	0	7	53	0	0	60	60	72.08±5.05b	S
Yanbian-3	0	0	0	0	0	60	60	60	100.00±0.00a	HS
Xingtai-23	0	0	0	0	60	0	60	60	100.00±0.00a	HS
Lingchuan C1	0	0	0	60	0	0	60	60	60.00±0.00d	S
Fangshan	0	60	0	0	0	0	60	60	25.00±0.00e	R
Wan 95-24	0	0	0	60	0	0	60	60	60.00±0.00d	S
Daziwang-24	0	0	0	60	0	0	60	60	75.00±0.00b	S

Appendix A1–A4: Growth and Physiological Responses and Disease Resistance Identification of Pumpkin Hybrid Combinations and Parental Lines After Infection by Fusarium Wilt Pathogen

Note: Different lowercase letters in the same column show significant difference ($P<0.05$).

APPENDICES B.1

Effects of Root-Knot Nematode Infection on Growth Indicators of Pumpkin Materials

Pumpkin Materials	Relative growth rate / %			
	Plant height(cm)	Stem diameter(mm)	Chlorophyll(SPAD)	Root Fresh Weight
Hetou a2 ×041-1	81.95±0.59f	84.6±0.57c	87.54±1.71a	85.36±0.47gh
Yanbian-3×Lingchuan C1	91.51±1.17bcdef	90.78±1.64abc	89.64±2.28a	91.01±0.84efgh
Yanbian-3×360-3	96.74±0.73bcdef	97.52±0.74abc	98.71±0.86a	98.56±0.67defg
Hetou a2 ×360-3	93.65±1.17bcdef	94.57±0.48abc	95.11±1.97a	92.32±1.62defgh
Yanbian-4×Lingchuan C1	90.97±0.38cdef	90.73±1.65abc	92.03±1.47a	92.16±0.55defgh
Yanbian-2×041-1	96.68±0.73bcdef	97.18±0.66abc	98.18±0.43a	97.01±0.29defg
360-3×041-1	84.90±3.91ef	86.95±1.61bc	86.00±3.57a	86.07±0.72fgh
Renhe-1×041-1	94.43±9.66bcdef	106.41±17.38a	93.79±7.22a	108.04±8.99cd
041-1×Xingtai	110.88±1.56abcd	96.13±8.34abc	87.36±19.62a	126.13±16.51b
Yanbian-4×041-1	129.52±16.76a	105.52±20.90a	102.8±7.95a	126.90±23.32b
Xingtai×Lingchuan C1	82.39±12.05f	94.02±1.17abc	87.73±7.96a	150.37±18.56a
Xingtai×Yanbian-4	102.13±10.03bcdef	96.42±3.99abc	93.02±13.86a	98.55±8.00defg
041-1×Hetou a2	89.59±10.97def	98.73±2.50abc	99.90±18.10a	118.46±13.61bc
Xingtai×487	102.11±22.82bcdef	101.03±5.57abc	96.48±14.01a	105.56±7.02cde
Xingtai×041-1	127.79±13.69a	99.90±3.25abc	95.77±16.61a	76.53±15.88h
Hetou a2 ×Lingchuan C1	113.12±23.71ab	96.34±2.23abc	102.00±6.60a	101.76±7.30def
Lingchuan C1×360-3	84.39±14.92ef	101.05±3.52abc	99.03±7.406a	96.87±13.68defg
Lingchuan C1×Xingtai	91.95±14.9bcdef	103.3±2.05ab	86.68±19.87a	102.79±7.27cde
Hetou a2 ×112-2	92.09±23.88bcdef	90.04±5.22abc	100.04±7.16a	104.62±0.87cde
Zhangzhou×041	112.33±12.50abc	95.65±13.33abc	101.78±13.52a	103.36±5.59cde
Renhe-1×360-3	87.44±17.55c	98.61±1.40abc	93.57±23.91a	104.42±13.77cde
Yanbian-4×360-3	105.83±7.14bcde	93.60±9.90abc	93.88±29.88a	96.35±10.50defg
360-3×487	88.20±10.68ef	90.32±2.68abc	84.45±8.49a	99.65±5.17defg
Renhe-1×Lingchuan C1	84.95±3.72ef	96.62±3.78abc	112.46±4.36a	100.05±0.68defg
041-1	111.11±6.23de	106.88±5.54ab	46.59±12.95e	120.93±37.49e

112-2	93.59±23.98fg	116.16±10.65a	63.81±13.02bcd	306.39±31.73a
360-3	98.1±13.11ef	88.41±10.32d	54.92±13.79cde	85.8±12.09f
487	81.19±11.43gh	96.71±3.62cd	50.4±8.99de	186.44±13.69d
Renhe-1	123.85±7.97cd	92.84±7.31d	39.54±8.72e	57.72±15.08h
Hetou a2	83.33±10.5gh	106.74±12.36b	72.07±19.96b	63.25±13.69gh
Yanbian-3	135.63±16.12c	102.55±12.3bc	74.33±25.33b	120.9±15.77e
Xingtai-23	78.32±20.45h	89.72±10.03d	78.36±25.14b	71.77±10.05fgh
Lingchuan C1	123.98±21.1cd	103.31±10.84bc	67.53±19.59bc	186.36±36.59d
Fangshan	238.46±0a	111.07±0ab	136.61±0a	82.11±0fg
Wan 95-24	120±0d	106.19±0b	63.95±0bcd	211.63±0c
Daziwang-24	200±0b	108.05±0ab	143.08±0a	234.85±0b

APPENDICES B.2

Effects of Root-Knot Nematode Infection on Growth Indicators of Pumpkin Materials

Pumpkin Materials	Gall Index	Egg Index	Reproduction Factor	Disease Inde
Hetou a2 ×041-1	21.87±1.81cde	4417.15±114.85c	7.54±0.22a	56.33±1.53d
Yanbian-3×Lingchuan C1	15.74±1.59cde	3068.37±34.81cde	5.58±0.05de	46.67±1.15f
Yanbian-3×360-3	3.72±0.57e	741.55±28.62h	1.46±0.07i	19.00±1.00j
Hetou a2 ×360-3	9.77±2.30cde	1914.15±102.32fg	3.53±0.15g	26.67±1.15i
Yanbian-4×Lingchuan C1	14.47±1.73cde	2900.70±205.07ef	5.35±0.35e	42.00±1.00g
Yanbian-2×041-1	5.50±0.60de	1091.02±97.07gh	2.12±0.19h	19.67±0.58j
360-3×041-1	20.92±2.37cde	4340.58±245.13cd	7.47±0.40a	51.33±0.58e
Renhe-1×041-1	29.97±1.35bc	3068.86±179.84cde	6.62±0.53b	76.33±2.52a
041-1×Xingtai	12.59±1.96cde	2263.80±401.07ef	5.63±0.37de	66.33±4.04b
Yanbian-4×041-1	15.53±2.63cde	2475.18±637.46de	6.09±0.51bcd	68.33±1.53b
Xingtai×Lingchuan C1	14.27±3.86cde	2123.89±228.40ef	6.35±0.60bc	75.33±1.53a
Xingtai×Yanbian-4	20.30±1.44ab	3144.38±473.71ab	6.15±0.41bcd	76.00±3.46a
041-1×Hetou a2	12.28±5.97cde	1765.77±331.90ef	4.12±0.26fg	60.33±0.58c
Xingtai×487	12.45±4.53cde	1980.99±170.81cde	4.18±0.44f	57.00±3.00cd
Xingtai×041-1	23.72±8.78ab	4102.65±1606.51a	5.94±0.89cde	66.33±3.51b

Hetou a2 ×Lingchuan C1	10.50±2.11cde	2120.74±365.67ef	4.28±0.44f	55.33±3.51d
Lingchuan C1×360-3	22.54±1.91bcd	2299.19±525.62de	4.36±0.36f	58.33±3.06cd
Lingchuan C1×Xingtai	19.28±3.24cde	2134.73±365.30def	4.37±0.61f	56.33±2.89d
Hetou a2 ×112-2	6.69±0.93de	597.37±84.82h	1.25±0.18i	33.00±1.00h
Zhangzhou×041	18.12±14.62a	1998.82±170.89b	4.12±0.16fg	57.33±1.53cd
Renhe-1×360-3	11.64±6.00cde	1955.51±218.45ef	4.07±0.54fg	56.33±1.53d
Yanbian-4×360-3	14.14±4.16cde	2330.06±407.32ef	4.44±0.40f	56.67±3.79cd
360-3×487	5.66±2.76de	706.05±94.31h	1.40±0.14i	33.33±3.79h
Renhe-1×Lingchuan C1	14.66±5.67cde	2081.68±141.14ef	4.17±0.31f	58.00±5.20cd
041-1	0.65±0.18b	118.62±33.21b	2.42±0.48cd	46.67±6.67c
112-2	0.65±0.18b	118.94±34.88b	5.20±1.12b	64.44±3.85a
360-3	0.17±0.12g	32.57±22.56f	0.81±0.55e	22.22±7.70e
487	0.38±0.09def	70.48±16.84cde	1.53±0.29de	35.56±7.7cd
Renhe-1	0.40±0.20cde	71.73±31.19cd	1.30±0.66de	22.22±10.18e
Hetou a2	0.25±0.31defg	47.64±57.85def	0.81±0.91e	20.00±13.33e
Yanbian-3	0.44±0.07cd	76.18±13.53cd	2.43±0.24cd	35.56±7.70cd
Xingtai-23	0.22±0.10efg	41.06±18.24def	0.79±0.35e	26.67±6.67de
Lingchuan C1	1.02±0.40a	186.91±72.65a	10.18±2.06a	62.22±3.85b
Fangshan	0.20±0.00fg	36.24±0.00ef	0.73±0.00e	20.00±0.00e
Wan 95-24	0.71±0.00b	132.53±0.00b	4.82±0.00b	40.00±0.00bc
Daziwang-24	0.58±0.00bc	103.10±0.00bc	3.20±0.00c	40.00±0.00bc

APPENDICES B.3

Effects of Root-Knot Nematode on Growth and Membership Function Values of Resistance Indexes in Pumpkin Hybrid Combinations

Pumpkin Hybrid	Plant height	Stem diameter	Chlorophyll	Root Fresh Weigh	Gall Index	Egg Index	Reproduction Factor	Disease Inde	Total	Rank

				t						
Hetou a2 ×041-1	0.61	0.58	0.05	0.86	0.92	0.88	0.00	0.35	4.25	8
Yanbian-3×Lingchuan C1	0.78	0.65	0.00	0.77	0.94	0.91	0.31	0.52	4.88	6
Yanbian-3×360-3	1.03	1.00	0.60	0.51	1.00	1.00	0.97	1.00	7.10	1
Hetou a2 ×360-3	0.93	0.64	0.13	0.65	0.97	0.95	0.64	0.87	5.77	3
Yanbian-4×Lingchuan C1	0.69	0.55	0.05	0.77	0.94	0.92	0.35	0.60	4.87	7
Yanbian-2×041-1	1.00	0.93	0.25	0.57	0.99	0.98	0.86	0.99	6.58	2
360-3×041-1	0.62	0.45	0.00	0.87	0.92	0.88	0.01	0.44	4.19	9
Renhe-1×041-1	0.14	0.21	0.65	0.86	0.00	0.26	0.15	0.00	2.26	22
041-1×Xingtai	0.10	0.17	0.42	0.84	0.60	0.47	0.30	0.17	3.08	18
Yanbian-4×041-1	0.15	0.40	0.75	0.90	0.50	0.41	0.23	0.14	3.49	14
Xingtai×Lingchuan C1	0.01	0.20	0.36	1.00	0.54	0.50	0.19	0.02	2.83	21
Xingtai×Yanbian-4	0.07	0.19	0.49	0.19	0.33	0.24	0.22	0.01	1.74	24
041-1×Hetou a2	0.00	0.14	0.58	0.56	0.61	0.60	0.54	0.28	3.31	16
Xingtai×487	0.08	0.31	0.67	0.49	0.60	0.54	0.53	0.34	3.56	12
Xingtai×041-1	0.13	0.24	0.67	0.11	0.21	0.00	0.25	0.17	1.79	23
Hetou a2 ×Lingchuan C1	0.18	0.20	0.90	0.62	0.67	0.50	0.52	0.37	3.95	10
Lingchuan C1×360-3	0.04	0.21	0.79	0.58	0.26	0.46	0.51	0.31	3.16	17
Lingchuan C1×Xingtai	0.01	0.27	0.48	0.55	0.37	0.50	0.50	0.35	3.04	19
Hetou a2 ×112-2	0.07	0.00	0.80	0.93	0.80	0.89	1.00	0.76	5.25	4
Zhangzhou×041	0.13	0.06	0.93	0.00	0.41	0.54	0.54	0.33	2.94	20
Renhe-1×360-3	0.08	0.11	0.69	0.54	0.63	0.55	0.55	0.35	3.51	13
Yanbian-4×360-3	0.14	0.22	0.61	0.68	0.54	0.45	0.49	0.34	3.48	15
360-3×487	0.16	0.40	0.59	0.50	0.84	0.86	0.98	0.75	5.07	5

Renhe-1×Lingchuan C1	0.06	0.36	1.00	0.56	0.53	0.51	0.54	0.32	3.88	11

APPENDICES B.4

Effects of Root-Knot Nematode on Growth and Membership Function Values of Resistance Indexes in Pumpkin Parents

Pumpkin Parents	Plant height	Stem diameter	Chlorophyll	Root Fresh Weight	Gall Index	Egg Index	Reproduction Factor	Disease Inde	Total	Rank
041-1	0.40	0.61	0.20	0.08	0.43	0.44	0.82	0.40	3.38	9
112-2	0.13	0.30	0.40	0.67	0.43	0.44	0.53	0.00	2.90	11
360-3	0.40	0.53	0.49	0.15	1.00	1.00	0.99	0.95	5.51	2
487	0.59	0.05	0.32	0.09	0.75	0.75	0.92	0.65	4.11	8
仁和-1	0.45	0.43	0.00	0.00	0.73	0.75	0.94	0.95	4.24	7
河头 a2	0.07	0.90	0.34	0.01	0.90	0.90	0.99	1.00	5.11	4
盐边-3	0.00	1.00	0.16	0.35	0.69	0.72	0.82	0.65	4.39	6
邢台-23	1.00	0.00	0.42	0.01	0.94	0.94	0.99	0.85	5.16	3
陵川 C1	0.43	0.37	0.16	1.00	0.00	0.00	0.00	0.05	2.02	12
方山	0.74	0.90	0.42	0.04	0.97	0.98	1.00	1.00	6.04	1
皖 95-24	0.20	0.64	0.01	0.46	0.36	0.35	0.57	0.55	3.14	10
大籽旺-24	0.28	0.72	1.00	0.32	0.52	0.54	0.74	0.55	4.67	5

Appendix B1–B4: Growth Responses and Comprehensive Resistance Evaluation of Pumpkin Rootstock Hybrid Combinations and Parental Lines Under Root-Knot Nematode Infection

Note: Different lowercase letters in the same column show significant difference ($P<0.05$).

APPENDICES C

ID and Functional Annotation of 30 Core Hub Genes

Gene_ID	Module	kME_Value	NR_annotation
CmoCh20G004420	ME17	0.938604	triosephosphate isomerase, cytosolic-like [Cucurbita moschata]
CmoCh20G011790	ME17	0.931598	thioredoxin-like protein YLS8 [Cucumis sativus]
CmoCh12G008560	ME17	0.915295	F-box protein SKIP1-like [Cucurbita moschata]
CmoCh02G005650	ME17	0.91377	probable calcium-binding protein CML20 [Cucurbita moschata]
CmoCh02G013370	ME17	0.906355	putative axial regulator YABBY 2 isoform X1 [Cucurbita moschata]
CmoCh01G013700	ME20	0.94177	protein ASPARTIC PROTEASE IN GUARD CELL 1-like [Cucurbita moschata]
CmoCh15G014290	ME20	0.939067	peroxidase 2-like [Cucurbita moschata]
CmoCh19G010650	ME20	0.933837	uncharacterized protein LOC111454865 [Cucurbita moschata]
CmoCh19G007930	ME20	0.929501	expansin-like A2 [Cucurbita moschata]
CmoCh06G001350	ME20	0.927398	hypothetical protein Csa_010510 [Cucumis sativus]
CmoCh01G015120	ME23	0.943313	phosphoenolpyruvate carboxykinase (ATP) [Cucurbita moschata]
CmoCh01G003210	ME23	0.927164	UDP-glucuronic acid decarboxylase 2-like [Cucurbita moschata]
CmoCh14G020350	ME23	0.922485	uncharacterized protein LOC111432091 [Cucurbita moschata]
CmoCh14G013030	ME23	0.921032	PRA1 family protein F3-like [Cucurbita moschata]
CmoCh06G014030	ME23	0.921003	folate-biopterin transporter 1, chloroplastic-like [Cucurbita moschata]
CmoCh18G000410	ME26	0.940643	reticulon-like protein B9 [Cucurbita moschata]
CmoCh06G014460	ME26	0.938414	uncharacterized protein LOC111456543 [Cucurbita moschata]
CmoCh11G007950	ME26	0.927772	inactive protein RESTRICTED TEV MOVEMENT 2-like [Cucurbita moschata]
CmoCh12G008210	ME26	0.923401	uncharacterized protein At1g08160 [Cucurbita moschata]
CmoCh04G010140	ME26	0.922918	early nodulin-like protein 3 [Cucurbita moschata]
CmoCh11G004390	ME5	0.967458	heptahelical transmembrane protein 2 [Cucurbita moschata]
CmoCh10G001630	ME5	0.965469	mannose-1-phosphate guanyltransferase alpha-B-like [Cucurbita moschata]
CmoCh03G007050	ME5	0.954519	thaumatin-like protein 1 isoform X1 [Cucurbita moschata]

CmoCh07G007090	ME5	0.949113	floral homeotic protein APETALA 2-like isoform X1 [Cucurbita moschata]
CmoCh08G006540	ME5	0.948153	uncharacterized protein LOC111464187 [Cucurbita moschata]
CmoCh13G007330	ME9	0.972324	large ribosomal RNA subunit accumulation protein YCED homolog 1, chloroplastic-like [Cucurbita moschata]
CmoCh13G003480	ME9	0.955749	ras-related protein RABB1c-like [Cucurbita moschata]
NewGene_2423	ME9	0.954696	NA
NewGene_1791	ME9	0.954034	NA
CmoCh01G000940	ME9	0.953286	protein IQ-DOMAIN 14-like isoform X1 [Cucurbita moschata]

Note: This table contains the complete information of the 30 core hub genes screened by WGCNA analysis in this study, including gene module affiliation, connectivity, and functional annotation. The complete data file is available in the supplementary materials of the paper: Supplementary_Table_S1_30_Hubs_Annotation.csv

APPENDICES D

Full Table of TF-Gene Regulatory Relationships in Rifu and Rimu

TF_Gene_ID	TF_Family	Target_Hub_ID	Distance_to_TSS	FIMO_Pvalue	WGCNA_Cor	Regulation	matched_sequence
CmoCh01G003210	ERF9	CmoCh03G007050	-586	1.43E-09	-0.62173	Negative	GACGGCGGAGGCGGCGGTG
CmoCh01G015120	ERF9	CmoCh03G007050	-586	1.43E-09	-0.7451	Negative	GACGGCGGAGGCGGCGGTG
CmoCh01G003210	Sl-ERF_C_6	CmoCh03G007050	-586	3.94E-09	-0.62173	Negative	TCACCGCCGCCTCCGCCGTC
CmoCh01G015120	Sl-ERF_C_6	CmoCh03G007050	-586	3.94E-09	-0.7451	Negative	TCACCGCCGCCTCCGCCGTC
CmoCh01G003210	GLYMA-12G117000	CmoCh03G007050	-586	5.83E-09	-0.62173	Negative	GACGGCGGAGGCGGCGG
CmoCh01G015120	GLYMA-12G117000	CmoCh03G007050	-586	5.83E-09	-0.7451	Negative	GACGGCGGAGGCGGCGG
CmoCh01G003210	DREB2G	CmoCh03G007050	-583	7.90E-09	-0.62173	Negative	GGCGGAGGCGGCGG
CmoCh01G015120	DREB2G	CmoCh03G007050	-583	7.90E-09	-0.7451	Negative	GGCGGAGGCGGCGG
CmoCh01G003210	Sl-ERF_F_4	CmoCh03G007050	-587	7.98E-09	-0.62173	Negative	ACCGCCGCCTCCGCCGTCA
CmoCh01G015120	Sl-ERF_F_4	CmoCh03G007050	-587	7.98E-09	-0.7451	Negative	ACCGCCGCCTCCGCCGTCA
CmoCh01G003210	RAP2-6	CmoCh03G007050	-587	1.18E-08	-0.62173	Negative	TGACGGCGGAGGCGG
CmoCh01G015120	RAP2-6	CmoCh03G007050	-587	1.18E-08	-0.7451	Negative	TGACGGCGGAGGCGG
CmoCh01G003210	DOF3.6	CmoCh03G007050	-151	1.42E-08	-0.62173	Negative	TTTTTTTTTTATTTTTTTTT

CmoCh01G015120	DOF3.6	CmoCh03G007050	-151	1.42E-08	-0.7451	Negative	TTTTTTTTTTATTTTTTTT
CmoCh01G003210	Sl-ERF_F_5	CmoCh03G007050	-586	1.62E-08	-0.62173	Negative	CCGCCGCCTCCGCCGTC

Note: This table contains 16,275 records of regulatory relationships between transcription factors (TFs) and target genes. The meanings of core columns correspond strictly to the actual fields in the table.

The complete data file is available in the supplementary materials of the paper:

Table_S2_Final_Optimized.csv

APPENDICES E

Photo of the field experiment at Henan Institute of Science and Technology, Xinxiang, China: Field hybridization and seed production

Photo of the plastic greenhouse experiment at Henan Institute of Science and

Technology, Xinxiang, China: Nursery preparation

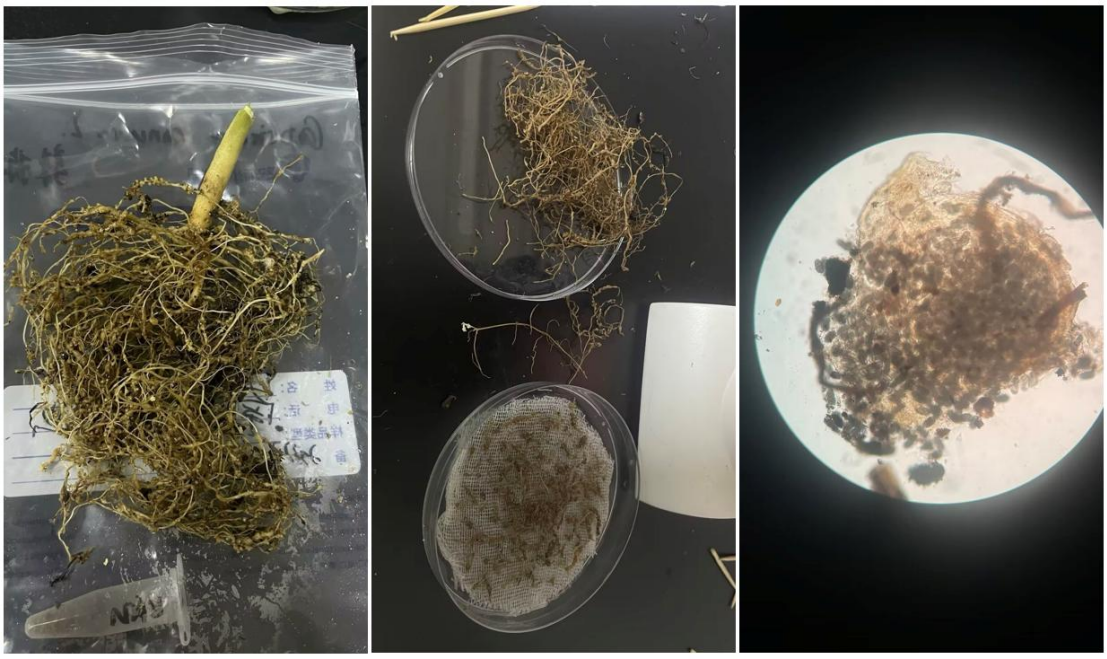

Photo of the laboratory experiment at Henan Institute of Science and Technology, Xinxiang, China: Collection of root galls and observation of egg masses

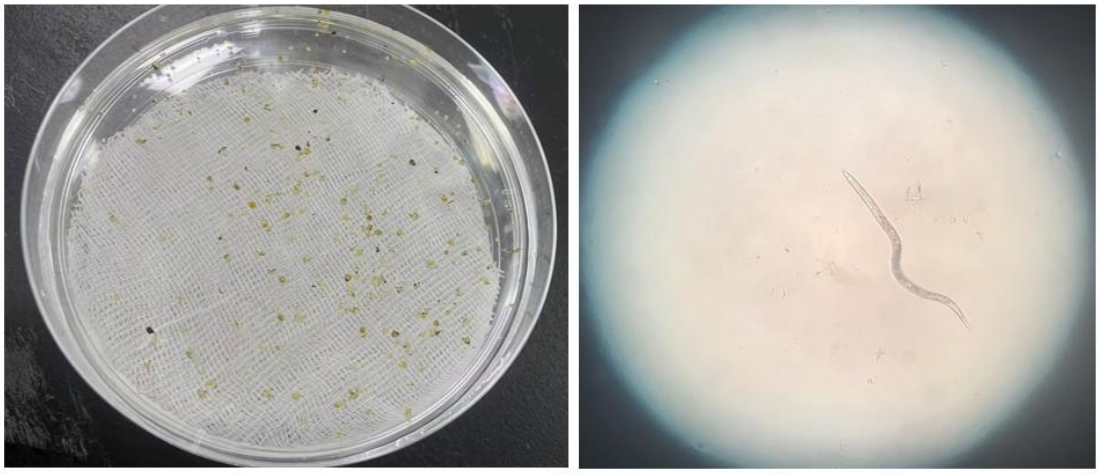

Photo of the laboratory experiment at Henan Institute of Science and Technology, Xinxiang, China: Hatching and observation of J2

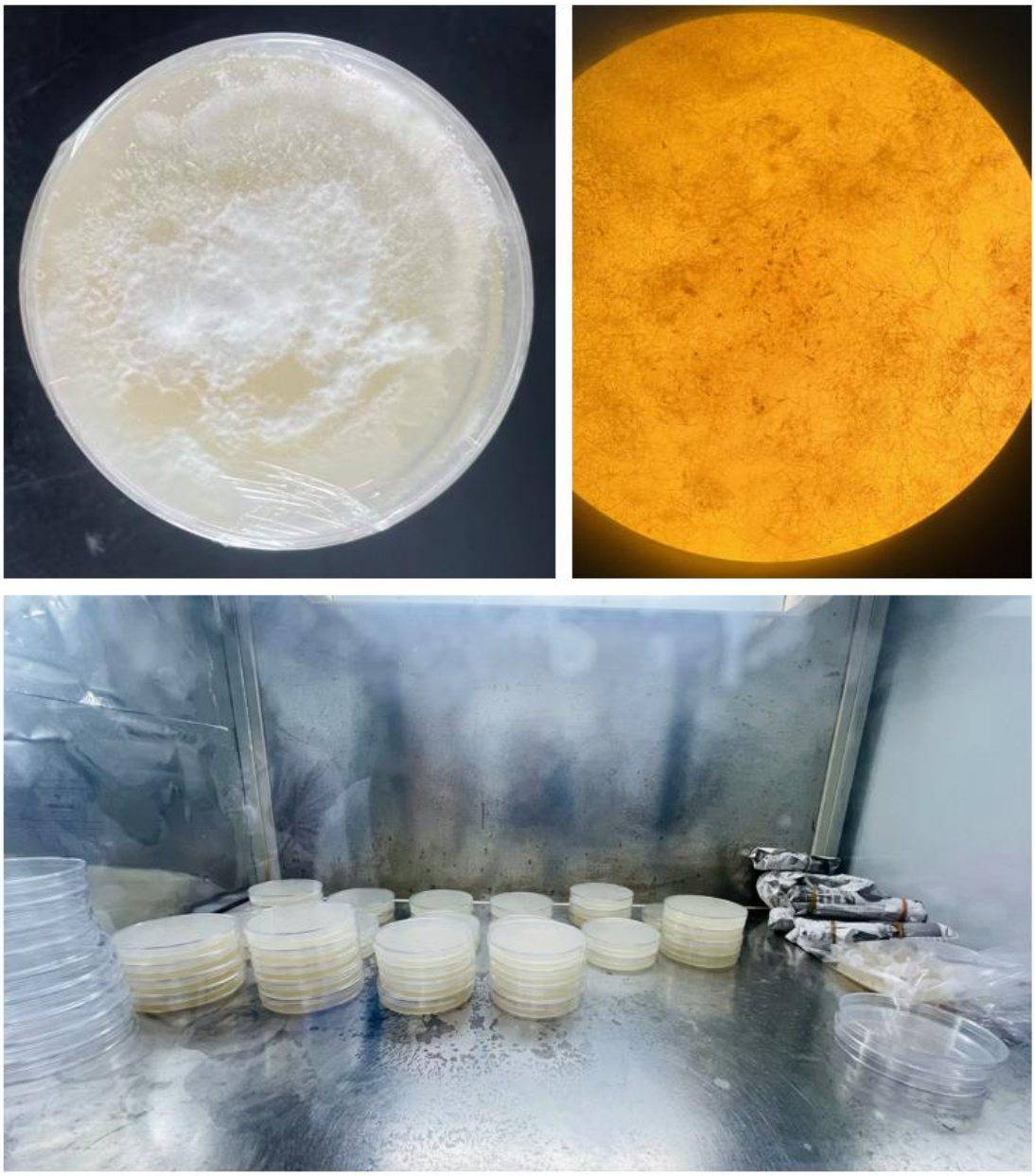

Photo of the laboratory experiment at Henan Institute of Science and Technology, Xinxiang, China: Propagation and observation of Fusarium wilt pathogen

Photo of the plastic greenhouse experiment at Henan Institute of Science and Technology, Xinxiang, China: Inoculation with Fusarium wilt pathogen and root-knot nematode

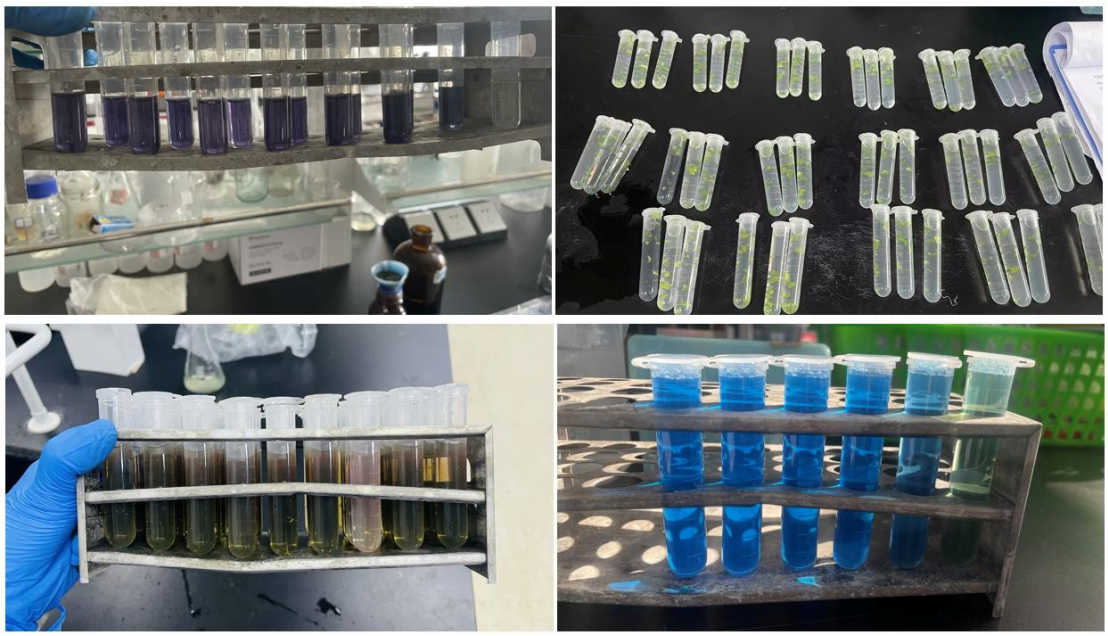

Photo of the laboratory experiment at Henan Institute of Science and Technology, Xinxiang, China: Determination of leaf antioxidant enzyme activities, MDA content, soluble sugar content and soluble protein content